REPORT DOCUMENTATION PAGE

AFRL-SR-BL-TR-00-

0768

1. AGENCY USE ONLY *(Leave blank)*	2. REPORT DATE
	December, 1997

4. TITLE AND SUBTITLE
1997 Summer Research Program (SRP), High School Apprenticeship Program (HSAP), Final Reports, Volume 12A, Armstrong Laboratory

5. FUNDING NUMBERS
F49620-93-C-0063

6. AUTHOR(S)
Gary Moore

7. PERFORMING ORGANIZATION NAME(S) AND ADDRESS(ES)
Research & Development Laboratories (RDL)
5800 Uplander Way
Culver City, CA 90230-6608

8. PERFORMING ORGANIZATION REPORT NUMBER

9. SPONSORING/MONITORING AGENCY NAME(S) AND ADDRESS(ES)
Air Force Office of Scientific Research (AFOSR)
801 N. Randolph St.
Arlington, VA 22203-1977

10. SPONSORING/MONITORING AGENCY REPORT NUMBER

11. SUPPLEMENTARY NOTES

12a. DISTRIBUTION AVAILABILITY STATEMENT
Approved for Public Release

12b. DISTRIBUTION CODE

13. ABSTRACT *(Maximum 200 words)*

The United States Air Force Summer Research Program (USAF-SRP) is designed to introduce university, college, and technical institute faculty members, graduate students, and high school students to Air Force research. This is accomplished by the faculty members (Summer Faculty Research Program, (SFRP)), graduate students (Graduate Student Research Program (GSRP)), and high school students (High School Apprenticeship Program (HSAP)) being selected on a nationally advertised competitive basis during the summer intersession period to perform research at Air Force Research Laboratory (AFRL) Technical Directorates, Air Force Air Logistics Centers (ALC), and other AF Laboratories. This volume consists of a program overview, program management statistics, and the final technical reports from the HSAP participants at the Armstrong Laboratory.

14. SUBJECT TERMS
Air Force Research, Air Force, Engineering, Laboratories, Reports, Summer, Universities, Faculty, Graduate Student, High School Student

15. NUMBER OF PAGES

16. PRICE CODE

17. SECURITY CLASSIFICATION OF REPORT	18. SECURITY CLASSIFICATION OF THIS PAGE	19. SECURITY CLASSIFICATION OF ABSTRACT	20. LIMITATION OF ABSTRACT
Unclassified	Unclassified	Unclassified	UL

UNITED STATES AIR FORCE

SUMMER RESEARCH PROGRAM -- 1997

HIGH SCHOOL APPRENTICESHIP PROGRAM
FINAL REPORTS

VOLUME 12A

ARMSTRONG LABORATORY

RESEARCH & DEVELOPMENT LABORATORIES

5800 Uplander Way

Culver City, CA 90230-6608

Program Director, RDL
Gary Moore

Program Manager, AFOSR
Major Linda Steel-Goodwin

Program Manager, RDL
Scott Licoscos

Program Administrator, RDL
Johnetta Thompson

Program Administrator, RDL
Rebecca Kelly-Clemmons

Submitted to:

AIR FORCE OFFICE OF SCIENTIFIC RESEARCH

Bolling Air Force Base

Washington, D.C.

December 1997

HSAP FINAL REPORT TABLE OF CONTENTS i-xv

1. INTRODUCTION 1

2. PARTICIPATION IN THE SUMMER RESEARCH PROGRAM 2

3. RECRUITING AND SELECTION 3

4. SITE VISITS 4

5. HBCU/MI PARTICIPATION 4

6. SRP FUNDING SOURCES 5

7. COMPENSATION FOR PARTICIPATIONS 5

8. CONTENTS OF THE 1995 REPORT 6

APPENDICIES:

A. PROGRAM STATISTICAL SUMMARY A-1

B. SRP EVALUATION RESPONSES B-1

HSAP FINAL REPORTS

PREFACE

Reports in this volume are numbered consecutively beginning with number 1. Each report is paginated with the report number followed by consecutive page numbers, e.g., 1-1, 1-2, 1-3; 2-1, 2-2, 2-3.

Due to its length, Volume 12A is bound in two parts, 12A and 12B. Volume 12A contains #1-20. Volume 12B contains reports #21-41. The Table of Contents for Volume 12 is included in both parts.

This document is one of a set of 16 volumes describing the 1997 AFOSR Summer Research Program. The following volumes comprise the set:

VOLUME	TITLE
1	Program Management Report
	Summer Faculty Research Program (SFRP) Reports
2A & 2B	Armstrong Laboratory
3A & 3B	Phillips Laboratory
4A & 4B	Rome Laboratory
5A, 5B & 5C	Wright Laboratory
6	Arnold Engineering Development Center, U.S. Air Force Academy, Air Logistic Centers, and Wilford Hall Medical Center
	Graduate Student Research Program (GSRP) Reports
7A & 7B	Armstrong Laboratory
8	Phillips Laboratory
9	Rome Laboratory
10A & 10B	Wright Laboratory
11	Arnold Engineering Development Center, U.S. Air Force Academy, Air Logistic Centers, and Wilford Hall Medical Center
	High School Apprenticeship Program (HSAP) Reports
12A & 12B	Armstrong Laboratory
13	Phillips Laboratory
14	Rome Laboratory
15A&15B	Wright Laboratory
16	Arnold Engineering Development Center

SRP Final Report Table of Contents

Author	University/Institution Report Title	Armstrong Laboratory Directorate	Vol-Page
Brandi L Black	Red Mountain High School , Mesa , AZ	AL/HRA	12- 1
Kimberly K Blazer	Oakwood High School , Dayton , OH Repeatability Evaluation of Night Vision Goggles for Geomentric Measurements	AL/CFHV	12- 2
Kristen R Bonnema	Wayne High School , Huber Heights , OH The Effects of Individual Differences and team processes on Team Member schema similarity and task P	AL/CFHI	12- 3
David M Brogan	Robert E. Lee High School , San Antonio , TX The use of 3-Dimensional modeling in the widespread Dissemination of complex scientific data	AL/OERS	12- 4
Matthew S Caspers	MacArthur High School , San Antonio , TX A Study of the 39-40 Hz Signal to determine an index of Gravitational induced loss of Consciousness	AL/CFTF	12- 5
Elizabeth M Cobb	Belmont High School , Dayton , OH A Study fo Pitch and Contact Associated with the Opening and Closing of Vaocal Cords	AL/CFBA	12- 6
Linda E Cortina	Theodore Roosevelt High School , San Antonio , TX The Effect of Hyperbaric Oxygenation on the Mitotic Div of Prostate Cancer Cells	AL/AOH	12- 7
Maria A Evans	John Jay High School , San Antonio , TX Mercury Analysis By Cold Vapor By Atomic Absortion	AL/OEAO	12- 8
Daniel L Hardmeyer	James Madison High School , San Antonio , TX Neuropsychological Examinations For Pilots	AL/AOC	12- 9
Nafisa Islam	Centerville High School , Centerville , OH Effects of timed exposure to Dibromobenzene on /arachidonic acid levels in skin using a methyl Este	AL/OET	12- 10
Kathleen S Kao	Keystone School , San Antonio , TX Effects of Brain Temperature ofn Fatigue in Rats Due to Maziaml Exercise and Radio Frequency Radiati	ALOERB	12- 11

SRP Final Report Table of Contents

Author	University/Institution Report Title	Armstrong Laboratory Directorate	Vol-Page
Lauren M Lamm	Keystone School , San Antonio , TX Analyses of Metal Concentrations By Flame Atomic Absorption Spectroscopy	AL/OEAO	12 - 12
Evan D Large	Northwestern High School , Springfield , OH ABDAR Remote Engineerigng	AL/HRGO	12 - 13
Jason L Law	Oliver Wendell Holmes High , San Antonio , TX	AL/CFT	12 - 14
Shaun M Little	Floresville High School , Floresville , TX The role of Microsoft's directx 3 software development Kit in the rapid development of high fidelity	AL/HRCC	12 - 15
Katie E Lorenz	Chaminade-Julienne High School , Dayton , OH Visual Acutiy between 6 and 60 Meters	AL/CFHP	12 - 16
Darby M Mahan	Tippecanoe High School , Tipp City . OH	AL/CF	12 - 17
Priscilla M Medina	PSJ High School , Port Saint Joe , FL A Look into the Air Force's Computer Department	AL/EQP	12 - 18
Mark T Meiners	Dobson High , Mesa , AZ A Study of Accuracy and Response Time in Tests of Spatial Ability	AL/HRA	12 - 19
David J Miller	Texas Academy of Mathematics , Denton , TX An Analysis of Radiofrequency Radiation Induced Temperature gradients in the Rat Brain	AL/OERS	12 - 20
Joseph R Moate	Rutherford High School , PANAMA CITY , FL	AL/EQM	12 - 21
Shannon J Murphy	Keystone School , San Antonio , TX An Investigation of The Precision of the El-Mar Fixation Analysis Software Technology	AL/CFTF	12 - 22

SRP Final Report Table of Contents

Author	University/Institution Report Title	Armstrong Laboratory Directorate	Vol-Page
Katrina A Navalta	Health Careers High School , San Antonio , TX Metals Analysis by Atomic Absorption Using A Graphite Furnace	AL/OEAO	12 - 23
Christine P Pan	Health Careers High School , San Antonio , TX Spinning a Web	AL/HRCC	12 - 24
Kavitha K Reddy	Miami Valley School , Dayton , OH Study of factors Influencing Injury Potential Associated with Emergency Egress	AL/CFBE	12 - 25
Anitha K Reddy	Miami Valley School , Dayton , OH A Study of the Methodology Used In An Experiment Testing The Effect of Localizing Auditory Signals O	AL/CFBA	12 - 26
Ester I Resendiz	William Howard Taft High School , San Antonio , TX A study of the shifts in scene perception memory	AL/CFTF	12 - 27
Amanda M Scheidt	Wayne High School , Huber Heights , OH	AL/OET	12 - 28
Rachel A Sharp	William Howard Taft High School , San Antonio , TX A study of the Analysis of Urinary Benzodiazepines Using Enzyme Hydrolysis	AL/AOEL	12 - 29
James E Sovel	Rutherford High School , PANAMA CITY , FL	AL/EQA	12 - 30
Curtis J Sparks	Xenia High School , Xenia , OH ABDR:Remote Engineering Requests	AL/HRGO	12 - 31
Lauren M Spencer	Rutherford High School , PANAMA CITY , FL Alternative Training Agents Laboratory-Scale Work	AL/EQL	12 - 32
Tyler W Standage	Gilbert High School , Gilbert , AZ A Study of Accuracy and Response time in tests of Spatial Ability	AL/HRA	12 - 33

SRP Final Report Table of Contents

Author	University/Institution Report Title	Armstrong Laboratory Directorate	Vol-Page
Rachel J Strickland	A. Crawford Mosely High School , Lynn Haven , FL the Process ofd Technical Publicaation/Documentation Via Electronic Media For the Armstrong Laborato	AL/EQP	12 - 34
Lydia R Strickland	A. Crawford Mosely High School , Lynn Haven , FL Anaerobic Degradatin Products of Toluene and Laboratory MSDS Management	AL/EQL	12 - 35
Kelly C Todd	Theodore Roosevelt High School , San Antonio , TX The Effect of Hyperbaric Oxygenation on the Mitotic Div of Prostate Cancer Cells	AL/AOH	12 - 36
Tammy L Venema	Stebbins High School , Dayton , OH Cerebral hemodynamic Response to a Squat-Stand at IG	AL/CFBS	12 - 37
Max P Vilimpoc	Beavercreek High School , Dayton , OH A Study of Psycho-Physiological Effects on Brainwave Activity During Varying levels of Activity	AL/CFHP	12 - 38
Elizabeth A Walker	Theodore Roosevelt High School , San Antonio , TX The Effect of Hyperbaric Oxygenation on the Mitotic Div of Prostate Cancer Cells	AL/AOH	12 - 39
Nathan L Wright	Dayton Christian High School , Dayton , OH CG and MOI Study of Human and Manikin Segments	AL/CFBV	12 - 40
Muchieh A Yu	Theodore Roosevelt High School , San Antonio , TX Detection of Clostridium Difficile Toxins by Polymerase Chain Reaction	AL/AOE	12 - 41

SRP Final Report Table of Contents

Author	University/Institution Report Title	Phillips Laboratory Directorate	Vol-Page
Emily R Blundell	Rosamond High School , Rosamond , CA Engineering Assistant	PL/RKO	13- 1
Lauren A Ferguson	Moriarity High School , Moriarity , NM Experimental Validation of Three-Dimensional Reconstruction of Inhomogeneity Images in turbid Media	PL/LIMI	13- 2
Erica S Gerken	Manzano High School , Albuquerque , NM Chaotic Dynamics in a Nd:YAG laser	PL/LIDD	13- 3
Ngan B Kha	Chelmsford High School , North Chelmsford , MA	PL/GPOS	13- 4
Paul G Loftsgard	Quartz Hill High School , Quartz Hill , CA A Study on Optical Paternation	PL/RKS	13- 5
Fawn R Miller	Manzano High School , Albuquerque , NM A Study of Space Structure's Isolation	PL/VTV	13- 6
Amy W Mok	Newton North High School , Newtonville , MA A study of the Effect of fuel Sulfur Content on the Production of Aerosols in Aircraft Exhaust Plum	PL/GPID	13- 7
Martin P Morales	Palmdale High School , Palmdale , CA the Separations and Reacrions of Cyclohexyl Poss Compounds	PL/RKS	13- 8
David D Parker	Boron High School , Boron , CA Intranet Web Page, Design and Development	PL/RKD	13- 9
Kimberly A Robinson	Sandia High School , Albuquerque , NM Scientific Visualization methods at the Center for Plasma Theory and Computation	PL/WSQA	13- 10
Michael P Schoenfeld	NewMexico Military Ins. , Roswell , NM Study of the Effect of Heat Flow on the Performance of an Alkali Metal Thermal-to-Electric Converter	PL/VTV	13- 11

SRP Final Report Table of Contents

Author	University/Institution Report Title	Phillips Laboratory Directorate	Vol-Page
Thomas J Shea	Tehachapi High School , Tehachapi , CA A study of the Characterization of reduced Toxicity Monopropellants	PL/RKS	13 - 12
Carl W Steinbach	Lincoln-Sudbury Regional High , Sudbury , MA A Study of the Interrelation of Cloud Thickness and Cloud Liquid Water Content in Maritime Stratocum	PL/GPAB	13 - 13
Nhi T Tran	Manzano High School , Albuquerque , NM Optically Addressed Spatial Light Modulators as real-time Holographic Media	PL/LIMS	13 - 14
Jeremy L White	Sandia High School , Albuquerque , NM Constructing a Computer Model of the Space Shuttle and The Effects of Lassers on Materials in Space	PL/WSAT	13 - 15
Joanne Wu	Newton North High School , Newtonville , MA Development of Algorithms to Objectively Forecast Present Weather and Surface VisibilityBy Means fo	PL/GPAB	13 - 16
Aaron Zimmerman	Sandia High School , Albuquerque , NM IDASS ADDITIONS	PL/WSAT	13 - 17

SRP Final Report Table of Contents

Author	University/Institution Report Title	Rome Laboratory Directorate	Vol-Page
Kristine A Angell	Camden High School , Camden , NY HTML Computer Language	RL/C3CA	14- 1
Stefan M Enjem	Whitesboro Senior High School , Marcy , NY Writiing World-Wide Web (WWW) Pages	RL/IRAE	14- 2
Jared S Feldman	Rome Free Academy , Rome , NY AFOSR SUMMER 1997 INTERNSHIP	RL/ERDR	14- 3
Douglas M Feldmann	Oneida Senior High School , Oneida , NY Examination of the neaarest-neighbor rule in voice pattern Classification	RL/OCSS	14- 4
Patrick X Fitzgerald	Holland Patent High School , Holland Patent , NY The Multi-Temporal Trainable Delay(MTTD) neural Network Architecture	RL/IRDS	14- 5
Daniel E Grabski	Holland Patent High School , Holland Patent , NY RF Module Life Test System Design	RL/ERDA	14- 6
Sandra L Jablonka	Oneida Senior High School , Oneida , NY Antenna Patten Measurements Using Infrared Imaging Techniques	RL/ERST	14- 7
Colin M Kinsella	Oneida Senior High School , Oneida , NY A Study of Genetic Algorithms	RL/C3CA	14- 8
Matthew A Miling	VVS Senior High School , Verona , NY A Study of Hostile Electromagnetic Environments within Multichip Modules	RL/ERST	14- 9
Francis P Ruiz	Rome Free Academy , Rome , NY	RL/ERDD	14- 10
Roshan P Shah	Camden High School , Camden , NY Multi-Paradigmatic Programming: Intergrating Prolog and Visual Basic	RL/C3CA	14- 11

SRP Final Report Table of Contents

Author	University/Institution Report Title	Rome Laboratory Directorate	Vol-Page
Brian B Tuch	New Hartford Senior High School , New Hartford , NY A Study of the Application, Uses, and Performance of Spread Spectrum Technology in Digital Signal Pr	RL/IRAA	14 - 12
Brian S Walsh	Whitesboro High School , Whitesboro , NY Web based Computer Programming	RL/IRDS	14 - 13
David A Young	Rome Free Academy , Rome . NY Reproducing the Copper/Gold Eutectic Curve Using Computer Simulations	RLERDR	14 - 14

SRP Final Report Table of Contents

Author	University/Institution Report Title	Wright Laboratory Directorate	Vol-Page
Michael C Austin	Fairborn High School , Fairborn , OH System Administration	WL/AASE	15- 1
Gaurav K Bedi	Wayne High School , Huber Heights , OH Synthesis & Characterization of Melt Intercalated Nanocomposites	WL/MLBP	15- 2
Crystal W Bhagat	Dayton Christian High School , Dayton , OH A Study of the Effects of Varying Pulse Width and Duty Cycle On Polymer Dispersed	WL/MLPJ	15- 3
Margaret A Bruns	Dixie High School , New Lebanon , OH Surface Structure and Optical Properties of a Sensitive Snake Infared Detector	WL/DOR	15 – 4
Shannon M Campbell	Carroll High School , Dayton , OH Window Design for Laser Velocimetere Data Aquisition	WL/POTF	15- 5
Percio B Castro	Belmont High School , Dayton , OH	WL/AACF	15- 6
Jason R Caudill	Fairborn High School , Fairborn , OH 2 PhotonIonization and Disassociative Attachment of Eletrons To Excited Molcules	WL/POOX	15- 7
Bernardo V Cavour	Fairmont High School , Kettering , OH High School Appentice Program Accomplishments	WL/FIBT	15- 8
Christopher R Clark	Niceville Senior High School , Niceville , FL Neural Networks & Digital Image Processing	WL/MNGA	15- 9
Aaron Davis	Niceville Senior High School , Niceville , FL Electronic Studies of Polypyrrole Films Grown on Semiconductor Wafers	WL/MNMF	15- 10
Debbie L Dressler	Centerville High School , Centerville , OH Traction Models	WL/POSL	15- 11

SRP Final Report Table of Contents

Author	University/Institution Report Title	Wright Laboratory Directorate	Vol-Page
Molly M Flanagan	Chaminade-Julienne High School , Dayton , OH	WL/POTF	15- 12
Landon W Frymire	Laurel Hill High School , Laurel Hill , FL Technical Report Library User's Manual	WL/MNAV	15- 13
Allison D Gadd	Carroll High School , Dayton , OH	WL/FIVS	15- 14
Matthew A Gerding	Fairborn High School , Fairborn , OH The Study of the Electro-Optic Coefficients of DR-1 and Dans	WL/MLPO	15- 15
Jon M Graham	Carroll High School , Riverside , OH The Flight Dynaics Lab	WL/DOR	15 – 16
Trenton Hamilton	Rocky Bayou Christian School , Niceville , FL Cast Ductile Iron (CDI) (A Controlled Fragmentation Study)	WL/MNM	15- 17
Neil Harrison	Ft Walton Beach High SC , Ft Walton BEACH , FL Comparison of Experimental Penetration Data with Various Penetration Prediction Methodologies	WL/MNM	15- 18
Angela C Helm	Carroll High School , Dayton , OH	WL/AACT	15- 19
Anna S Hill	Carroll High School , Dayton , OH Window design for Laser velocimeter Data Aquisition	WL/POTF	15- 20
Erek A Kasse	Bellbrook High School , Bellbrook , OH Friction and Solid Lubricants	WL/MLBT	15- 21
Maria Lee	Wayne High School , Huber Heights , OH the Database Design for a Configuration Mnagement Library	WL/AAST	15- 22

SRP Final Report Table of Contents

Author	University/Institution Report Title	Wright Laboratory Directorate	Vol-Page
Colleen A Lefevre	Lehman High School , Sidney , OH the Effect of Chain Lengths on Bond Orders and Geometry in Simple Cyanines0	WL/DOR	15 – 23
John P Lightle	Tippecanoe High School , Tipp City , OH A Study of two methods for Predicting fin Center of Pressure position	WL/FIGC	15 - 24
Alexander R Lippert	Choctawhatchee High School , Ft Walton BEACH , FL Nanoparticle Doped Organic Electronic Junction Devices	WL/MNMF	15 - 25
Marcus W Mac Nealy	Chaminade-Julienne High School , Dayton , OH Web Page Design to Display Infrared Imagery	WL/AACA	15 - 26
Jonathan S Mah	Centerville High School , Centerville , OH The Integration of Circuit synthesis and Schematic Programs Using Prolog, ad Evaluatation of a Graph	WL/AASH	15 - 27
David Mandel	Niceville Senior High School , Niceville , FL Terminal Ballistics Data Acquisition & Analysis	WL/MNM	15 - 28
Michele V Manuel	Crestview High School , Crestview , FL The Mechanical & Metallurgical Characterization of Liquid Phase Sintered Tungsten Alloyw	WL/MNM	15 - 29
Lori M Marshall	Carroll High School , Dayton , OH A Study of Chemical Vapor Depositiion and Pulse Laser Deposition	WL/DOR	15 – 30
Terrence J McGregor	Fairborn High School , Fairborn , OH Chain Armor Ballistic Testing : Establishing the Ballistic Limit	WL/FIVS	15 - 31
Deborah S Mills	West Liberty-Dalem Jr./Sr. High School , West Liberty , OH A Summer at Wright Patterson Air Force Base	WL/DOR	15 – 32
Ryan M Moore	Centerville High School . Centerville , OH Studies in Computational Chemistry and Biomimetics	WL/MLPJ	15 - 33

SRP Final Report Table of Contents

Author	University/Institution Report Title	Wright Laboratory Directorate	Vol-Page
Jeremy M Mount	Bellbrook High School , Bellbrook , OH	WL/FIIB	15 - 34
John D Murchison	Ft Walton Beach High SC , Ft Walton BEACH , FL Methodology for the Creation of a Randomized Shot-Line Generator	WL/MNSA	15 - 35
Disha J Patel	Fairmont High School , Kettering , OH	WL/AACT	15 - 36
Neill W Perry	Crestview High School , Crestview , FL Empirical Characterization of Mid-Infrared Photodetectors for a Dual-Wavelength Ladar System	WL/MNGS	15 - 37
Kathleen A Pirog	Niceville Senior High School , Niceville , FL The Implications of Photomodeler on the Generation of 3D Models	WL/MNGA	15 - 38
Nathan A Power	Heritage Christian School , Xenia , OH The World Wide Web and Hyper Text Markup Language	WL/AAOP	15 - 39
Shaun G Power	Heritage Christian School , Xenia , OH	WL/AACI	15 - 40
Josh J Pressnell	Fairmont High School , Kettering , OH A Study n Internet Programming and World Wide Web Publishing	WL/AACN	15 - 41
Stephanie M Puterbaugh	Beavercreek High School , Dayton , OH Initial Experimental evaluation of an Axial Groove Heat Pipe for Aircraft Applications	WL/POOS	15 - 42
Matthew R Rabe	Carroll High School , Dayton , OH	WL/POSC	15 - 43
Kristan M Raymond	Ft Walton Beach High SC , Ft Walton BEACH , FL Immersion Corrosion Testing of Tungsten Heavy-Metal Alloys	WL/MNSE	15 - 44

SRP Final Report Table of Contents

Author	University/Institution Report Title	Wright Laboratory Directorate	Vol-Page
David S Revill	Choctawhatchee High School , Ft Walton BEACH , FL Verification of State of Chemical Equations & Generation of Textures for Phenomenology Modeling	WL/MNGA	15 - 45
Harris T Schneiderman	Miami Valley School , Dayton , OH A Study of the capabilities of computational fluid dynamics technology to simulate the flight perfor	WL/FIMC	15 - 46
Nicole L Speelman	Stebbins High School , Dayton , OH Development and Application of Materials Characterization web Site	WL/MLIM	15 - 47
Kari D Sutherland	Dayton Christian High School , Dayton , OH A Study of the Effects of the Performance of Polymer Dispersed Liquid Crystal Holographic Gratings w	WL/MLPJ	15 - 48
Christine M Task	Stebbins High School , Dayton , OH	WL/MLIM	15 - 49
Rebecca M Thien	Chaminade-Julienne High School , Dayton , OH A Study of the Corrosion Resistence of Sol-Gels	WL/DOR	15 – 50
Jonathan D Tidwell	Rocky Bayou Christian School , Niceville . FL Data Reduction for Blast Arena Lethality Enhancement	WL/MNM	15 - 51
Robert L Todd	Carroll High School , Dayton , OH The Characterization of A Scud Fragment	WL/MLLI	15 - 52
Elizabeth A Walker	Niceville Senior High School , Niceville , FL Concept vs Reality:Developing a Theoretical Sequencing Program for Shock Induced Combustion	WL//MNA	15 - 53
Darren C Wells	Bellbrook High School , Bellbrook , OH A Study of the Tension and Shear Strength of Bidirectonal Epoxy-Resin Composites	WL/DOR	15 – 54
Tuan P Yang	Choctawhatchee High School , Ft Walton BEACH , FL Thermal Characterization of the 1,3,3-Trinitroazetidine (ADNAZ) Binary Mixture	WL/MNM	15 - 56

SRP Final Report Table of Contents

Author	University/Institution Report Title	Arnold Engineering Development Center Directorate	Vol-Page
Karllee R Barton	Coffee County Central High , Manchester , TN A Math Model of the Flow Characteristics of The J4 gaseous Nitrogen Repress Systems	AEDC	16 - 1
Jason G Bradford	Franklin County Senior High School , Winchester , TN Design of A Serchable Data Retreving Web Based Page	AEDC	16 - 2
James R Brandon	Coffee County Central High , Manchester , TN	AEDC	16 - 3
Barbara E King	Franklin County Senior High School , Winchester , TN Assessment of Microwave Horn Antenna Radiation Pattern	AEDC	16 - 4
Kaitrin T Mahar	Coffee County Central High , Manchester , TN Analysis of DWSG Characterizations	AEDC	16 - 5
Steven W Marlowe	Franklin County Senior High School , Winchester , TN Writing a Cost Estimate Program Using The Java Programming Language	AEDC	16 - 6
Michael R Munn	Coffee County Central High , Manchester , TN Construction of a Graphical User Interface for the Thermally Perfect Gas Code	AEDC	16 - 7
Jason A Myers	Coffee County Central High , Manchester , TN Intranet Development Problem with Powerpoint	AEDC	16 - 8
James P Nichols	Tullahoma High School , Tullahoma , TN Assessment of Reflecting Microwave Horn Data Within A Plasma	AEDC	16 - 9
James M Perryman	Shelbyville Central High School , Shelbyville , TN Computer Manipulation of Raman Spectroscopy Test	AEDC	16 - 10
Kristin A Pierce	Coffee County Central High , Manchester , TN Evaluation of Arc Heater Performance and Operational Stability	AEDC	16 - 11

Author	University/Institution Report Title	Arnold Engineering Development Center Directorate	Vol-Page
Daniel M Thompson	Shelbyville Central High School , Shelbyville , TN Maintenance of Facilities	AEDC	16- 12
James R Williamson	Franklin County Senior High School , Winchester , TN Access Conversions	AEDC	16- 13

1. INTRODUCTION

The Summer Research Program (SRP), sponsored by the Air Force Office of Scientific Research (AFOSR), offers paid opportunities for university faculty, graduate students, and high school students to conduct research in U.S. Air Force research laboratories nationwide during the summer.

Introduced by AFOSR in 1978, this innovative program is based on the concept of teaming academic researchers with Air Force scientists in the same disciplines using laboratory facilities and equipment not often available at associates' institutions.

The Summer Faculty Research Program (SFRP) is open annually to approximately 150 faculty members with at least two years of teaching and/or research experience in accredited U.S. colleges, universities, or technical institutions. SFRP associates must be either U.S. citizens or permanent residents.

The Graduate Student Research Program (GSRP) is open annually to approximately 100 graduate students holding a bachelor's or a master's degree; GSRP associates must be U.S. citizens enrolled full time at an accredited institution.

The High School Apprentice Program (HSAP) annually selects about 125 high school students located within a twenty mile commuting distance of participating Air Force laboratories.

AFOSR also offers its research associates an opportunity, under the Summer Research Extension Program (SREP), to continue their AFOSR-sponsored research at their home institutions through the award of research grants. In 1994 the maximum amount of each grant was increased from $20,000 to $25,000, and the number of AFOSR-sponsored grants decreased from 75 to 60. A separate annual report is compiled on the SREP.

The numbers of projected summer research participants in each of the three categories and SREP "grants" are usually increased through direct sponsorship by participating laboratories.

AFOSR's SRP has well served its objectives of building critical links between Air Force research laboratories and the academic community. opening avenues of communications and forging new research relationships between Air Force and academic technical experts in areas of national interest, and strengthening the nation's efforts to sustain careers in science and engineering. The success of the SRP can be gauged from its growth from inception (see Table 1) and from the favorable responses the 1997 participants expressed in end-of-tour SRP evaluations (Appendix B).

AFOSR contracts for administration of the SRP by civilian contractors. The contract was first awarded to Research & Development Laboratories (RDL) in September 1990. After completion of the

1990 contract, RDL (in 1993) won the recompetition for the basic year and four 1-year options.

2. PARTICIPATION IN THE SUMMER RESEARCH PROGRAM

The SRP began with faculty associates in 1979; graduate students were added in 1982 and high school students in 1986. The following table shows the number of associates in the program each year.

YEAR	SRP Participation, by Year			TOTAL
	SFRP	GSRP	HSAP	
1979	70			70
1980	87			87
1981	87			87
1982	91	17		108
1983	101	53		154
1984	152	84		236
1985	154	92		246
1986	158	100	42	300
1987	159	101	73	333
1988	153	107	101	361
1989	168	102	103	373
1990	165	121	132	418
1991	170	142	132	444
1992	185	121	159	464
1993	187	117	136	440
1994	192	117	133	442
1995	190	115	137	442
1996	188	109	138	435
1997	148	98	140	427

Beginning in 1993, due to budget cuts, some of the laboratories weren't able to afford to fund as many associates as in previous years. Since then, the number of funded positions has remained fairly constant at a slightly lower level.

3. RECRUITING AND SELECTION

The SRP is conducted on a nationally advertised and competitive-selection basis. The advertising for faculty and graduate students consisted primarily of the mailing of 8,000 52-page SRP brochures to chairpersons of departments relevant to AFOSR research and to administrators of grants in accredited universities, colleges, and technical institutions. Historically Black Colleges and Universities (HBCUs) and Minority Institutions (MIs) were included. Brochures also went to all participating USAF laboratories, the previous year's participants, and numerous individual requesters (over 1000 annually).

RDL placed advertisements in the following publications: *Black Issues in Higher Education, Winds of Change,* and *IEEE Spectrum.* Because no participants list either *Physics Today* or *Chemical & Engineering News* as being their source of learning about the program for the past several years, advertisements in these magazines were dropped, and the funds were used to cover increases in brochure printing costs.

High school applicants can participate only in laboratories located no more than 20 miles from their residence. Tailored brochures on the HSAP were sent to the head counselors of 180 high schools in the vicinity of participating laboratories, with instructions for publicizing the program in their schools. High school students selected to serve at Wright Laboratory's Armament Directorate (Eglin Air Force Base, Florida) serve eleven weeks as opposed to the eight weeks normally worked by high school students at all other participating laboratories.

Each SFRP or GSRP applicant is given a first, second, and third choice of laboratory. High school students who have more than one laboratory or directorate near their homes are also given first, second, and third choices.

Laboratories make their selections and prioritize their nominees. AFOSR then determines the number to be funded at each laboratory and approves laboratories' selections.

Subsequently, laboratories use their own funds to sponsor additional candidates. Some selectees do not accept the appointment, so alternate candidates are chosen. This multi-step selection procedure results in some candidates being notified of their acceptance after scheduled deadlines. The total applicants and participants for 1997 are shown in this table.

1997 Applicants and Participants			
PARTICIPANT CATEGORY	TOTAL APPLICANTS	SELECTEES	DECLINING SELECTEES
SFRP	490	188	32
(HBCU/MI)	(0)	(0)	(0)
GSRP	202	98	9
(HBCU/MI)	(0)	(0)	(0)
HSAP	433	140	14
TOTAL	1125	426	55

4. SITE VISITS

During June and July of 1997, representatives of both AFOSR/NI and RDL visited each participating laboratory to provide briefings, answer questions. and resolve problems for both laboratory personnel and participants. The objective was to ensure that the SRP would be as constructive as possible for all participants. Both SRP participants and RDL representatives found these visits beneficial. At many of the laboratories, this was the only opportunity for all participants to meet at one time to share their experiences and exchange ideas.

5. HISTORICALLY BLACK COLLEGES AND UNIVERSITIES AND MINORITY INSTITUTIONS (HBCU/MIs)

Before 1993, an RDL program representative visited from seven to ten different HBCU/MIs annually to promote interest in the SRP among the faculty and graduate students. These efforts were marginally effective, yielding a doubling of HBCI/MI applicants. In an effort to achieve AFOSR's goal of 10% of all applicants and selectees being HBCU/MI qualified, the RDL team decided to try other avenues of approach to increase the number of qualified applicants. Through the combined efforts of the AFOSR Program Office at Bolling AFB and RDL, two very active minority groups were found, HACU (Hispanic American Colleges and Universities) and AISES (American Indian Science and Engineering Society). RDL is in communication with representatives of each of these organizations on a monthly basis to keep up with the their activities and special events. Both organizations have widely-distributed magazines/quarterlies in which RDL placed ads.

Since 1994 the number of both SFRP and GSRP HBCU/MI applicants and participants has increased ten-fold, from about two dozen SFRP applicants and a half dozen selectees to over 100 applicants and two dozen selectees, and a half-dozen GSRP applicants and two or three selectees to 18 applicants and 7 or 8 selectees. Since 1993, the SFRP had a two-fold applicant increase and a two-fold selectee increase. Since 1993, the GSRP had a three-fold applicant increase and a three to four-fold increase in selectees.

In addition to RDL's special recruiting efforts, AFOSR attempts each year to obtain additional funding or use leftover funding from cancellations the past year to fund HBCU/MI associates. This year, 5 HBCU/MI SFRPs declined after they were selected (and there was no one qualified to replace them with). The following table records HBCU/MI participation in this program.

SRP HBCU/MI Participation, By Year				
YEAR	SFRP		GSRP	
	Applicants	Participants	Applicants	Participants
1985	76	23	15	11
1986	70	18	20	10
1987	82	32	32	10
1988	53	17	23	14
1989	39	15	13	4
1990	43	14	17	3
1991	42	13	8	5
1992	70	13	9	5
1993	60	13	6	2
1994	90	16	11	6
1995	90	21	20	8
1996	119	27	18	7

6. SRP FUNDING SOURCES

Funding sources for the 1997 SRP were the AFOSR-provided slots for the basic contract and laboratory funds. Funding sources by category for the 1997 SRP selected participants are shown here.

1997 SRP FUNDING CATEGORY	SFRP	GSRP	HSAP
AFOSR Basic Allocation Funds	141	89	123
USAF Laboratory Funds	48	9	17
HBCU/MI By AFOSR (Using Procured Addn'l Funds)	0	0	N/A
TOTAL	9	98	140

SFRP - 188 were selected, but thirty two canceled too late to be replaced.
GSRP - 98 were selected, but nine canceled too late to be replaced.
HSAP - 140 were selected, but fourteen canceled too late to be replaced.

7. COMPENSATION FOR PARTICIPANTS

Compensation for SRP participants, per five-day work week, is shown in this table.

1997 SRP Associate Compensation

PARTICIPANT CATEGORY	1991	1992	1993	1994	1995	1996	1997
Faculty Members	$690	$718	$740	$740	$740	$770	$770
Graduate Student (Master's Degree)	$425	$442	$455	$455	$455	$470	$470
Graduate Student (Bachelor's Degree)	$365	$380	$391	$391	$391	$400	$400
High School Student (First Year)	$200	$200	$200	$200	$200	$200	$200
High School Student (Subsequent Years)	$240	$240	$240	$240	$240	$240	$240

The program also offered associates whose homes were more than 50 miles from the laboratory an expense allowance (seven days per week) of $50/day for faculty and $40/day for graduate students. Transportation to the laboratory at the beginning of their tour and back to their home destinations at the end was also reimbursed for these participants. Of the combined SFRP and GSRP associates, 65 % (194 out of 286) claimed travel reimbursements at an average round-trip cost of $776.

Faculty members were encouraged to visit their laboratories before their summer tour began. All costs of these orientation visits were reimbursed. Forty-three percent (85 out of 188) of faculty associates took orientation trips at an average cost of $388. By contrast, in 1993, 58 % of SFRP associates took

orientation visits at an average cost of $685; that was the highest percentage of associates opting to take an orientation trip since RDL has administered the SRP. and the highest average cost of an orientation trip. These 1993 numbers are included to show the fluctuation which can occur in these numbers for planning purposes.

Program participants submitted biweekly vouchers countersigned by their laboratory research focal point, and RDL issued paychecks so as to arrive in associates' hands two weeks later.

This is the second year of using direct deposit for the SFRP and GSRP associates. The process went much more smoothly with respect to obtaining required information from the associates, only 7% of the associates' information needed clarification in order for direct deposit to properly function as opposed to 10% from last year. The remaining associates received their stipend and expense payments via checks sent in the US mail.

HSAP program participants were considered actual RDL employees, and their respective state and federal income tax and Social Security were withheld from their paychecks. By the nature of their independent research. SFRP and GSRP program participants were considered to be consultants or independent contractors. As such, SFRP and GSRP associates were responsible for their own income taxes, Social Security, and insurance.

8. CONTENTS OF THE 1997 REPORT

The complete set of reports for the 1997 SRP includes this program management report (Volume 1) augmented by fifteen volumes of final research reports by the 1997 associates, as indicated below:

1997 SRP Final Report Volume Assignments

LABORATORY	SFRP	GSRP	HSAP
Armstrong	2	7	12
Phillips	3	8	13
Rome	4	9	14
Wright	5A, 5B	10	15
AEDC, ALCs, WHMC	6	11	16

APPENDIX A – PROGRAM STATISTICAL SUMMARY

A. Colleges/Universities Represented

Selected SFRP associates represented 169 different colleges, universities, and institutions. GSRP associates represented 95 different colleges, universities, and institutions.

B. States Represented

SFRP -Applicants came from 47 states plus Washington D.C. Selectees represent 44 states.

GSRP - Applicants came from 44 states. Selectees represent 32 states.

HSAP - Applicants came from thirteen states. Selectees represent nine states.

Total Number of Participants	
SFRP	189
GSRP	97
HSAP	140
TOTAL	426

Degrees Represented			
	SFRP	GSRP	TOTAL
Doctoral	184	0	184
Master's	2	41	43
Bachelor's	0	56	56
TOTAL	186	97	298

SFRP Academic Titles	
Assistant Professor	64
Associate Professor	70
Professor	40
Instructor	0
Chairman	1
Visiting Professor	1
Visiting Assoc. Prof.	1
Research Associate	9
TOTAL	186

Source of Learning About the SRP		
Category	Applicants	Selectees
Applied/participated in prior years	28%	34%
Colleague familiar with SRP	19%	16%
Brochure mailed to institution	23%	17%
Contact with Air Force laboratory	17%	23%
IEEE Spectrum	2%	1%
BIIHE	1%	1%
Other source	10%	8%
TOTAL	100%	100%

APPENDIX B – SRP EVALUATION RESPONSES

1. OVERVIEW

Evaluations were completed and returned to RDL by four groups at the completion of the SRP. The number of respondents in each group is shown below.

Table B-1. Total SRP Evaluations Received

Evaluation Group	Responses
SFRP & GSRPs	275
HSAPs	113
USAF Laboratory Focal Points	84
USAF Laboratory HSAP Mentors	6

All groups indicate unanimous enthusiasm for the SRP experience.

The summarized recommendations for program improvement from both associates and laboratory personnel are listed below:

A. Better preparation on the labs' part prior to associates' arrival (i.e., office space, computer assets, clearly defined scope of work).

B. Faculty Associates suggest higher stipends for SFRP associates.

C. Both HSAP Air Force laboratory mentors and associates would like the summer tour extended from the current 8 weeks to either 10 or 11 weeks; the groups state it takes 4-6 weeks just to get high school students up-to-speed on what's going on at laboratory. (Note: this same argument was used to raise the faculty and graduate student participation time a few years ago.)

2. 1997 USAF LABORATORY FOCAL POINT (LFP) EVALUATION RESPONSES

The summarized results listed below are from the 84 LFP evaluations received.

1. LFP evaluations received and associate preferences:

Table B-2. Air Force LFP Evaluation Responses (By Type)

		How Many Associates Would You Prefer To Get ? (% Response)											
		SFRP				GSRP (w/Univ Professor)				GSRP (w/o Univ Professor)			
Lab	Evals Recv'd	0	1	2	3+	0	1	2	3+	0	1	2	3+
AEDC	0	-	-	-	-	-	-	-	-	-	-	-	-
WHMC	0	-	-	-	-	-	-	-	-	-	-	-	-
AL	7	28	28	28	14	54	14	28	0	86	0	14	0
USAFA	1	0	100	0	0	100	0	0	0	0	100	0	0
PL	25	40	40	16	4	88	12	0	0	84	12	4	0
RL	5	60	40	0	0	80	10	0	0	100	0	0	0
WL	46	30	43	20	6	78	17	4	0	93	4	2	0
Total	84	32%	50%	13%	5%	80%	11%	6%	0%	73%	23%	4%	0%

LFP Evaluation Summary. The summarized responses, by laboratory, are listed on the following page. LFPs were asked to rate the following questions on a scale from 1 (below average) to 5 (above average).

2. LFPs involved in SRP associate application evaluation process:
   a. Time available for evaluation of applications:
   b. Adequacy of applications for selection process:
3. Value of orientation trips:
4. Length of research tour:
5. a. Benefits of associate's work to laboratory:
   b. Benefits of associate's work to Air Force:
6. a. Enhancement of research qualifications for LFP and staff:
   b. Enhancement of research qualifications for SFRP associate:
   c. Enhancement of research qualifications for GSRP associate:
7. a. Enhancement of knowledge for LFP and staff:
   b. Enhancement of knowledge for SFRP associate:
   c. Enhancement of knowledge for GSRP associate:
8. Value of Air Force and university links:
9. Potential for future collaboration:
10. a. Your working relationship with SFRP:
    b. Your working relationship with GSRP:
11. Expenditure of your time worthwhile:

(Continued on next page)

12. Quality of program literature for associate:
13. a. Quality of RDL's communications with you:
    b. Quality of RDL's communications with associates:
14. Overall assessment of SRP:

Table B-3. Laboratory Focal Point Reponses to above questions

	AEDC	*AL*	*USAFA*	*PL*	*RL*	*WHMC*	*WL*
# Evals Recv'd	0	7	1	14	5	0	46
Question #							
2	-	86 %	0 %	88 %	80 %	-	85 %
2a	-	4.3	n/a	3.8	4.0	-	3.6
2b	-	4.0	n/a	3.9	4.5	-	4.1
3	-	4.5	n/a	4.3	4.3	-	3.7
4	-	4.1	4.0	4.1	4.2	-	3.9
5a	-	4.3	5.0	4.3	4.6	-	4.4
5b	-	4.5	n/a	4.2	4.6	-	4.3
6a	-	4.5	5.0	4.0	4.4	-	4.3
6b	-	4.3	n/a	4.1	5.0	-	4.4
6c	-	3.7	5.0	3.5	5.0	-	4.3
7a	-	4.7	5.0	4.0	4.4	-	4.3
7b	-	4.3	n/a	4.2	5.0	-	4.4
7c	-	4.0	5.0	3.9	5.0	-	4.3
8	-	4.6	4.0	4.5	4.6	-	4.3
9	-	4.9	5.0	4.4	4.8	-	4.2
10a	-	5.0	n/a	4.6	4.6	-	4.6
10b	-	4.7	5.0	3.9	5.0	-	4.4
11	-	4.6	5.0	4.4	4.8	-	4.4
12	-	4.0	4.0	4.0	4.2	-	3.8
13a	-	3.2	4.0	3.5	3.8	-	3.4
13b	-	3.4	4.0	3.6	4.5	-	3.6
14	-	4.4	5.0	4.4	4.8	-	4.4

3. 1997 SFRP & GSRP EVALUATION RESPONSES

The summarized results listed below are from the 257 SFRP/GSRP evaluations received.

Associates were asked to rate the following questions on a scale from 1 (below average) to 5 (above average) - by Air Force base results and over-all results of the 1997 evaluations are listed after the questions.

1. The match between the laboratories research and your field:
2. Your working relationship with your LFP:
3. Enhancement of your academic qualifications:
4. Enhancement of your research qualifications:
5. Lab readiness for you: LFP, task, plan:
6. Lab readiness for you: equipment, supplies, facilities:
7. Lab resources:
8. Lab research and administrative support:
9. Adequacy of brochure and associate handbook:
10. RDL communications with you:
11. Overall payment procedures:
12. Overall assessment of the SRP:
13. a. Would you apply again?
    b. Will you continue this or related research?
14. Was length of your tour satisfactory?
15. Percentage of associates who experienced difficulties in finding housing:
16. Where did you stay during your SRP tour?
    a. At Home:
    b. With Friend:
    c. On Local Economy:
    d. Base Quarters:
17. Value of orientation visit:
    a. Essential:
    b. Convenient:
    c. Not Worth Cost:
    d. Not Used:

SFRP and GSRP associate's responses are listed in tabular format on the following page.

Table B-4. 1997 SFRP & GSRP Associate Responses to SRP Evaluation

	Arnold	Brooks	Edwards	Eglin	Griffis	Hanscom	Kelly	Kirtland	Lackland	Robins	Tyndall	WPAFB	average
# res	6	48	6	14	31	19	3	32	1	2	10	85	257
1	4.8	4.4	4.6	4.7	4.4	4.9	4.6	4.6	5.0	5.0	4.0	4.7	4.6
2	5.0	4.6	4.1	4.9	4.7	4.7	5.0	4.7	5.0	5.0	4.6	4.8	4.7
3	4.5	4.4	4.0	4.6	4.3	4.2	4.3	4.4	5.0	5.0	4.5	4.3	4.4
4	4.3	4.5	3.8	4.6	4.4	4.4	4.3	4.6	5.0	4.0	4.4	4.5	4.5
5	4.5	4.3	3.3	4.8	4.4	4.5	4.3	4.2	5.0	5.0	3.9	4.4	4.4
6	4.3	4.3	3.7	4.7	4.4	4.5	4.0	3.8	5.0	5.0	3.8	4.2	4.2
7	4.5	4.4	4.2	4.8	4.5	4.3	4.3	4.1	5.0	5.0	4.3	4.3	4.4
8	4.5	4.6	3.0	4.9	4.4	4.3	4.3	4.5	5.0	5.0	4.7	4.5	4.5
9	4.7	4.5	4.7	4.5	4.3	4.5	4.7	4.3	5.0	5.0	4.1	4.5	4.5
10	4.2	4.4	4.7	4.4	4.1	4.1	4.0	4.2	5.0	4.5	3.6	4.4	4.3
11	3.8	4.1	4.5	4.0	3.9	4.1	4.0	4.0	3.0	4.0	3.7	4.0	4.0
12	5.7	4.7	4.3	4.9	4.5	4.9	4.7	4.6	5.0	4.5	4.6	4.5	4.6
Numbers below are percentages													
13a	83	90	83	93	87	75	100	81	100	100	100	86	87
13b	100	89	83	100	94	98	100	94	100	100	100	94	93
14	83	96	100	90	87	80	100	92	100	100	70	84	88
15	17	6	0	33	20	76	33	25	0	100	20	8	39
16a	-	26	17	9	38	23	33	4	-	-	-	30	
16b	100	33	-	40	-	8	-	-	-	-	36	2	
16c	-	41	83	40	62	69	67	96	100	100	64	68	
16d	-	-	-	-	-	-	-	-	-	-	-	0	
17a	-	33	100	17	50	14	67	39	-	50	40	31	35
17b	-	21	-	17	10	14	-	24	-	50	20	16	16
17c	-	-	-	-	10	7	-	-	-	-	-	2	3
17d	100	46	-	66	30	69	33	37	100	-	40	51	46

4. 1997 USAF LABORATORY HSAP MENTOR EVALUATION RESPONSES

Not enough evaluations received (5 total) from Mentors to do useful summary.

5. 1997 HSAP EVALUATION RESPONSES

The summarized results listed below are from the 113 HSAP evaluations received.

HSAP apprentices were asked to rate the following questions on a scale from 1 (below average) to 5 (above average)

1. Your influence on selection of topic/type of work.
2. Working relationship with mentor, other lab scientists.
3. Enhancement of your academic qualifications.
4. Technically challenging work.
5. Lab readiness for you: mentor, task, work plan, equipment.
6. Influence on your career.
7. Increased interest in math/science.
8. Lab research & administrative support.
9. Adequacy of RDL's Apprentice Handbook and administrative materials.
10. Responsiveness of RDL communications.
11. Overall payment procedures.
12. Overall assessment of SRP value to you.
13. Would you apply again next year? Yes (92 %)
14. Will you pursue future studies related to this research? Yes (68 %)
15. Was Tour length satisfactory? Yes (82 %)

	Arnold	Brooks	Edwards	Eglin	Griffiss	Hanscom	Kirtland	Tyndall	WPAFB	Totals
# resp	5	19	7	15	13	2	7	5	40	113
1	2.8	3.3	3.4	3.5	3.4	4.0	3.2	3.6	3.6	3.4
2	4.4	4.6	4.5	4.8	4.6	4.0	4.4	4.0	4.6	4.6
3	4.0	4.2	4.1	4.3	4.5	5.0	4.3	4.6	4.4	4.4
4	3.6	3.9	4.0	4.5	4.2	5.0	4.6	3.8	4.3	4.2
5	4.4	4.1	3.7	4.5	4.1	3.0	3.9	3.6	3.9	4.0
6	3.2	3.6	3.6	4.1	3.8	5.0	3.3	3.8	3.6	3.7
7	2.8	4.1	4.0	3.9	3.9	5.0	3.6	4.0	4.0	3.9
8	3.8	4.1	4.0	4.3	4.0	4.0	4.3	3.8	4.3	4.2
9	4.4	3.6	4.1	4.1	3.5	4.0	3.9	4.0	3.7	3.8
10	4.0	3.8	4.1	3.7	4.1	4.0	3.9	2.4	3.8	3.8
11	4.2	4.2	3.7	3.9	3.8	3.0	3.7	2.6	3.7	3.8
12	4.0	4.5	4.9	4.6	4.6	5.0	4.6	4.2	4.3	4.5
Numbers below are percentages										
13	60%	95%	100%	100%	85%	100%	100%	100%	90%	92%
14	20%	80%	71%	80%	54%	100%	71%	80%	65%	68%
15	100%	70%	71%	100%	100%	50%	86%	60%	80%	82%

Associate did not participate in the program.

Repeatability Evaluation of Night Vision Goggles for Geometric Measurements

Kimberly Blazer
Oakwood High School
1400 Far Hills Ave.
Dayton, OH 45419

Katie Lorenz
Chaminade-Julienne High School
505 S. Ludlow St.
Dayton, OH 45402

Final Report for:
High School Apprentice Program
Armstrong Laboratory

Sponsored by:
Air Force Office of Scientific Research
Bolling Air Force Base, DC

and

Armstrong Laboratory

August 1997

Repeatability Evaluation of Night Vision Goggles for Geometric Measurements

Kimberly Blazer
Oakwood High School

Katie Lorenz
Chaminade-Julienne High School

Abstract

A repeatability evaluation of an apparatus for testing NVG geometric distortion was performed. Multiple measurements were taken in order to quantify the margin of error in the equipment and procedure. Two pairs of NVGs were tested on a rotating scan table equipped with a collimated light source, CCD camera, frame grabber, and viewing monitor. Means and 95% confidence intervals were computed for each NVG channel for measures of magnification, image rotation, and "S" distortion.

Repeatability Evaluation of Night Vision Goggles for Geometric Measurements

Kimberly Blazer
Katie Lorenz

Introduction

Night vision goggles are used in low light environments with light levels that range from starlight to half moon. Binocular goggles are comprised of two viewing channels/oculars. These channels include an objective lens, light amplifier, and eye piece. The light amplifier tube, which consists of photocathode tube, micro channel plate, and a phosphor screen, is located in between the objective lens and the eye piece. The available light enters the objective lens and then is multiplied 20,000 or 30,000 times in the light amplifier tube allowing more light to reach the eye. In the amplifying process, the optics focus the photons of light on the cathode and convert them to photoelectrons. This number is proportional to the input photons. This photoelectron image is focused on the micro channel plate, where the light is amplified while maintaining the information. The intensified image is then transferred to the phosphor screen which gives a green appearance to the image.

The scan table in the Night Vision Operations facility of Armstrong Laboratory, which tests NVGs, is the only apparatus of its kind. Because it is a unique set-up, it is necessary to quantify the reliability of the measurements by computing confidence intervals. The scan table is used for measurements of magnification, an increase or decrease in size; image rotation, rotation of the image as a whole; and "S" distortion, distortion within the image. As new goggles are tested, it's crucial to find fairly accurate values of magnification, image rotation, and "S" distortion, to ensure that there are no manufacturing defects. If the tests result in varying data, it's still important to be able to quantify confidence intervals so users are aware of the potential error in the system.

Methodology

The experiment included multiple measurements over a three week period. Geometric tests were conducted on both the left and right channels of two pairs of NVGs. The procedure was designed to measure magnification, image rotation, and "S" distortion, all of which arise out of the geometric aspects of the NVG image. These three parameters can be derived from the same data, so a single measurement procedure was developed to quantify them.

In the magnification analysis, horizontal errors are subtracted from the input angle at which the data point was measured. The difference is plotted as a function of input angle. A least-squares reduction to the central 80% of the data is performed to obtain a straight line, approximating the data. The slope of the line is the magnification. The system magnification is usually around one, signifying the absence of any magnification. The image produced is, therefore, its original size when viewed through the goggles.

Image rotation takes the whole image and rotates it due to the twisting of the fiber optic bundles within the NVG. A discrepancy between image rotation in the two individual channels causes a distorted picture not allowing the two images to fuse properly. A discrepancy of no more than one degree is permitted by Air Force spec. The analysis of image rotation involves plotting the vertical movements of a pinhole image as a function of input angle at which the data point was measured. To best fit a straight line, a least-squares reduction is performed. The slope of this line is the image rotation. Values in this area tended to vary somewhat.

Distortion within the image itself is referred to as "S" distortion. To obtain this value, the constant average rotation is subtracted from the image rotation data. This leaves only the vertical variations. The extreme of variation above and below the straight line fit is determined. The difference of the two extremes is the "S" distortion. In other words, the image rotation graph is fitted to the x-axis and the difference between the highest and lowest points then becomes the value for "S" distortion.

Apparatus:

The scan table utilized in the experiment consists of: a light source (1) focused to infinity, a collimating lens (2), a mounted NVG (3), a CCD camera (4) which is connected to a frame grabber (5) that takes a picture of the pinhole position, a monitor (6) which displays the image, and a computer (7) which controls rotation of the goggles. It's this rotation that gives us measurements across the entire field of view of the NVG.

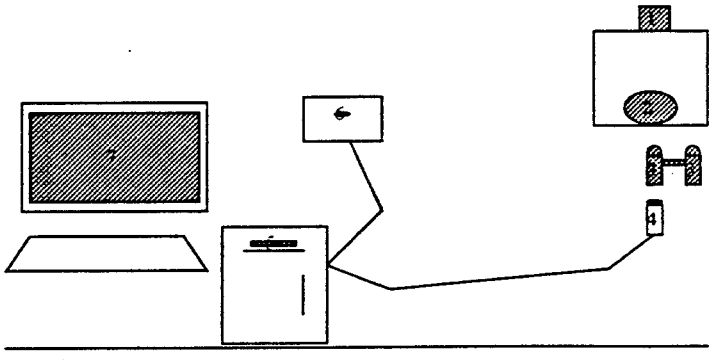

Figure 1. Scan table used to measure geometric distortion

Procedure:

The NVGs were focused and mounted on the rotary table between the video camera and the collimator such that the table rotated about the NVG eye piece. The threshold test was run achieving the clearest pinhole image with the least noise. This test is also used to check system alignment and assure that the pinhole image is centered on the monitor. Geometric image parameter testing was begun by taking both the intensified (with goggles) and unintensified (without goggles) references. This recorded the horizontal and vertical position of the pinhole image. After these tests were performed, the X and Y calibration tests were conducted in order to convert the linear measurements into angular values. A 15 mrad glass wedge was placed in front of the collimator lens, first in the horizontal plane then in the vertical plane. The computer recorded the horizontal and vertical distance the pinhole moved and then divided the deviation of the glass wedge by the distance the image moved in pixels in order to obtain the conversion factor. All measurements were multiplied by this conversion factor to obtain horizontal and vertical errors in angular units. The collimator was adjusted to one edge of the field of view and scanning was begun. After half of the field of view of the goggle was scanned, the collimator was readjusted to scan the other half. The data that was collected should resemble a V when plotted as a function of input angle, preferably symmetric towards the vertex. The data was transferred to an Excel spreadsheet to calculate magnification, image rotation, and "S" distortion. It was then transferred to another spreadsheet which calculated means and confidence intervals.

Results

The exhibited results are for two pairs of goggles identified by their serial numbers, 698 and 356. Magnification, image rotation, and "S" distortion are shown for each goggle in the graphs and tables below.

Table 1. Data Summary

NVG	n=11	MEAN	95% CONFIDENCE	
698L			UPPER	LOWER
	MAGNIFICATION	0.99	1.00	0.99
	IMAGE ROTATION	1.81	3.56	0.05
	"S" DISTORTION	2.41	2.71	2.11
698R				
	MAGNIFICATION	0.99	0.99	0.98
	IMAGE DISTORTION	15.31	16.43	14.20
	"S" DISTORTION	4.18	4.48	3.88

356L			
	0.98	0.98	0.97
MAGNIFICATION	-4.93	-2.74	-7.12
IMAGE DISTORTION	0.91	1.31	0.51
"S" DISTORTION			
356R			
MAGNIFICATION	0.98	0.98	0.97
IMAGE DISTORTION	-9.83	-8.57	-11.09
"S" DISTORTION	0.97	1.34	0.60

Magnification:

Magnification values appeared to stay relatively equivalent, not showing inconsistencies in the data or a significant change in slope. The values for magnification, as shown in Figure 2, all rounded to one and varied from 0.97 to 1.00 on both goggles. Since the values are similar in range, only one graph of representative data is shown for magnification.

#698:

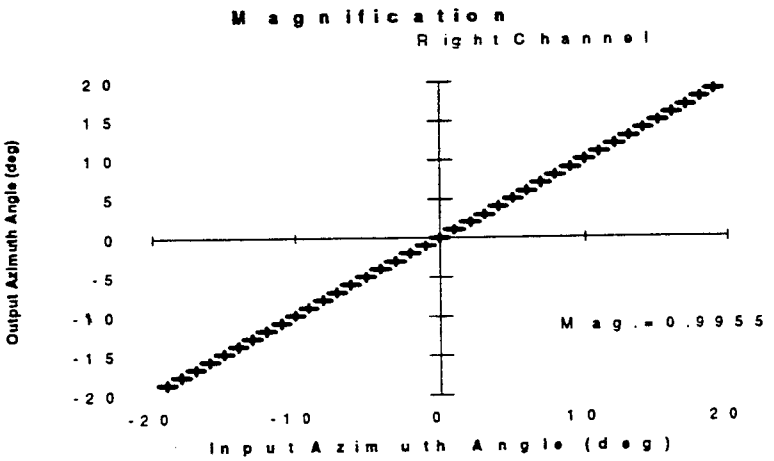

Figure 2.

Image rotation:

Figures 3, 4, 5, and 6 represent the typical outcome of the trials for image rotation. The 698 right channel's data tended to display a steeper slope than the left channel, signifying that the right channel had a greater rotation of the image. The data for the two sets of goggles indicates that there are differing image rotation values between them. The means for image rotation of the 698 goggles were 1.81 for the left channel and 15.31 for the right. The means for left and right channels of the 356 set were recorded as -4.93 and -9.83, respectively.

#698

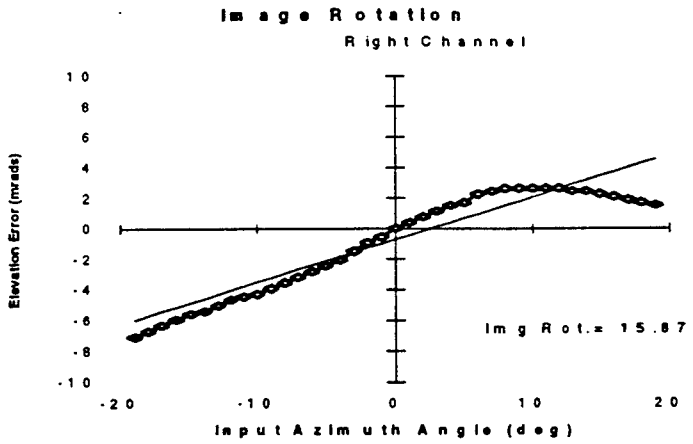

Figure 3.

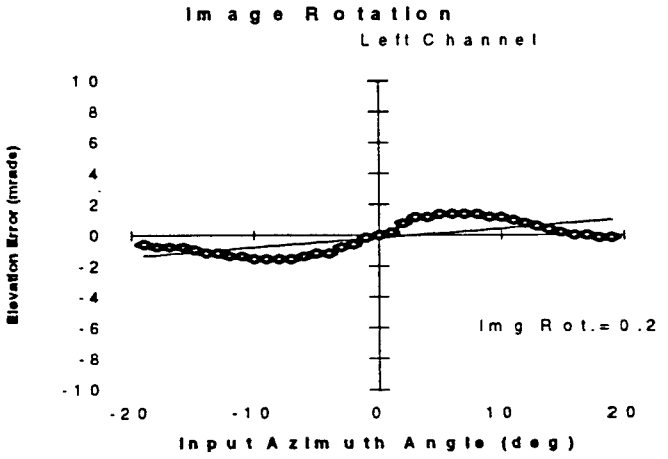

Figure 4.

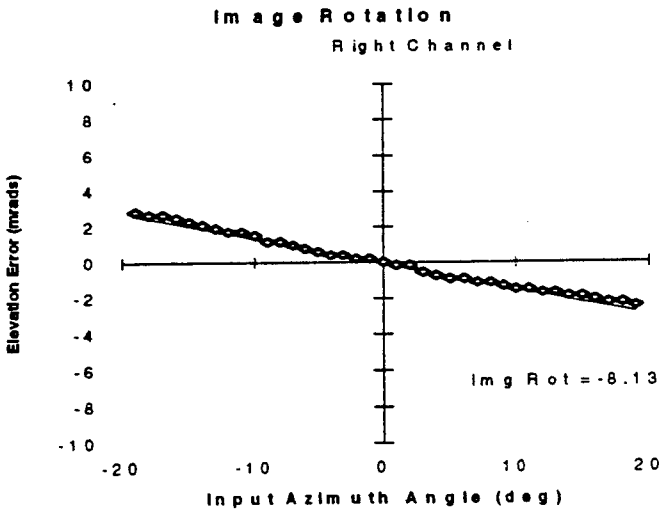

Figure 5.

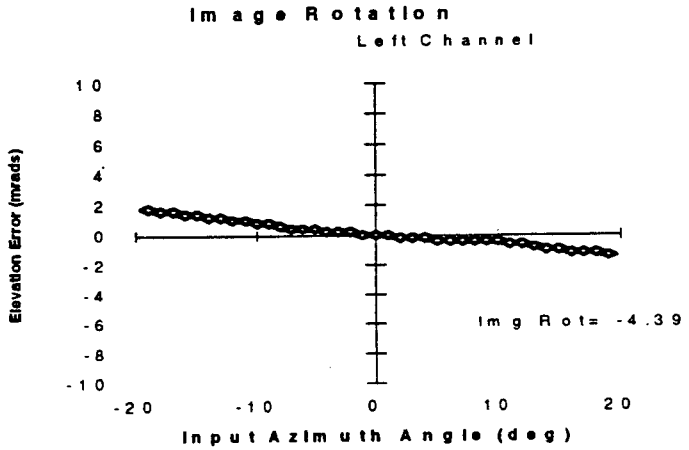

Figure 6.

"S" distortion:

"S" distortion is represented in Figures 7, 8, 9, and 10. This simply shows the image rotation data aligned with the x-axis. The means for "S" distortion were 2.41 for the left channel of the 698 goggle and 4.18 for the right channel. The mean for the left channel of the 356 goggles was 0.91 and 0.97 for the right channel. Since image rotation and "S" distortion originate from a single scan, if the scan is incorrect or defective, both data sets show greater distortion.

#698

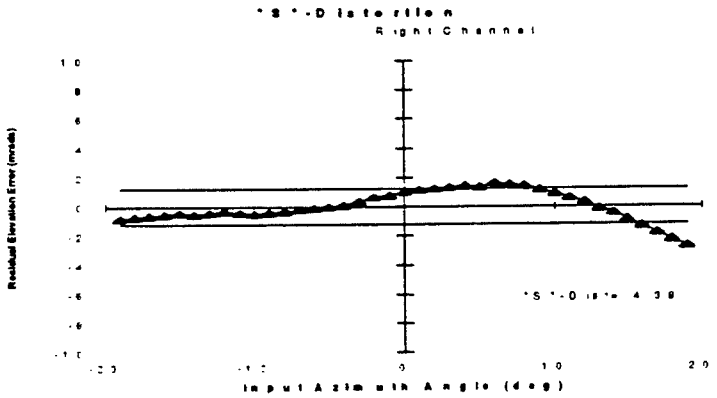

Figure 7.

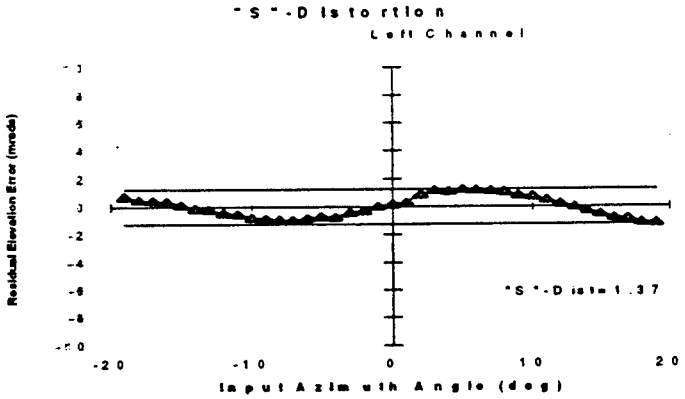

Figure 8.

#356

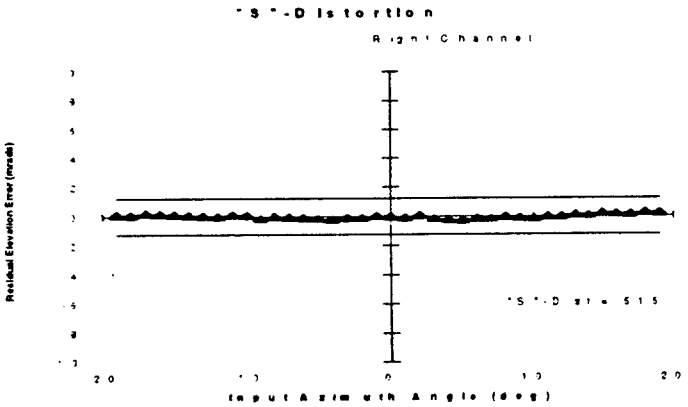

Figure 9.

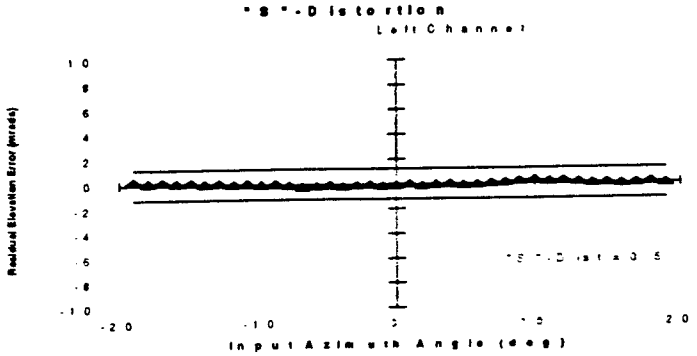

Figure 10.

Discussion:

As shown in Table 1 the results for magnification, image rotation, and "S" distortion were reasonably consistent within the 95% confidence interval. A few occurrences of inconsistent data did exist, however. Differences in image rotation of channels of the same goggles is influenced by the overall condition of the goggles as well as the twisting of the fiber optic bundles within the goggles. Atypical data sets are shown in Figures 11, 12, 13, and 14 below. Primarily, the image rotation and "S" distortion data sets exhibited a "jump" in the data located near the center of the graph. This misalignment at the center of the field of view was not observed when the experimenters looked through the goggles. It was, therefore, believed to be an anomaly introduced by the measurement procedure. A possible explanation for the apparent misalignment of the points near the center is that the collimator did not remain level when adjusted from side to side for the two halves of the scan. Another possible explanation is that the goggle mount apparatus did not keep the NVGs in a stable position throughout the scan. Either of these conditions could have caused the image to move from its original position. Since "S" distortion originates from the same data set, this hypothesis would also explain the inconsistency within that data as well.

Image rotation:

#698

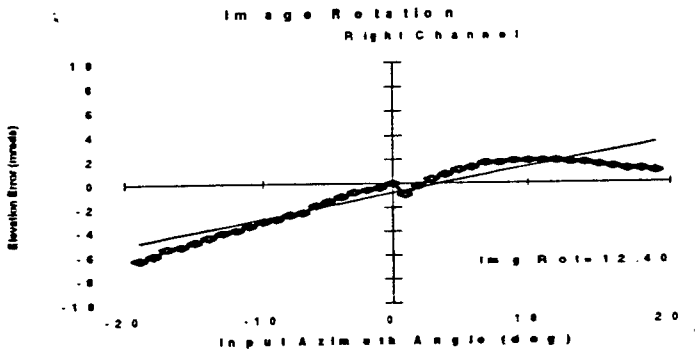

Figure 11.

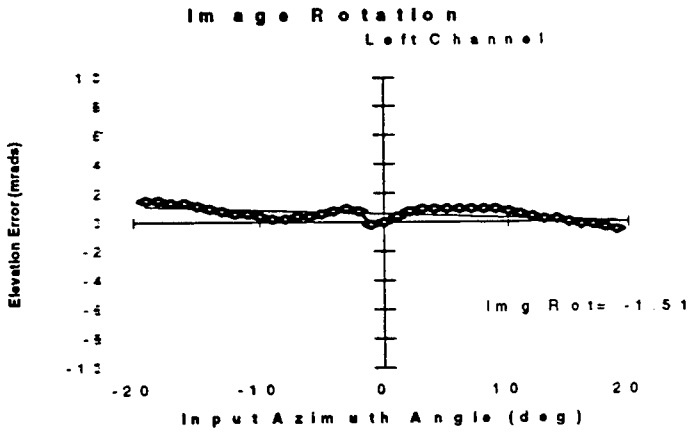

Figure 12.

#356

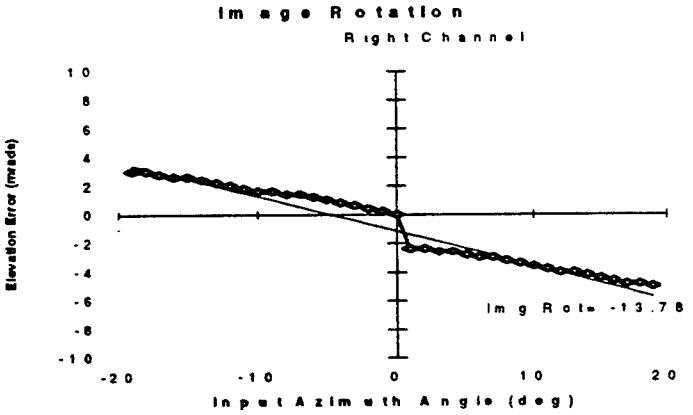

Figure 13.

"S" Distortion:

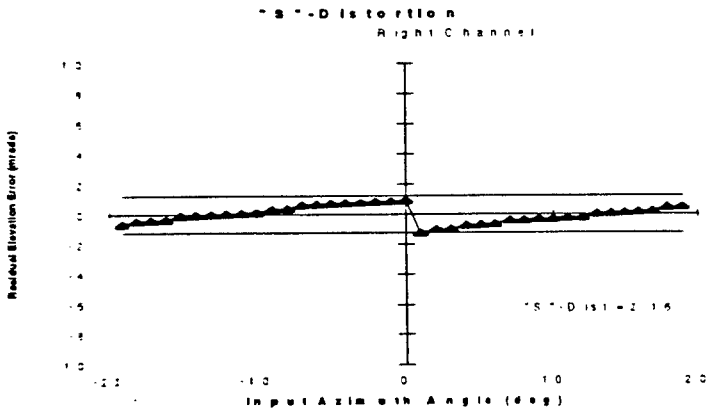

Figure 14.

Follow-up Examination of the Lab Equipment:

In order to explain the inconsistencies in data (Figures 10-13), an examination of the lab set-up was conducted. Scan table rotation, collimator adjustment, and camera position were investigated. The scan table and the collimator appeared to be relatively stable, not causing the apparent "jumps" in the data. The camera, however, was easily shifted out of position. Because of this discovery, it is hypothesized that the shifting of the camera during experimentation caused the inconsistencies in data collection.

Since there were a few scans which exhibited the disjointed data at the center of the NVG field of view, these scans were deleted and the calculations of the means and confidence intervals were recomputed with the remaining data sets. Magnification varied little, therefore, the values remained the same. Means ranged from 0.99 to 0.98. Image rotation values changed, and thus decreased the range of the confidence intervals (See Table 2), improving the accuracy of the means. "S" distortion did not deviate from the original calculations as greatly as image rotation. Because of this, the revised values are not extremely different from Table 1. After the elimination of the stray data, the geometric distortion values are more consistent and accurate, providing a more realistic picture of the data collected.

Table 2. Revised Data Summary

NVG	Mean	95% Confidence	
		Upper	Lower
698L			
Magnification n=11	0.99	0.99	0.99
Image Rotation n=10	3.16	3.78	2.53
"S" Distortion n=10	2.51	2.72	2.31
698R			
Magnification n=11	0.99	0.99	0.98
Image Rotation n=8	16.19	16.67	15.71
"S" Distortion n=10	4.26	4.51	4.02
356L			
Magnification n=8	0.98	0.98	0.97
Image Rotation n=8	-5.44	-4.79	-6.09
"S" Distortion n=8	0.68	0.80	0.56
356R			
Magnification n=8	0.98	0.98	0.97
Image Rotation n=8	-8.82	-8.40	-9.24
"S" Distortion n=8	0.68	0.79	0.56

Conclusions and Recommendations:

According to the revised data, the 95% confidence interval for the magnification produced very little variation across all of the goggle channels. Both left channels had no variation from the means. The 95% confidence interval for the right channels were equivalent to the mean +/-1%. The left channel of the 698 goggles had a large interval of +/-20% while that of the right channel was +/-3%. The 356 goggles produced 12% and 5% variations, left and right, respectively. "S" distortion values were pretty consistent within goggles. The 698 goggles had 8% and 6% variations, left and right, and the 356 goggles produced 18% and 16%, left and right.

In order to obtain more accurate and consistent data, it is recommended that all of the equipment is thoroughly stabilized before scanning. Sturdy goggle and camera mounts are a necessity if consistent data is desired. Consistently correct alignment of the collimator, NVG's, and CCD camera would reduce deviation among the data sets as well.

THE EFFECTS OF INDIVIDUAL DIFFERENCES AND TEAM PROCESSES ON TEAM MEMBER SCHEMA SIMILARITY AND TASK PERFORMANCE

Kristen R. Bonnema

Wayne High School
5400 Chambersburg Road
Huber Heights, OH 45424

Final Report for:
High School Apprentice Program
Armstrong Laboratory

Sponsored by:
Air Force Office of Scientific Research
Bolling Air Force Base, Washington, DC

And

Armstrong Laboratory

August 1997

THE EFFECTS OF INDIVIDUAL DIFFERENCES AND TEAM PROCESSES ON TEAM MEMBER SCHEMA SIMILARITY AND TASK PERFORMANCE

Kristen R. Bonnema
High School Student
Wayne High School

Joan R. Rentsch
Associate Professor of Psychology
Department of Psychology, Wright State University

Michael D. McNeese
Research Scientist
CFHI, Armstrong Laboratory

Dawn D. Burnett
Graduate Student
Department of Psychology, Wright State University

Abstract

The research reported here examined team member schema similarity, its predictors, and its relationship to team performance. This research has implications for applied Air Force problems such as UCAV (Unmanned Combat Air Vehicle) operation, transport command centers, information warfare, battlefield management, C^3I, and joint collaborative systems such as data walls, avatars, intelligent agents, and knowledge rooms.

One purpose of the present study was to test a portion of the Team Member Schema Similarity Model with modifications. It was hypothesized that team member individual differences would predict team process variables (team interaction process variables and group process variables) and team member schema similarity (TMSS). Team process variables and TMSS were hypothesized to predict team performance.

Data were collected in a laboratory setting. Forty-five two member teams attempted to solve a complex, ill-defined problem. Team members completed individual difference measures before working on the problem. After solving the problem, team members completed teamwork schema measures. TMSS was operationalized as schema agreement and schema accuracy. Team performance and team interaction processes were coded by raters. Preliminary results are reported that indicate some support for portions of the modified model. Future research and potential applications are discussed.

THE EFFECTS OF INDIVIDUAL DIFFERENCES AND TEAM PROCESSES ON TEAM MEMBER SCHEMA SIMILARITY AND TASK PERFORMANCE

Kristen R. Bonnema
Joan R. Rentsch
Michael D. McNeese
Dawn D. Burnett

Teams, crews, multi-operator units, and collaborative systems abound in the Air Force. Dr. Michael McNeese has developed a research program to study the socio-cognitive variables operating within these multi-person units. Because Air Force teams operate in environments that are characterized by ill-defined and emergent situations, McNeese's research program has incorporated theories of situational awareness, crew schemata, shared cognition, social construction of knowledge, and interpersonal interaction to understand the development of meanings necessary for effective functioning in these environments (e.g., Brown, Whitaker, Selvaraj, & McNeese, 1995; McNeese, Zaff, Citera, Brown, & Whitaker, 1995; McNeese, 1993; Nosek & McNeese, 1997; Wellens & McNeese, 1987; Young & McNeese, 1995). This type of research will produce knowledge that will be applicable to the development of joint collaborative systems technology within the Air Force. The research study reported in this document is part of this research program.

The research reported below focused on cognitive processes within teams. Specifically, the research examined team member schema similarity, its predictors, and its relationship to team performance. This research is relevant to co-located or distributed teams. It also has implications for applied Air Force problems such as UCAV (Unmanned Combat Air Vehicle) operation, transport command centers, information warfare, battlefield management, C^3I, and joint collaborative systems such as data walls, avatars (Wells & Hoffman, 1996), intelligent agents, and knowledge rooms.

For example, UAV operation requires that pilots coordinate with field controllers, tower personnel, and manned air vehicles in complex, dynamic, ill-defined situations. During the chaos of combat, the UCAV crew must be able to construct meaning quickly in these ambiguous situations. UAV crew members must be able to

understand each other and they must have shared situational awareness. This ability to understand one another and to develop shared situational awareness is developed, in part, through team member schema similarity. Thus, team member schema similarity (TMSS) will enhance the performance of these types of teams.

Below, the conceptual model used to guide the current research is described, relevant past research is reviewed, and a modified version of the model is presented. Then the present study is described.

Team Member Schema Similarity Model

The Team Member Schema Similarity Model (Rentsch & Hall, 1994) is shown in Figure 1. The critical variable in the model is team member schema similarity (TMSS). Team member schema similarity (TMSS) refers to the degree to which team members have similar team-related schemas. A schema is a complex knowledge structure that organizes new information and facilitates understanding (Poole, Gray, & Gioia, 1990).

Although team members may develop many team-related schemas (e.g., schemas of team members, schemas of the task), the focus of the present study is on teamwork schemas (Cannon-Bowers & Salas, 1990). Teamwork schemas contain knowledge and information regarding communicating about, evaluating, and compensating for teammates' performance (Cannon-Bowers & Salas, 1990). Teamwork schemas will guide team members' assumptions, expectations, and behavior regarding teamwork.

Rentsch and Hall (1994) extended the concept of coorientation (Poole & McPhee, 1983), which is typically studied with respect to attitudes, to the study of teamwork schemas. They suggested that TMSS refers to schema accuracy as well as schema agreement. Schema agreement among individuals exists when individuals have similar schemas. This type of schema similarity has received research attention in the past (e.g., Walsh, Henderson, & Deighton, 1988). Schema accuracy exists when individuals are able to describe another individuals' schema accurately. This type of schema similarity has received very little research attention. A critical or optimal level of TMSS, in terms of both accuracy and agreement, is hypothesized to enhance team effectiveness. Empirical research has revealed some support for this hypothesis (Rentsch, Pape, & Brickman, 1997; Rentsch, 1993).

Team members who have schema similarity have similar knowledge about teamwork and they organize this information in a similar way. Teamwork schema similarity is hypothesized to enhance team effectiveness

because similar teamwork schemas in terms of agreement and accuracy among team members will allow team members to interact efficiently and effectively. Team members with high TMSS will be able to anticipate, to facilitate, and to compensate for one another's behavior.

Communication among team members is also likely to be enhanced as team members' teamwork schemas become increasingly similar. Team members may be aware of the information required by each other and fully understand the information that is being communicated to each other. Moreover, team members are likely to anticipate and understand each other's actions due to teamwork schema similarity.

Researchers in the military realm have studied team cognitions as team mental models. They have examined the relationship between team cognitions and team performance (e.g., Cannon-Bowers, Salas, & Converse, 1993). Much of this research provides indirect evidence that team mental models predict team performance (Cannon-Bowers et al., 1993).

Most researchers have conceptualized team cognitions in terms of schema agreement. The accuracy component of TMSS has not been explored extensively to the authors' knowledge. Thus, one purpose of the present study was to test the roles of team member schema accuracy and agreement in the prediction of team effectiveness. Rentsch, Pape, and Brickman (1997) examined TMSS conceptualized as schema agreement and schema accuracy. Their results revealed that agreement and accuracy predicted team effectiveness significantly. They suggested that schema accuracy may be more important in predicting team effectiveness than schema agreement. They suggested that future research examine these relationships in detail.

Antecedents of TMSS. As shown in Figure 1, two antecedents of team-related schema similarity are team membership influences, such as person-environment fit, and schema related communications, such as communication that occurs during socialization processes. These antecedents are expected to regulate the degree of schema similarity among team members to an optimal level. It is assumed that an optimal level of schema similarity exists for any given team and that when schema content is of high quality, the optimal level of schema similarity will enhance team effectiveness maximally.

In the present study, we focused on a subset of team membership influences and a subset of schema related communications as predictors of TMSS. The team membership influences we examined were individual differences. The schema related communications in our study were team interaction process variables. Below, we elaborate these portions of the model.

Team membership influences as individual differences. Schneider (1987) hypothesized that individuals are attracted to organizations containing people who are similar to themselves (Attraction), organizations select individuals who are similar to others already in the organization (Selection), and individuals who gain entry into the organization, but who are significantly different from those already in the organization are predicted to leave the organization (Attrition). One outcome of the ASA process is excessive similarity among organizational members. In the extreme, Schneider hypothesized, organizations may fail due to excessive homogeneity among organizational members, because too much homogeneity among organizational members would limit organizational creativity.

Thus, this organizational theorist predicted that similarity among organizational members will be associated with organizational members thinking similarly. In other words, individuals who are similar in terms of individual difference characteristics are likely to have similar schemas. Extending this logic to teams implies that similarity among team members' individual difference characteristics may enhance TMSS. Thus, an optimal level of TMSS may be due, in part, to similarities among team members' individual difference characteristics (Rentsch & Hall, 1994).

Although similarity among team member individual differences characteristics may be related to TMSS, it may also be the case that the level of the individual difference characteristics existing within the team may also be related to TMSS. Pape (1997) hypothesized that high levels of teamwork schema accuracy and agreement would exist when perceivers were high on trust and perspective taking, and when targets were high on private self-consciousness[1]. She hypothesized that targets high on self-monitoring would have low levels of accuracy and agreement. Team members who are high and similar in terms of several individual difference variables, such as perspective taking, trust, and private self-consciousness, and who are low and similar on self-monitoring are likely to experience high TMSS. These variables were investigated in the present study.

Schema related communications as team interaction processes. Schema related communication processes include communication that occurs during training, team member socialization, and team member interactions. In the present study we examined schema communication processes that occur while team members interact to complete a task. Within the team context, there is evidence that team member interaction is a primary cause of schema similarity among team members (Bettenhausen & Murnighan, 1991; Gersick, 1989; Walsh, Henderson, & Deighton, 1988). Many researchers agree that groups require social construction of knowledge and metacognitive processes to solve problems successfully (e.g., Young & McNeese, 1995). However, the research has not addressed the nature of the interactions leading to socially constructed meaning. No definitive theory for studying these interaction processes has been developed. Therefore, another purpose of the present study was to determine team interaction process variables that predict TMSS and team performance. We drew upon the group communication and crew coordination literatures. Our summary of this literature is presented next.

Team Interaction Processes

As Tower and Elliott (1996) note, although team member communication and coordination are hypothesized to be related to team performance, very little empirical research has been conducted to test the nature of these linkages. However, according to Tannenbaum, Beard, and Salas (1992), existing research evidence tends to support communication processes, coordination processes, and decision making processes as predictors of team performance.

For example, Hakel, Weil, and Hakel (1988) reported that intrateam communication patterns differentiated high from low performing teams. Among other findings, Kimble and McNeese (1987), found that teams that talked in longer utterances performed better than teams that spoke in shorter utterances.

Team interaction processes and TMSS are likely to have a reciprocal relationship. Team member communication is important because it is critical to developing similar understandings, and similar understandings, in turn, imbue communication with meaning (Fischer, 1996). Again, the research evidence is indirect. For example, Dyer (1984) reported research by Obermayer and colleagues revealing that experienced aircrews communicated more frequently during nonroutine missions than during routine missions compared to less

experienced crews. This suggests that experienced aircrews might have had TMSS for routine situations and, therefore, did not require high levels of communication for these situations.

Although there are many approaches for studying team interaction processes, there is none that specifically addresses the sense-making, or socially constructed aspect of interaction. Interaction seems to enhance performance and it seems to be related to TMSS. Yet, there exists a need for additional study of interactions and communication within teams (Duffy, 1993).

Team Interaction Process Variables

We developed a coding scheme to record the nature of the interactions occurring among team members. In particular, we focused on the degree to which team members tended to share interpretive information with one another. We assessed: depth of meaning of informing oriented communication, depth of meaning of learning oriented communication, quality of exchange, consensus evaluation communication, openness and acceptance of communication, and egocentricity versus mutuality of interaction. We also included group process variables in the present study. The group process variables were team cohesion, task motivation, and team metacognition.

The Present Study

The primary purpose of the present study was to test a portion of the TMSS model with modifications. The variables explored in the present study are presented in Figure 2. It was hypothesized that team member individual differences will predict team process variables (team interaction process variables and group process variables) and TMSS. Team process variables and TMSS are hypothesized to predict team performance.

Method

Participants

The participants were 90 undergraduate students who comprised 45 two member same-sex teams. There were 20 male teams and 25 female teams.

Task

The task used for the present study was *The Adventures of Jasper Woodbury: Rescue at Boone's Meadow.* The Jasper task is a complex, ill-defined task that requires problem solvers to identify the problem and the

subproblems needed to solve the problem, to distinguish between relevant and ill-relevant information, to coordinate relevant information, and to evaluate alternative possible solutions. Middle-school level mathematics are required to solve the problem (McNeese, 1993; Vye, Goldman, Voss, Hmelo, & Williams, undated).

The Jasper task is presented on laser video disc. A story problem is presented in which an injured eagle must be rescued from a remote location. Alternative routes, modes of transportation, and individuals are available for rescuing the eagle. Two problems are to be solved: (1) What is the quickest way to move the eagle? (2) How long will that take?

When solving the problem, team members could refer back to the video disc by using a Macintosh computer system. They were to record their answer and any information used to arrive at their answer in writing. The teams were videotaped as they attempted to solve the problem. They were stopped after 60 minutes, if they had not reached a solution. Only three teams were stopped. All other teams reached a solution in 12 to 56 minutes.

Measures

Individual differences. Traditional individual difference measures were used. The Interpersonal Trust Scale (Rotter, 1967) was used to assess trust. It had an internal consistency reliability estimate of .63 in the present study. In past research internal consistency reliability has been estimated at .76 (Rotter, 1967). Perspective taking was measured using the Interpersonal Reactivity Index (Davis, 1980), which is a 7 item measure. The internal consistency reliability estimate obtained in the present study was .77, which is consistent with past research findings (Davis, 1980). The Self Monitoring Scale (Snyder & Gangestad, 1986) was used to evaluate self-monitoring. An internal consistency reliability estimate of .70 is typical in past research (Snyder & Gangestad, 1986) and it was .69 in the present sample. Private and public self-consciousness were measured by the Self-Consciousness Scale (Fenigstein, Scheier, & Buss, 1975). The public self-consciousness scale contains seven items and had an internal consistency reliability estimate of .76. The private self-consciousness scale consists of 10 items and had an internal consistency reliability estimate of .54 in the present study.

Teamwork schema similarity. Teamwork schema similarity was assessed using a measure developed for this study based on pilot research (Pape, 1997). The measure was developed using the procedure advanced by

Rentsch (1993). The measure consisted of 15 items that assessed teamwork schema. Each team member rated the 15 items for how important they were to his or her concept of teamwork. Then each team member completed the items as he or she believed his or her teammate would rate them.

Team Performance. Eight aspects of team performance were coded: problem space identification, constraint violations, misconceptions, confusions, math errors, speed, accuracy, corrections, and solution quality. Similar types of performance measures for the employed task have precedence in the research literature (e.g., McNeese, 1993; Vye, Goldman, Voss, Hmelo, & Williams, undated). Two raters coded performance independently by reviewing each team's written work and the videotape of the team. Interrater reliability was 93% agreement. The raters resolved any discrepancies in ratings through consensus.

Team processes. Team processes were coded using a coding scheme developed for this study. Two categories of team processes were assessed: team interaction processes and group processes. Team interaction processes included: depth of meaning in informing oriented communication, depth of meaning in learning oriented communication, quality of exchange, consensus evaluation communication, egocentricity versus mutuality, openness and acceptance of communication. Group processes were: group cohesion, task motivation, and team metacognition.

The total time during which the team worked was divided into quarters. Each process variable was rated for each quarter. The team received a rating for depth of meaning in informing oriented communication, depth of meaning in learning oriented communication, quality of exchange, consensus evaluation communication, egocentricity versus mutuality, group cohesion, and team metacognition for each quarter. Each team member was rated on depth of meaning in informing oriented communication, depth of meaning in learning oriented communication, consensus evaluation communication, openness and acceptance of communication, task motivation and team metacognition for each quarter.

Each variable was rated by two raters. One rater prepared a transcript of the videotape and then reviewed the videotape using the transcript to rate the team members and the team on the process measures. The other rater

used the transcripts when reviewing the videotape to make the ratings. The raters achieved interrater reliability of 77% agreement on all of the ratings. All discrepancies were resolved through consensus.

Preliminary Results

Variables

The results reported here are very preliminary. The similarity among team members on the individual difference measures was assessed using the within team standard deviations on each variable. Team level on the individual difference measures was assessed using the within team level mean for each variable. Two forms of TMSS accuracy and agreement were calculated. One form was based on absolute difference scores. Using the absolute difference score method, TMSS agreement was calculated as the average of the summed absolute difference scores between members' ratings on each teamwork schema item. TMSS accuracy scores were calculated as the average of the summed absolute differences scores between each member's ratings of the other member's schema and the other member's actual schema ratings. Stated differently, the absolute difference was calculated for each item, then summed for each team member, and the sums were averaged for the team level accuracy measure. The second form of TMSS was calculated using the square root of the sum of the squared difference scores. Both forms of TMSS produced similar results, therefore, the results from the absolute difference form are presented.

Each process variable was aggregated across quarters for a total score. An aggregated team level score was computed for those variables on which each team member was assessed. All analyses involving process variables are based on a sample size of 30. All other analyses are based on a sample size of 45.

Individual Differences as Predictors of TMSS

The similarity and level of the individual difference scores were correlated with TMSS accuracy and agreement scores. The bivariate correlations revealed no statistically significant relationships. Regression analyses were conducted using a backward stepwise strategy. These results revealed that TMSS Accuracy was predicted by team member similarity on trust and on public self-consciousness ($\underline{R} = .37$, $\underline{p} < .05$; $\beta = .24, .28$, respectively, $\underline{p} > .05$). TMSS Agreement was predicted by team level on team experience, trust, public self-consciousness, and

private self-consciousness ($R = .45$, $p < .05$; $\beta = -.24, .26, .28, -.38$ respectively). Private self-consciousness and team experience had negative beta weights. These are unexpected results. Additional analyses are required to test for suppression effects.

Team Interaction Processes as Predictors of TMSS

The only team interaction process variable that predicted TMSS was the aggregated team level openness variable. This variable predicted both TMSS Accuracy and Agreement with correlations of .44 ($p < .05$). This result was unexpected, because it was in the opposite direction of the prediction. Remember a low value indicates high TMSS. Therefore, the positive correlations suggest that low TMSS is related to a high level of openness. After reviewing this result, the process coders suggested that perhaps, the measure of openness was assessing some other variable such as acquiescence or passivity. They believed that this may be the case, because team members were given high ratings on openness and acceptance when they were willing to consider the other team members' input. A high degree of openness and acceptance was characterized by immediate discussion of another's input. The more persuasion required before input is considered or discussed, the lower the level of openness and acceptance. These behaviors might also characterize high levels of acquiescence or passivity. If this is true, then these correlations may make sense.

TMSS Accuracy and Agreement as Predictors of Team Performance

TMSS Accuracy correlated significantly with how completely teams identified the problem space, with the solution rating, and with making a constraint violation ($r = -.33, -.30, .36$, $p < .05$). Higher TMSS accuracy was related to better problem identification and a higher solution rating. However, it was an unexpected finding that high TMSS Accuracy was related to making more constraint violations.

Simultaneous regression equations were computed in which TMSS accuracy and agreement were entered as predictors of team performance. Significant results were obtained for a constraint violation and for problem space identification. In both cases TMSS Accuracy had a significant beta weight and TMSS Agreement did not. Furthermore, in both cases, the multiple R was .39. Although an additional hierarchical regression analysis is required, it appears that TMSS Accuracy alone predicts as well as TMSS Accuracy and Agreement combined.

Team Interaction Processes as Predictors of Team Performance

Correlational analyses have been conducted to provide preliminary results regarding the nature of the relationship between team interaction processes and team performance. Problem space identification was correlated significantly with aggregated team level openness, team depth of informing oriented communication, and team learning oriented communication, and team cohesion (r = -.39, .42, .36, -.51, respectively, $p < .05$). Team cohesion and team level openness were related negatively to team performance. Again, this pattern of results may indicate that the openness measure really assessed acquiescence. It might also suggest that highly cohesive teams suffered from a bit of groupthink causing them to ignore some information.

Aggregated team openness, team cohesion, and quality of exchange were correlated significantly with constraint violations (r = .41, .38, .47, respectively, $p < .05$). All of these correlations were in the direction opposite of that predicted. Again, the acquiescence and groupthink hypotheses may explain these results.

Egocentricity versus mutuality and team depth of meaning in informing oriented communication predicted corrections (r = -.37, .40, respectively, $p < .05$). Egocentricity also predicted misconceptions (r = -.47, $p < .05$). Solution rating was predicted significantly by team depth of information processing (r = .38, $p < .05$).

Discussion Based on Preliminary Results

We would like to remind the reader that these results are preliminary for several reasons. First, the analyses involving the process variables were based on a sample size of 30. Data from all 45 teams will be analyzed in the near future. Second, additional analyses are required to further explore the nature of the predicted relationships and the nature of the unexpected results. Some of the analyses to be conducted were mentioned in the results section. Third, our dataset contains variables that may serve as control variables (e.g., time to solution, demographic characteristics). These variables have not yet been analyzed. Therefore, due to the preliminary nature of the data analysis, our discussion of these results is presented tentatively and cautiously.

In this study we tested a model of team member schema similarity (TMSS) that included individual difference and team process variables as predictors of TMSS, and TMSS and team process variables as predictors of team performance. The results revealed that the individual difference variables predicted TMSS in combination

only. In addition, similarity of individual differences predicted TMSS Accuracy and level of individual differences predicted Agreement. These results reflect the complex nature of personality. Also, we suggest that future research include the Armstrong Laboratory Aviation Personality Survey (ALAPS; Retzlaff, King, McGlohn, Callister, 1996) as a measure of individual differences related to teams and collaborative work. The variables on the ALAPS may be related more strongly to TMSS than the individual difference variables assessed in the present study.

The process variable related to openness or acquiescence predicted TMSS. This relationship requires additional study. However, we hesitate to interpret any of the process correlations in depth due to the preliminary sample size.

In past research, team effectiveness has often been assessed by the teams rating their own performance. This practice is common (Tannenbaum, Beard, & Salas, 1992). However, Tannenbaum et al. (1992) advocate the use of objective measures. In the present study, we employed objective performance measures. TMSS was not a strong predictor of these performance measures. Interestingly, included on the background survey was a single item on which team members rated their satisfaction with the teamwork that had occurred on their team. This item correlated significantly with TMSS accuracy and agreement (r = -.37, -.35, respectively).

Although based on only part of the dataset, it appears that team processes have weak relationships to TMSS. However, team processes do predict team performance. The nature of these relationships requires additional analyses.

This study has revealed that TMSS Accuracy and Agreement predict team performance differently and are related differentially to individual differences. TMSS Accuracy deserves additional investigation.

Future Research

The next step in this line of research is to test the TMSS model within the context of an ecologically valid synthetic task environment, such as the VIPER/VECTOR tasks (McNeese, personal communication) that were developed in Armstrong Laboratory, or such as the TRAP task (Wilson, McNeese, Brown, & Wellens, 1987) modified to realistically portray the UCAV or the command-post environment. This research will contribute to the

Collaborative Systems Technology Lab at The Fitts Human Factors Engineering Laboratory at the Collaborative Systems Technology Branch of Armstrong Labs at Wright Patterson AFB.

Baker and Salas (1992) suggest that teamwork may evolve, therefore researchers need to develop teamwork measures that are generalizable to teams in many settings and different team tasks. Our efforts to develop team interaction process measures are in line with this objective. Our measures will be useful in understanding the development of teamwork behaviors and the development of TMSS. We wish to pursue future research in which we will use these measures to study the development of teamwork and TMSS.

Future Applications

The theoretical constructs and the measures that we have developed as part of the Air Force Office of Scientific Research Summer Faculty Research Program applied within the ecologically valid synthetic task environment will provide the foundation for future research on Joint Cognitive Systems. As we acquire knowledge of team member schema similarity and its relation to shared responsibility and team performance, we can pursue research relating these variables to collaborative systems technologies such as datawalls or knowledge rooms. Understanding how team members interact will facilitate the design and development of human-machine communication (Wellens & McNeese, 1987).

We know that the *New World Vistas Air and Space Power for the 21st Century* publication indicates that collaborative computing is a high priority. Collaborative computing may take the form of advanced "groupware," which may be used to facilitate group interaction and decision making among co-located or distributed group members, and human-machine interaction. Clearly, understanding the effects of the joint cognitive system designs on TMSS will enhance the utility of these technologies. MUDs, or Multiple User Dimensions, are described as "....in effect social virtual realities"...."to manage the details of the social interaction... (NWV, p. 100)." The New World Vistas report goes so far as to suggest that a "virtual Pentagon (p. 101)" may become a reality. These innovations require extensive knowledge of socio-cognitive processes and their relationships to technology.

Footnotes

1. Perceiver refers to the individual who is asked to rate another person. The person being rated is referred to as the target.

References

Baker, D. P., & Salas, E. (1992). Principles for measuring teamwork skills. Human Factors, 34(4), 469-475.

Bettenhausen, K. L. & Murnighan, J. K. (1991). The development of an intragroup norm and the effects of interpersonal and structural challenges. Administrative Science Quarterly, 36, 20-35.

Brown, C. E., Whitaker, R. D., Selvaraj, J. A., & McNeese, M. D. (1995). The development of trace: An integrative bargaining paradigm for investigating multidisciplinary design tradeoffs. Air Force Material Command, Wright-Patterson Air Force Base, Ohio. (Al/CF-TR-1995-0073).

Cannon-Bowers, J. & Salas, E. (1990, April). Cognitive psychology and team training: Shared mental models in complex systems. Paper presented to the Meeting of the Society for Industrial/Organizational Psychology, Miami Beach, Florida.

Cannon-Bowers, J. A., Salas, E., & Converse, S. (1993). Shared mental models in expert team decision making. In N. J. Castellan (Ed.), Individual and group decision making (pp. 221-246). Hillsdale: Lawrence Erblaum Associates.

Davis, M. H. (1980). A multidimensional approach to individual differences in empathy. JSAS: Catalog of Selected Documents in Psychology, 10, 85.

Duffy, L. (1993). Team decision making and technology. In N. J. Castellan (Ed.), Individual and group decision making (pp. 247-265). Hillsdale: Lawrence Erblaum Associates.

Dyer, J. L. (1984). Team research and team training: A state of the art review. In F. A. Muckler (Ed.), Human factors review (pp. 285-323). Santa Monica: Human Factors Society.

Fenigstein, A., Scheier, M. F., & Buss, A. H. (1975). Public and private self-consciousness: Assessment and theory. Journal of Consulting and Clinical Psychology, 43(4), 522-527.

Fischer, U. M. (1996). Methods for analyzing group problem solving decision making. United States Army Research Institute for the Behavioral and Social Sciences. (ARI Research Note 96-64).

Gersick, C. (1989). Marking time: Predictable transitions in task groups. Academy of Management Journal, 32, 274-309.

Hakel, M. D., Weil, E. K., & Hakel, L. (1988). The analysis and clustering of navy ratings based on social interaction characteristics: A literature review and conceptual model. Naval Personnel Research and Development Center, San Diego, California. (TR-88-46).

Kimble, C. E., & McNeese, M. D. (1987). Emergent leadership and team effectiveness on a team resource allocation task. Harry G. Armstrong Aerospace Medical Research Lab, Wright-Patterson Air Force Base, Ohio. (AD-A192-105).

McNeese, M. D. (1993). Putting knowledge to use: The acquisition and transfer of knowledge in situated problem solving environments. Dayton, OH: Wright-Patterson Air Force Base, Armstrong Laboratory. (NTIS No. AL/CF-TR-1993-0052).

McNeese, M. D., Zaff, B. S., Citera, M., Brown, C. E., & Whitaker, R. (1995). AKADAM: Eliciting user knowledge to support participatory ergonomics. The International Journal of Industrial Ergonomics, 15(5), 345-363.

New World Vistas: Air and Space Power for the 21st Century. Information Technology Volume. Department of the Air Force. USAF Scientific Advisory Board.

Nosek, J. T., & McNeese, M. D. (1997). Issues for knowledge management from experiences in supporting group knowledge elicitation and creation in ill-defined, emerging situations. Paper presented to the AAAI Spring Symposia: Knowledge Management, Standford University, March.

Pape, L. J. (1997). The effect of personality characteristics on team member schema similarity. Unpublished master's thesis proposal. Wright State University, Dayton, Ohio.

Poole, M. S., Gray, B. & Gioia, D. A. (1990). Organizational script development through interactive accommodation. Group and Organization Studies, 15(2), 212-232.

Poole, M. S. & McPhee, R. D. (1983). A structural analysis of organizational climate. In L. L. Putnam & M. E. Pacanowsky (Eds.), Communication and organizations: An interpretive approach (pp. 195-219). Beverly Hills, CA: Sage Publications.

Rentsch, J. R. (1993, August). Predicting team effectiveness from teamwork schema similarity. Paper presented at the Academy of Management Meetings, Atlanta, Georgia.

Rentsch, J. R., & Hall, R. J. (1994). Members of great teams think alike: A model of team effectiveness and schema similarity among team members. In M. M. Beyerlein & D. A. Johnson (Eds.), Advances in interdisciplinary studies of work teams. Vol. 1. Series on self-managed work teams (pp. 223-262). Greenwich, CT: JAI Press.

Rentsch, J. R., Pape, L. P., & Brickman, N. M. (1997). Team member schema similarity: Exploring individual differences predictors. Unpublished manuscript. Wright State University.

Retzlaff, P. D. King, R. E., McGlohn, S. E., & Callister, J. D. (1996). The development of the Armstrong Laboratory Aviation Personality Survey (ALAPS). Air Force Material Command, Brooks Air Force Base, Texas. (AL/AO-TR-1996-0108).

Rotter, J. B. (1967). A new scale for the measurement of interpersonal trust. Journal of Personality, 35, 651-665.

Schneider, B. (1987). People make the place. Personnel Psychology, 40, 437-453.

Snyder, M., & Gangestad, S. (1986). On the nature of self-monitoring: Matters of assessment, matters of validity. Journal of Personality and Social Psychology, 51(1), 125-139.

Tannenbaum, S.I., Beard, R.L., & Salas, E. (1992). Team building and its influence on team effectiveness: an examination of conceptual and empirical developments. In K. Kelley (Ed.), Issues, theory, and research in industrial/organizational psychology (pp. 117-153). North-Holland: Elsvier.

Tower, S. L., & Elliott, L. R. (1996). The role of communication efficiency in teams with distributed expertise: Application of the multi-level theory. Proceedings of the International Association of Management Conference, Toronto, Canada.

Vye, N. J., Goldman, S. R., Voss, J. F., Hmelo, C., Williams, S., & Cognition and Technology Group at Vanderbilt. (undated). Complex Mathematical Problem Solving by Individuals and Dyads. Unpublished manuscript. Vanderbilt University, Nashville, Tennessee.

Walsh, J. P., Henderson, C. M, & Deighton, J. (1988). Negotiated belief structures and decision performance: An empirical investigation. Organizational Behavior and Human Decision Processes, 42, 194-216.

Wellens, A. R., & McNeese, M. D. (1987). A research agenda for the social psychology of intelligent machines. IEEE Systems, Man, and Cybernetics.

Wells, M. J., & Hoffman, H. G. (1996). The virtual crewmember. Paper presented to the Human Factors and Ergonomics Society, Philadelphia, September 2-6.

Wilson, D. L., McNeese, M. D., Brown, C. E., & Wellens, A. R. (1987). Utility of shared versus isolated work setting for dynamic team decision-making. Armstrong Aerospace Medical Research Laboratory, Wright-Patterson Air Force Base, Ohio. (AD-A192-434).

Young, M. F., & McNeese, M. D. (1995). A situated cognition approach to problem solving. In Hancock, P., Flach, J., Caird, J., & Vincente, K. (Eds.), Local applications of the ecological approach to human-machine systems. Hillsdale: Lawrence Erblaum Associates.

Figure 1: Team Member Schema Similarity Model
(Rentsch & Hall, 1994)

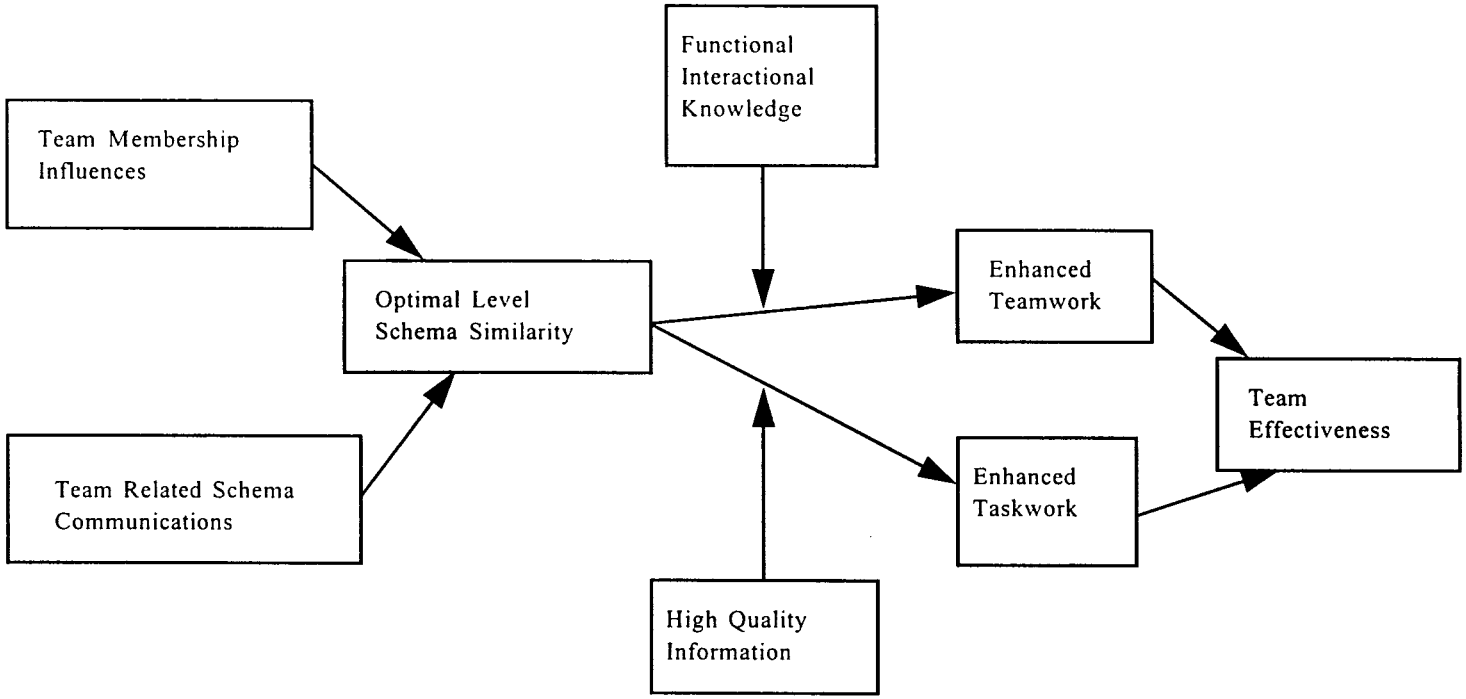

Figure 2: Model Modifications

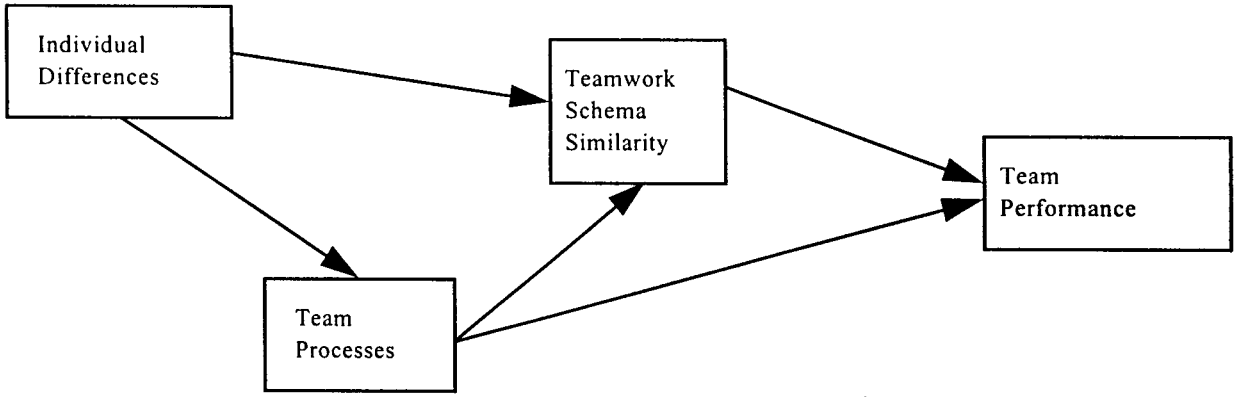

THE USE OF 3-DIMENSIONAL MODELING IN THE WIDESPREAD DISSEMINATION OF COMPLEX SCIENTIFIC DATA

David Brogan

Robert E. Lee High School
1600 Jackson-Keller
San Antonio, TX 78216

Final Report for:
High School Apprentice Program
Armstrong Laboratory

Sponsored by:
Air Force Office of Scientific Research
Bolling Air Force Base, Washington, DC

And

Armstrong Laboratory

August 1997

THE USE OF 3-DIMENSIONAL MODELING IN THE WIDESPREAD DISSEMINATION OF COMPLEX SCIENTIFIC DATA

David Brogan
Robert E. Lee High School

Abstract

A 3-Dimensional modeling program entitled "ElectroGIG" was used to create three animations. These included an eyeball, a rat brain and a radar dish. The purpose of these animations was to present recently collected data from experiments and demonstrate how the experiments were performed. Also, a UNIX-based program was used to create a wireframe model from sequential -TIFF images. Discussion includes inherent problems from working with computer animations. Also discussed were the possible uses for this technology in the future, especially in the health and medical fields.

THE USE OF 3-DIMENSIONAL MODELING IN THE WIDESPREAD DISSEMINATION OF COMPLEX SCIENTIFIC DATA

David Brogan

Introduction

As the world rapidly advances towards the 21st Century, the global community demands information faster and presented more effectively than ever before. Now, more than ever, companies and the scientific community are turning towards computers for new ways to present larger volumes of increasingly complex data. No longer will numerical tables, simple graphs or overheads be acceptable, instead advanced graphics and animations are expected. Three dimensional modeling, if used properly, could have an enormous impact on the presentation of all types of information. In the world of research, scientists must be able to demonstrate their findings in an effective manner, especially when dealing with others who do not possess the same scientific background and training. Computer modeling can be much more accurate and easier to comprehend than any medium discovered yet, although the challenges with dealing with it are numerous and great.

Methodology

ElectroGIG was the chosen modeling program because of its numerous features and capabilities. Before any work could be done, the manuals and tutorials were studied briefly, until the program was somewhat familiar. At that point, work on the models could begin. The first model that was needed was that of an eyeball. This eye would then be used to demonstrate the effects of non-ionizing radiation on the eye through an animation. The eyeball was purchased as a -DXF file from Viewpoint Datalabs, a company that produces and sells three-dimensional computer models. This eye included an inner and outer cornea, iris, optic nerve, retina, choroid and various lenses. Of course, all that could be seen was the outer cornea since it was fully opaque. The first step was to make this transparent so that the other parts of the eye, including

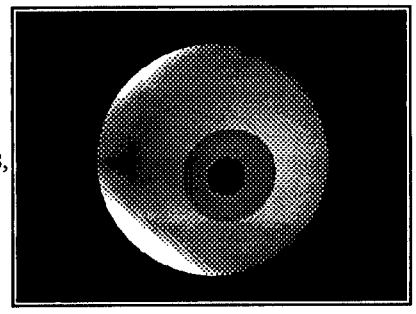

the iris, could be seen. This was done, however, the ridge between the choroid and the retina was then visible, which looked extremely unrealistic. The decision was then made to make the outer cornea opaque and cut away a part of the cornea to expose the iris. This was accomplished by creating a cone and using a feature entitled "subtract". The only problem with this is that the angle of the cone was extremely difficult to match up with the angle of the surface of the cornea. If the two were not aligned perfectly, one part of the cone could cut through the iris and the other part might not even reach the cornea. After numerous attempts, the two were finally lined up correctly. Then, the cone had to be made transparent so that it would not show up as part of the eye. The area of the base of the cone was then subtracted from the cornea, which allowed the viewer to see the iris, if sufficient lighting was available.

Lighting itself was another problem because of the numerous positions and intensities available to work with. Each light contained almost a dozen variables, including intensity, x-y-z position, coi, etc.

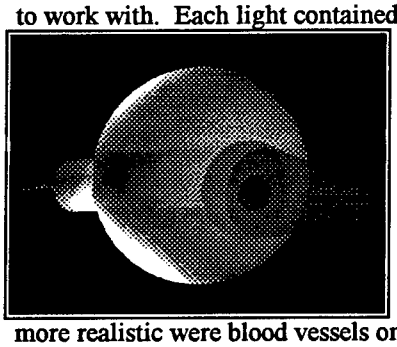

A spotlight was added to the front of the eye, which illuminated the iris very well. Two other lights were added to the top-back and the front-bottom to expose the eye, but also provided enough shadows to give the eye depth. Another attribute that was added to make the eye more realistic were blood vessels on the outer cornea. This was accomplished by making the blood vessels in Adobe Photoshop TM through use of the paintbrush and red paint. After the lines were done, they were saved as a .TIFF image and imported into the model inside of ElectroGIG. The inner lens of the eye was made black so that the impression of a black pupil would be given. The iris was given a light blue diffuse attribute and the optic nerve was colored red. Once the model itself was completed, the animation had to be made, also in ElectroGIG.

The camera first zoomed into the eye for three seconds, from a wide angle and was then supposed to rotate around the eye. However, the camera in GIG is not designed to rotate around an object, so instead the eye was made to rotate 50 degrees counterclockwise over a span of two seconds. Once this was done, a cone simulating the millimeter waves was to appear and focus on the iris of the eye. A yellow cone was created and then made transparent so it would not appear during the first part of the animation. After the eye finished its rotation, the cone became visible and the color of the iris changed from blue to

red to give the viewer some sense of the irradiation that occurred. One advantage that GIG possesses is that the model can be divided up into separate segments called solid tags. These tags can then be colored and moved individually. The animation part of GIG will display a separate track for each tag that is specified. That way, if one part of the animation needs to be changed, it is possible to edit the individual tags for movement of for colors, instead of the entire animation.

The next model that was desired was that of a rat brain. This model could then be used to show the placement of temperature probes in the rat brain for ongoing studies. No model of the rat brain could be found to purchase, so it was necessary to create one from scratch, using a feature of GIG called Nurbs. GIG itself constructs models out of five basic primitives, cone, sphere, torus, cylinder and cube. If any other shape is desired, a tool such as Nurbs must be used. Nurbs is a free form modeling program which allows the user to mold their own shape by adjusting various key points. The first decision that was to be made was whether the brain should be one solid object or an object made up of separate parts assembled together. After various experimentation and studious examination of an actual rat brain, the right lobe of the cerebral cortex was created. Then, a mirror function was used to mirror the points across the y-axis and create the corresponding left lobe. After this basic part of the brain was made, the cerebellum had to be constructed and added into the back of the cortex. The brain stem was then made in the same fashion and combined with the other three. Frontal lobes in the shapes of torpedoes were made and added in, as well as optic nerves. The optic nerves were created by first assembling a structure that looked like one nerve twisted into another. This nerve was copied, rotated and moved so that two of them created the beginning of a chain that extended off the bottom of the cortex. This chain was copied and moved so that one extended from the bottom of each cortex. With so much on the outside of the cortex, it was decided that more detail was needed inside the cortex, hence the introduction of the corpus collosum. It was attempted to model this in Nurbs, however, when it was made, Nurbs left the ends transparent so that it was possible to see through the corpus collosum from the beginning to the end. This was definitely not acceptable, so an attempt at using a tool called free-forms was made. Free-forms required more work with the individual

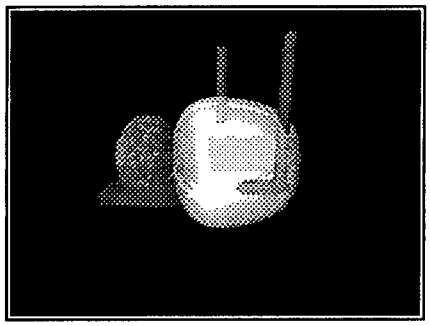

points, but it did not leave the ends open as Nurbs did. Next, an object representing the hypothalamus was created in Nurbs and placed in its proper position in the brain. Finally, two probes were made out of very thin cylinders and put into their places. one in the upper cortex, towards the middle of the brain, and the other into the hypothalamus.

It was also necessary to insure that every part was in the correct proportion to the rest of the brain. A stereotaxic map of the rat brain was used to measure the various parts. These measurements

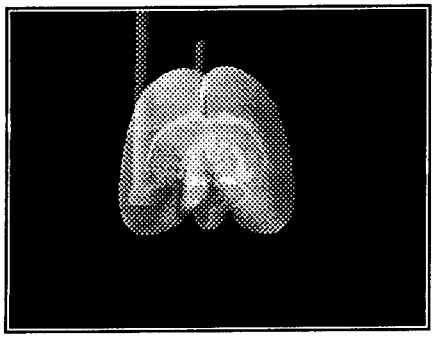

were then converted to the units of the screen and the different parts were multiplied by whatever factor was necessary to make it realistic. Once the structure of the brain was created, various color attributes needed to be added to make it more visually pleasing and easier to understand. The cortex was originally red and 70 percent transparent so that the inner part of the brain could be seen from the outside. However, the cerebellum was green and it was realized that a color blind person would not be able to easily distinguish the two. The cortex was then changed to white and the cerebellum an orangish tint. A blue color covered the brain stem and the hypothalamus, along with a 60 percent transparency on the brain stem. The corpus collosum and the frontal lobes were given a yellow shade and 60 percent transparency. Purple was chosen for the optic nerves while the probes were left a grayish-white. In addition to its color, a bump map was found in the Texture Editor and applied to the cerebellum. This gave the latter part of the brain a realistic, bumpy effect. The Texture Editor is another tool that contains many different types of textures which can be applied to an objects surface. After the colors of the brain pleased the viewer, the lighting had to once again be adjusted to properly illuminate the inside of the brain. It seemed that no matter how many lights were positioned on the sides, one side would be blacked out, or the entire cortex would turn up washed out. This problem was finally solved by putting a light underneath the brain, where there were hardly any structures (other than the cortex) to block the light.

A fly through of the brain then needed to be created to go along with the model. The first part of the animation involved camera movements, along with the rotation of the brain 90 degrees clockwise around the y-axis. Then the camera slowly straightened out and moved inside of the brain, traveling from

the front to the rear, through the middle. At the end of the cortex, the camera turned, looked up through the top of the brain at a 25 degree angle, then slowly backed out of the rear of the brain. The most difficult part of the animation was the mathematics involved with trying to keep the camera moving at equal speeds throughout the entire fly-through. Each key frame had to be positioned at a particular point in space, or the camera would randomly speed up or slow down. Also, in earlier versions of the animation, the camera did not turn around inside the brain, but rather went straight out the back and then turned. The problem with this was that too much time elapsed where nothing was shown on the screen as the camera was turning. This was solved by "skipping" over empty space and jumping between one spot and another in between key frames.

Another animation was requested as an opening for promotional videos. Since the work was done in the Radiofrequency Dosimetry Imaging Lab, it was decided that a radar would be more than appropriate to incorporate as part of the opening sequence. Since a -DXF file of a radar could not be found or bought, NURBS were once again used to create the dish of the radar. This was a fairly simple task as opposed to the parts of the brain since it simply consisted of a curved rectangular prism. A thin, sharp cone served as the attachment of the dish to the base of the radar unit, constructed from a large cube. Texture Editor provided a dark. black metallic texture for the entire object. A thin rectangular board, with the image of clouds at sunset on it, was positioned behind the radar to give the illusion of a background. After the setting was created, the animation remained as the sole task to perform. The radar dish was set to rotate continuously around the y-axis in a clockwise direction. With each new sweep of the dish, a new title appeared and a spotlight went over the title to highlight the individual letters. The first title displayed the title of the labs "Air Force Research Laboratories", followed in the next sweep by the location, "Brooks Air Force Base, Texas", and finally the division, "Radiofrequency Radiation Division". The title was given a shining gold texture, while the location displayed a chrome format. The division's texture required a little more work since it was desired that it be steel blue. GIG does not have steel blue as a texture, but rather, only offers black and gray steels. After some experimentation with the Red-

Green-Blue (RGB) values of the texture, a steel blue was created. The desired effect for the spotlight was to cause each letter to glint as it passed over it. This worked fine for the gold, however the chrome would not reflect the light. This is due to the fact that it was all ready reflecting nothing but light. Without the shadow of an image to bounce off the chrome, no change would be observed when it was highlighted. So, another cube was added with a light directly in front of it, which reflected onto the chrome. The steel blue could not be made to reflect the spotlight, even when the intensity was increased. All that the increased intensity served to do was to white out part of the dish.

The final project that was needed to be done in GIG involved a monkey phantom. Gel had been put into bags in the shape of a monkey phantom, and then scanned using Magnetic Resonance Imaging (MRI), producing 338 images showing the outline of a monkey at various points in the body. The goal was to then convert these images into a -DXF file so the entire wireframe model of a monkey could be manipulated inside of GIG. A program called NUAGES would extract the contours from each individual image, put the them all into one text file, and then convert the contours into one large wireframe. A copy of this program was obtained free-of-charge off of the Internet, and used to create a monkey wireframe.

Modifications

As with anything dealing with computers, problems always arise and change plans slightly. On the eyeball, the TIFF image of the arteries and capillaries would not remain in the same spot from frame to frame. This was discovered after the first rendering when red lines began to crawl all over the eyeball, an effect that was very undesirable. Upon this discovery, it was decided to take the image off of the retina and choroid, leaving them a solid white. Also, the effect of having the eye turn red when the cone came on, gave the false impression that millimeter waves are harmful to the eye. Instead of having such a dramatic change, it was decided that a solid blue color throughout would prove more effective and accurate.

On the rat brain, the two individual lobes of the brain overlapped in the middle, causing it to look very unrealistic and cluttered inside the cortex. So, a single cortex was created in Nurbs to replace the individual right and left lobes. Another problem with the animation was that the camera seemed to move

too quickly during its fly-through of the cortex, meaning that the entire animation had to be redone. This in itself is a large disadvantage of GIG, since the individual frames of each track can not be edited. Once an animation track is laid down, the track can be shortened or prolonged as a whole, but it is impossible to manipulate individual key frames. For instance, if the first fifteen frames were fine, but the last thirty needed to be redone, the entire track would have to be deleted. This is especially frustrating when an animation contains thousands of frames with many complex movements. Due to the complexity of the brain itself, rendering proved to be an extremely slow process. To solve that problem, it was decided to eliminate certain inconsequential features of the brain, such as the optic nerves and the frontal lobes. This rendering problem did not apply specifically to the brain, but affected everything that was done in GIG because a large amount of time was required just to render one frame in some cases. This made it very difficult to see the effects of the lights or any changes made to them as well as many other aspects of the model.

The radar also contained many inherent problems simply because of the length of the animation.

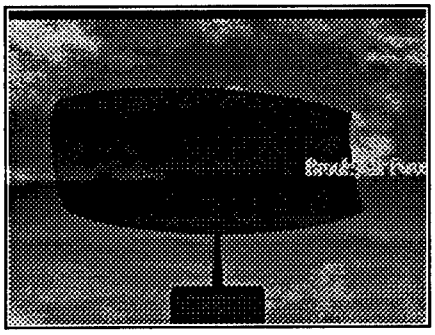

At 49 seconds, it was the longest of all the animations and thus provided the most opportunities for errors to occur. At first, the second set of words revolved around the back of the dish, however this did not look very realistic, so the entire animation track involving the words had to be deleted. Also, the dish would not rotate around its base, but rather the y axis, which was slightly offset. This caused the dish to move into space as it rotated. This problem was solved by maneuvering the radar onto the y-axis and then rotating it again. Also the words would not rotate facing outwards at all times to complete the half circle, instead they rotated around their local axes. This problem was solved by setting key frames at every 45 degrees and moving and resizing the words manually, instead of letting the animation perform the changes. Of course, this also created much more work when the track had to be redone. As always, lighting problems had to be dealt with so that the objects were appropriately lit, but not bleached out by the spotlights.

Finally, the conversion of the TIFF images to a -DXF file of a monkey was not nearly as easy as it seemed. It proved difficult simply to find the correct syntax for the commands to begin with, much less understand the proper order of them. The biggest problem was discovering how to perform batch processing with the command, since none of the normal UNIX batch variables, such as * or # seemed to be working. It was finally discovered how to create a loop to put all of the files into one large image file, whose contours could be extracted all at once. After this was accomplished, the -DFX file proved to be worthless, which meant that the extraction had gone awry. After careful examination of the code, it was realized that the image files could not be 24-bit images, so they were converted into 8-bit. However, this did not solve the problem, so they were converted into -PGM (Portable Gray Map) files, which also did not work. After several e-mails with Bernhard Geiger, the developer of NUAGES, he eventually sent us a shell script designed specifically for the monkey phantom files, along with a note suggesting that the images be converted into binary -PGM files. (see Appendix) The script was written to accept -TIFF images, so it was necessary to modify it to accept the binary images that had already been created. Once applied, this script proved to be successful and created a proper monkey phantom. However, this phantom was not hollow, although it was also very large in terms of file size. A quick study of the header for the nuage command yielded a "-no_int" option which allowed the -DXF file to be created without any internal vertices. Still, the file remained quite large, so a little more in-depth reading of the UNIX code showed a constant entitled "verbos", which was simply a BOOLEAN variable that could be switched from True to False and controlled the amount of vertices that were out into the wireframe. After changing "verbos" to True, the nuage command became interactive and allowed the user to greatly decrease the amount of vertices included in the file. This cut the file size by half, making it much easier to work with.

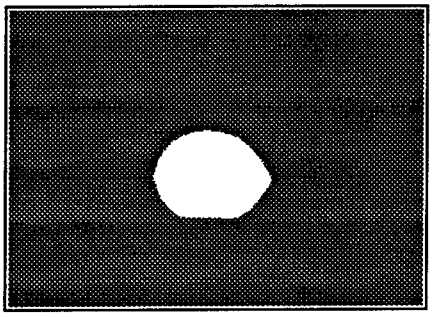

The next step was to take this phantom and turn it into an animation which would preceed the eyeball animation. As the viewer zoomed in on the monkey phantom, the eyeball would be superimposed on the face, then the camera would cut to the eyeball alone. When placed into the monkey phantom, the eyeball, looked greatly out of place, since the phantom had no facial features whatsoever. Since this

looked crude and elementary, the decision was made to use the MRI scans of an actual monkey. The same code and procedures could be used, however the image size had to be changed on the extraction command. A problem did arise when nuages was called for these images, since "verbose" needed to be false in order for the images to process correctly. This was easy to change, yet, as a result, the file size was doubled. Since the MRI monkey contained more than twice as many images as the phantom, this was a great cause for concern. In fact, when nuages did attempt to once again process the images, the disk that the temporary output file was assigned to, quickly filled up, thus terminating the program. This problem was eventually solved by editing the code and changing the destination of the output file to a disk with much more room. With this done, the monkey was created, in a file with a size of 70 megabytes. An enormous amount of space for one -DXF file.

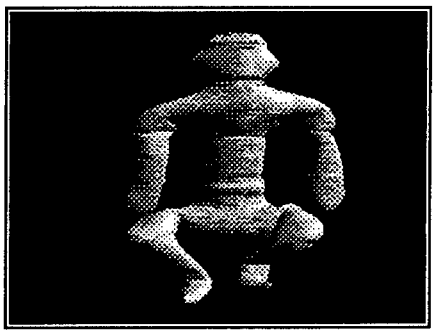

Conclusion

There can be no doubt that computers will play an increasingly important role in the development of science and the spread of information. More and more software is being developed to fit any imaginable need for presentations and entertainment. However, complexity must be balanced with versatility. The modeler used here was not designed for wide commercial use in homes and offices everywhere. The vast number of options and capabilities prevented that from occurring. Nobody in this day and age wants to have to read three separate and very large manuals to simply get started. Most home programs require very little knowledge or computer skills to operate, so that the average person can enjoy them. Therein lies the difference between industry and home software. The biggest disadvantage to this software was in fact its endless capabilities, because it was necessary for a person to sit down and literally read the manual if a problem was encountered. This took quite a bit of time, however, once a person is familiarized with the software, they can then create very complex projects in a relatively short amount of time.

Not only is knowledge of one program necessary, but proficiency with several others is also useful, because of the amazing interactive capabilities that many programs now share. Images and files can be designed in one program, then exported to the other. Of course, none of this can occur without the proper hardware. A fast computer is essential to have any hopes of completing any amount of work. As detail and quality increases, so does files size, while speed greatly decreases. Huge amounts of memory on the very best computers are needed simply to run some of the programs at their minimal capacity. It is essential that newer and newer technology is constantly invested in if any truly outstanding work is to be done. However, after great investments of time and money, the possibilities for creativity are as exciting as they are numerous. With the perfection of NUAGES, virtually any object can be scanned and turned into a realistic DXF file. It would be a very simple task to take MRI images of a human and create an individualized model of their body. This model could then be used to show the patient exaclty what is wrong with them and where the ailment is located. Also, a very useful teaching tool could be created for medical students who are just beginning to learn anatomy and physiology. Even more advanced doctors could benefit by possibly performing virtual surgeries without ever cutting into the patient. Without the use of computers in today's professional world, it is far too easy for crucial information to be lost in the endless expanses of the human memory, or be simply ignored. Truly, computers and modeling programs such as these are necessary to help science and researchers compete for their due recognition in the next millennium.

While all of this research and work has certainly given me a better knowledge of computers, I have come away from this summer with far more. Of all the benefits I have received, the most far reaching is the experience I have gained from working with others and depending upon my own abilities. Far too often, our educational system spoon feeds students the answers to any challenging problem and lowers the standards to make their ineptness seem acceptable. This summer, no one lowered any standards for me, and anytime a problem seemed too great, I was simply forced to work a little harder. This was often frustrating, but the satisfaction it provided at the end of a successful job was immense. Finally, I was able to do something that was of benefit to others, instead of completing worksheets and filling in the blanks on tests. Luckily, I was kept challenged throughout the summer, which increased my

confidence in myself as more and more difficult projects were assigned to me. Out of all the jobs I could have filled this summer, this was one of the few which would actually give me a sense of accomplishment upon its completion.

References

Adobe. Adobe Photoshop 3.0 User Guide. Adobe Systems Inc. : Mountain View, CA, 1994.

ElectrogGIG. GIG3DGO Reference Manuals. ElectroGIG BV : San Francisco, 1995.

Paxinos, George; Watson, Charles. The Rat Brain. Academic Press Inc. : San Diego, 1986.

Appendix

Syntax to Create a -DXF file

Convert -TIF to PGM Raw
foreach a (name*.tif)
cat b=$a:r'.pgm'
imconv -tif $a -rpgm $b
end

Extract Contours
extract.sh name output.cnt

Combine Contours into -DXF file
./nuages output.cnt -tri output.dxf -dxf -no_int

Respond yes to all questions, except object header query

Note: Make sure that "verbose" in 'nuages' is set to 1 to keep the file small. If it does not compile this way, set verbose back to 0. Check to make sure that the pixel sizes in the 'extract.sh' script are the same as the images to be extracted from.

A STUDY OF THE 39-40 HZ SIGNAL TO DETERMINE AN INDEX OF GRAVITATIONAL INDUCED LOSS OF CONSCIOUSNESS

M.S. Caspers

Douglas MacArthur High School
2923 Bitters Road
San Antonio, TX 78217

Final Report for:
High School Apprentice Program
Armstrong Laboratory

Sponsored by:
Air Force Office of Scientific Research
Bolling Air Force Base, Washington, DC

And

Armstrong Laboratory

August 1997

A STUDY OF THE 39-40 Hz SIGNAL TO DETERMINE AN INDEX OF GRAVITATIONAL INDUCED LOSS OF CONSCIOUSNESS

M.S. Caspers, R.M. Echon, P.W. Werchan

Abstract

For many years, humans have been the limiting factor in flying high-performance aircraft. Since G-LOC (Gravitational Induced Loss of Consciousness) is a very dangerous aspect of flying, many scientists have been looking for a reliable index to predict the onset of unconsciousness and thereby prevent G-LOC.

This study is concerned with finding a reliable and reproducible index of unconsciousness which presently has not been found. Our group decided to search EEG frequency in the 30-40 Hz range, hypothesizing that the 38-40 Hz range, specifically, would yield the best results for an index.

During an +Gz acceleration profile, the EEG signals from adult, male Sprague Dawley rats (*Rattus*) were recorded and used to test the hypothesis. First, the rats underwent EEG implantation surgery, where four brain electrodes were implanted. The rats were then put into a +Gz restraint and bolted into the centrifuge. Finally, a +Gz tolerance test consisting of +5Gz, +10Gz, +15Gz, +17.5Gz, +20Gz +22.5Gz, and +25Gz profiles was performed. Each profile is thirty seconds long with a five minute rest period between each profile. If the rat became iso-EEG, which means there is a total lack of EEG power on any given +Gz profile, then the experiment would cease and the data would be analyzed.

Using Fast Fourier Transforms (FFT), the raw EEG scores were changed to time (seconds) versus EEG power in μV rms /Hz. When the data was normalized, a significant reduction in EEG power occurred in the twelve to thirteen second window. To achieve a more pronounced representation, the data from the two to thirteen second window was changed to a percent reduction in EEG power, post acceleration. When the

twelve to thirteen second window was graphed, the +5Gz had the greatest percent of EEG power and the +25Gz the least. Therefore, an inverse relationship is identified between the +Gz's and percent of EEG power.

One interesting phenomenon is that an enormous power spike occurs at the eight to nine second window. Here, the two to nine second window was changed to a percent of EEG power increase, post acceleration. When this phenomenon is graphed, the +5Gz has the least percent of EEG power, and the +25Gz has the greatest percent power, thereby identifying a direct relationship between the +Gz and the increase in EEG power. This power spike is seen in all the tests at nine seconds where the EEG power spike is followed by iso-EEG three seconds later. It is possible that we could use this power spike to predict the onset of G-LOC.

Purpose

As technology advances and we build aircraft with astonishing maneuvering capabilities, humans continue to be the limitation in flying these marvels. Since these advanced, tactical aircraft can exert a punishing G-load on the pilot, they can easily render pilots incapacitated in seconds. In order to understand G-LOC (Gravitational Loss of Consciousness), it is imperative to have a dependable and reproducible index of unconsciousness which presently has not been identified. This project is to find a reliable index of unconsciousness.

Hypothesis

Other studies searching for an index of unconsciousness used the 0-30 Hz range and met with little or no success in finding a reliable index of unconsciousness. Our group decided to take the next logical step and examine the intra-hemispheric differential signal in the 30-40 Hz range at +5Gz, +10Gz, +15Gz, +20Gz, +22.5Gz, +25Gz (Review). We hypothesize that the best trends for the index of G-LOC lie specifically in the 38-40 Hz range. This experiment will test the 38-40 Hz range for a concrete representation of unconsciousness.

Materials

1. one adult, male Sprague Dawley rat
2. one electric razor
3. electro-cautery device
4. 2mm drill bit and threading device and 4mm screwdriver
5. stainless steel screws soldered to an insulated wired with gold plated connectors (used as electrodes)
6. plastic pedestal for the connector
7. methyl metacrylate (cranioplastic cement)
8. suture kit
9. Buprenex pain killer
10. +Gz restraining device
11. Small Animal Centrifuge (SAC)

} Brooks AFB, San Antonio, TX
Armstrong Laboratory

12. computer with LabView Power Slice Software for Fast Fourier Transforms (FFT) and Microsoft Excel

Method

1. Using halothane anesthetic (3%), put the rat to sleep for surgery.
2. Shave the scalp.
3. Make a 3.5 cm incision, and expose skull with the electro-cautery device.
4. Drill two sets of bilaterally symmetric holes with the 2mm drill bit. The first pair is located over the frontal cortex, and the second pair located over the parietal cortex. Then thread the holes for the screws (See Figure Below)
5. Insert stainless steel screws into the holes and the put the gold-plated connectors into the pedestal.
6. Mix methyl metacrylate to secure the electrode wires into the pedestal and secure pedestal to skull.
7. Suture the scalp together leaving no gaps.
8. Inject Buprenex as pain killer.
9. Wait at least four hours for rat to recover all preoperative motor abilities.
10. Secure rat in centrifuge restraint, and add the appropriate padding for the mass of the rat. (Fig. 8)
11. Run +Gz test of 5, 10, 15, 17.5, 20, 22.5, 25g's in the SAC. Each profile runs for a duration of thirty seconds, followed by a five minute rest period.
12. EEG Records Data of the intra-hemisphereic differential signal on an EEG strip chart. Also save the EEG signal in the computer for further study.
13. Take raw EEG score and run data though Power Slice for FFT.
14. Normalize the data using Equation 1.

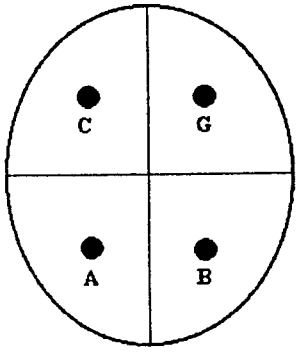

Method and Materials are for only one trial.

EEG
Implantation
Surgery

Recovery
Time

to centrifuge:
EEG monitor

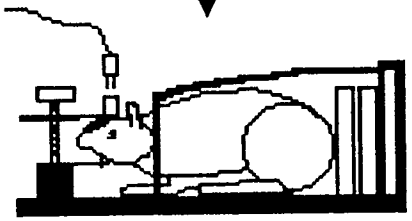

+Gz Restraining Device

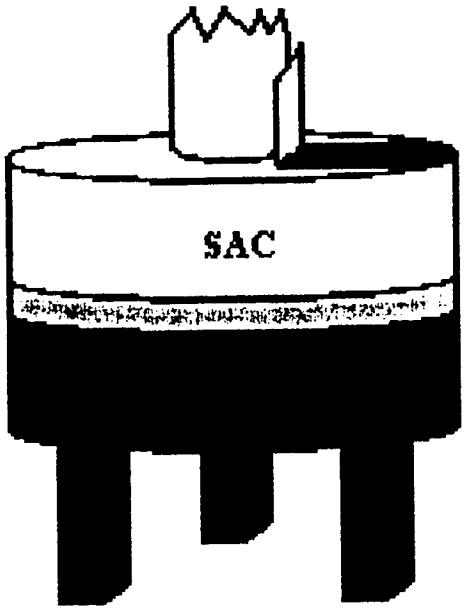

The +Gz Profile

+5Gz

5 Minute
Recovery

+10Gz

5 Minute
Recovery

Profile continues in this
manner with the +15Gz,
+17.5Gz, +20Gz,
+22.5Gz, +25Gz.

However, if the rat goes Iso-EEG on any of the +Gz profiles and does not recover immediately, then the experiment is over, and the rat does not proceed to the next +Gz profile.

Analyze the Data.

Conclusions

After all the data from the experiment had been normalized (Equation 1), some very interesting phenomena were observed. When the data from the two to nine second window was corrected to be a percentage of increase (Equation 3), post acceleration, an interesting phenomenon was observed. In this eight to nine second window, there is an extraordinary increase in EEG power, which illustrates a direct relationship between the +Gz and the EEG power. The two to nine second window is chosen for correction because at the zero to one second there is an enormous power spike due to the shock of acceleration, which gives an inaccurate representation. Since the rat does not lose consciousness in the +5Gz, but does in the +25Gz, this spike could be a last struggle to remain conscious before G-LOC (Gravitational Induced Loss of Consciousness). This is very important because this power spike at nine seconds could be a signal flag that G-LOC is going to occur three seconds later (Graph 1)

In the normalized graph (Equation 1) a reduction in EEG power can be observed in the 38-40 Hz range. In the +25Gz profile, the percentage of EEG power sharply decreased from 150.70% above baseline at eleven seconds to 30.57% above baseline at twelve seconds. After the twelve second mark, EEG power remained at an average 23.05% above baseline. In an ideal EEG profile, the normalized graph should show a significant EEG power reduction in the twelve to thirteen second window, and there should be no iso-EEG recovery. To test this window, the data from the two to thirteen seconds of all the +Gz tests were corrected and graphed (Equation 2) to show the percent of EEG power reduction, post acceleration. The two to thirteen second window is chosen because at zero to one seconds there is an enormous spike in EEG power due to the shock of acceleration. Moreover, the two to thirteen second area is a relative "plateau" of excited brain activity, post acceleration, but immediately prior to the EEG power reduction at the twelve to thirteen second window. When the reduction is plotted, it shows exactly what was anticipated. The graph has the highest percent of EEG power at

+5Gz, where the rat does not lose consciousness, then as the +Gz increase to +25Gz, the EEG power decreases, thus illustrating an inverse relationship between +Gz and the EEG power (Graph 2).

The 30 Hz signal produced no pattern to G-LOC in the selected profiles. You can easily see that the 39 Hz signal gives a better representation of the data, since the reduction pattern is visible at these lower +Gz. In order to see the reduction pattern in the 30 Hz signal the subject would most likely have to be subjected to excessive G-forces (Graph 3)

In the 38-40 Hz range on the normalized +25Gz profile (Equation 1), a power spike occurs at an average of 4.5 seconds after the twelve second mark with the first oscillation at fourteen seconds and the next at eighteen seconds. The maximum EEG power spike is at twenty-three seconds, which is followed by two more spikes at twenty-eight and thirty-two seconds respectively. Furthermore, the fourteen, eighteen, twenty-eight, and thirty two second spike are all approximately equal, and approximately one-half the power of the twenty-three second maximum. These oscillations could be autonomic brain functions being picked up by the EEG. This EEG profile is graphed on a bar graph instead of the area graph so a more pronounced representation could be achieved (Graph 4).

38-39 Hz EEG Power Increase at 8-9 Seconds

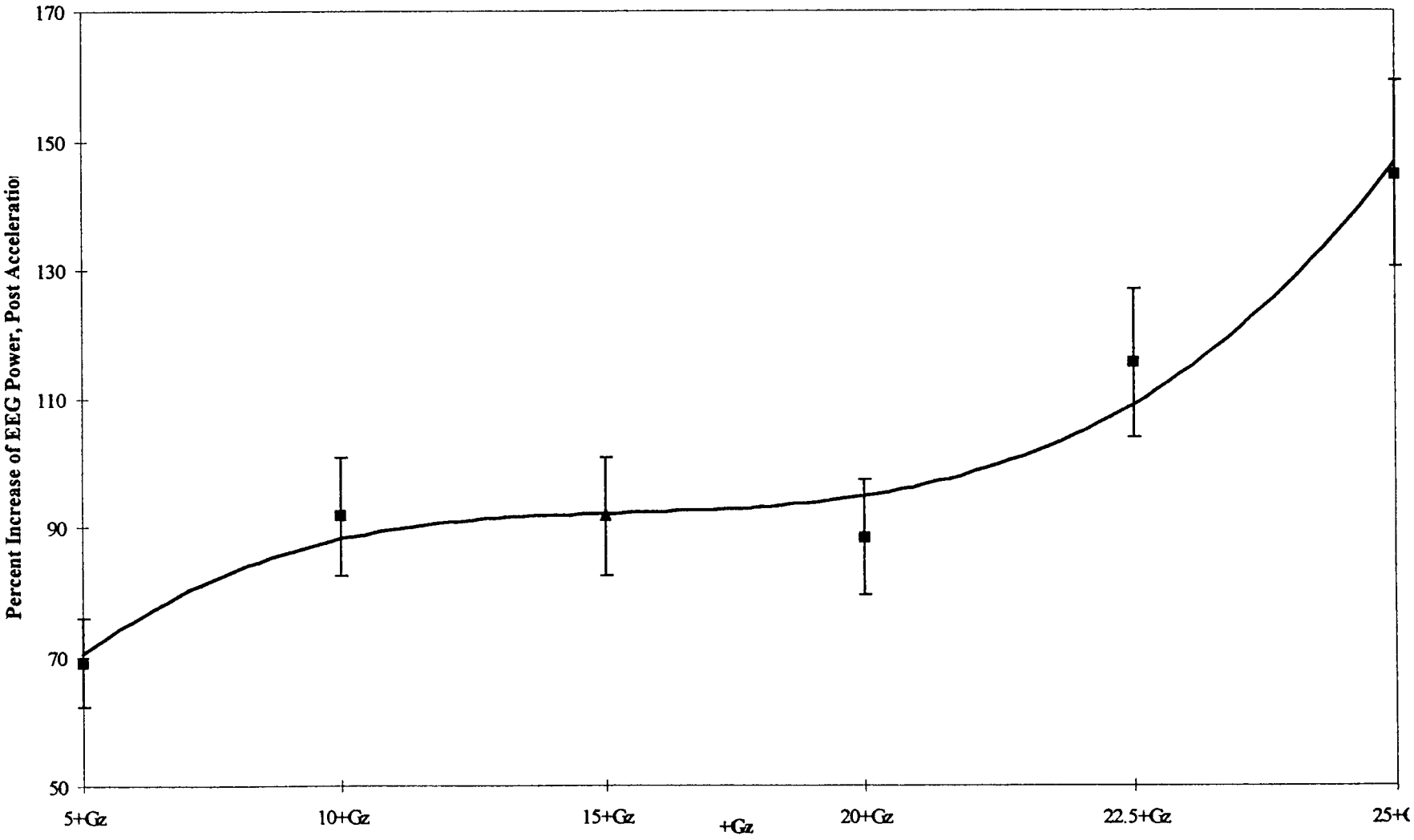

Graph 1

39 Hz EEG Power Reduction at 12-13 Seconds

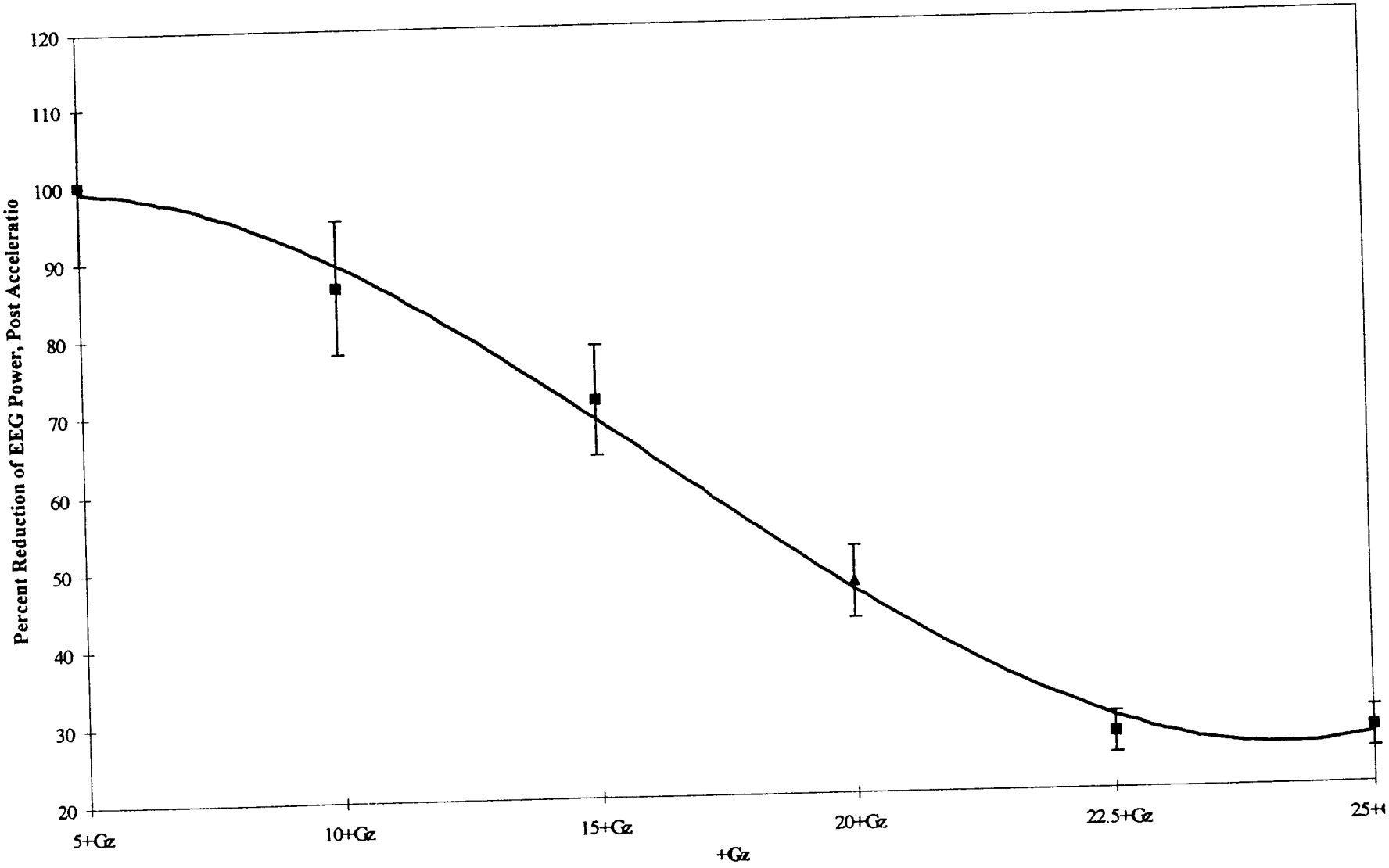

Graph 2

30 Hz EEG Power at 12-13 Seconds

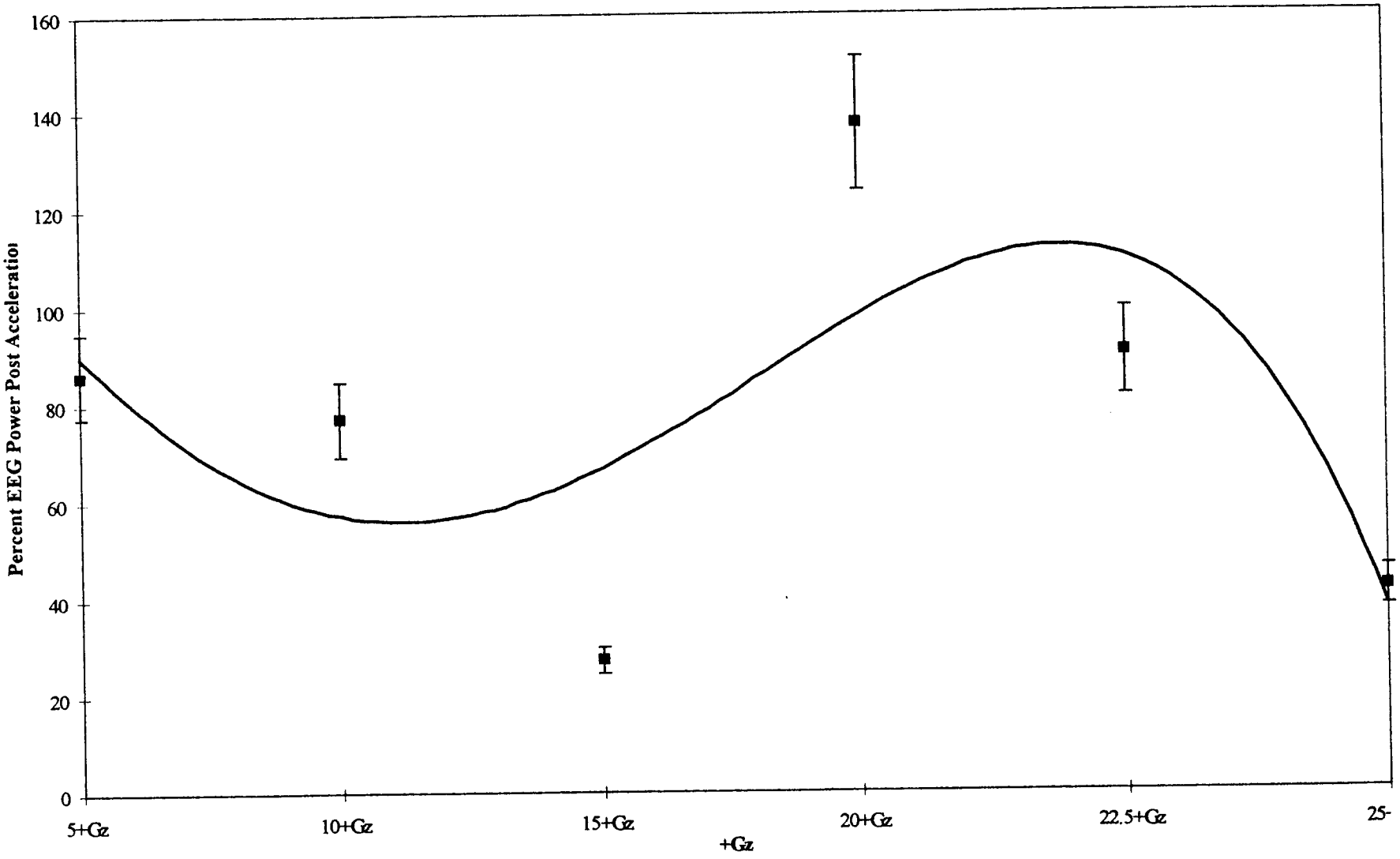

Graph 3

Normalized Average 38-40 Hz Signals at +25Gz

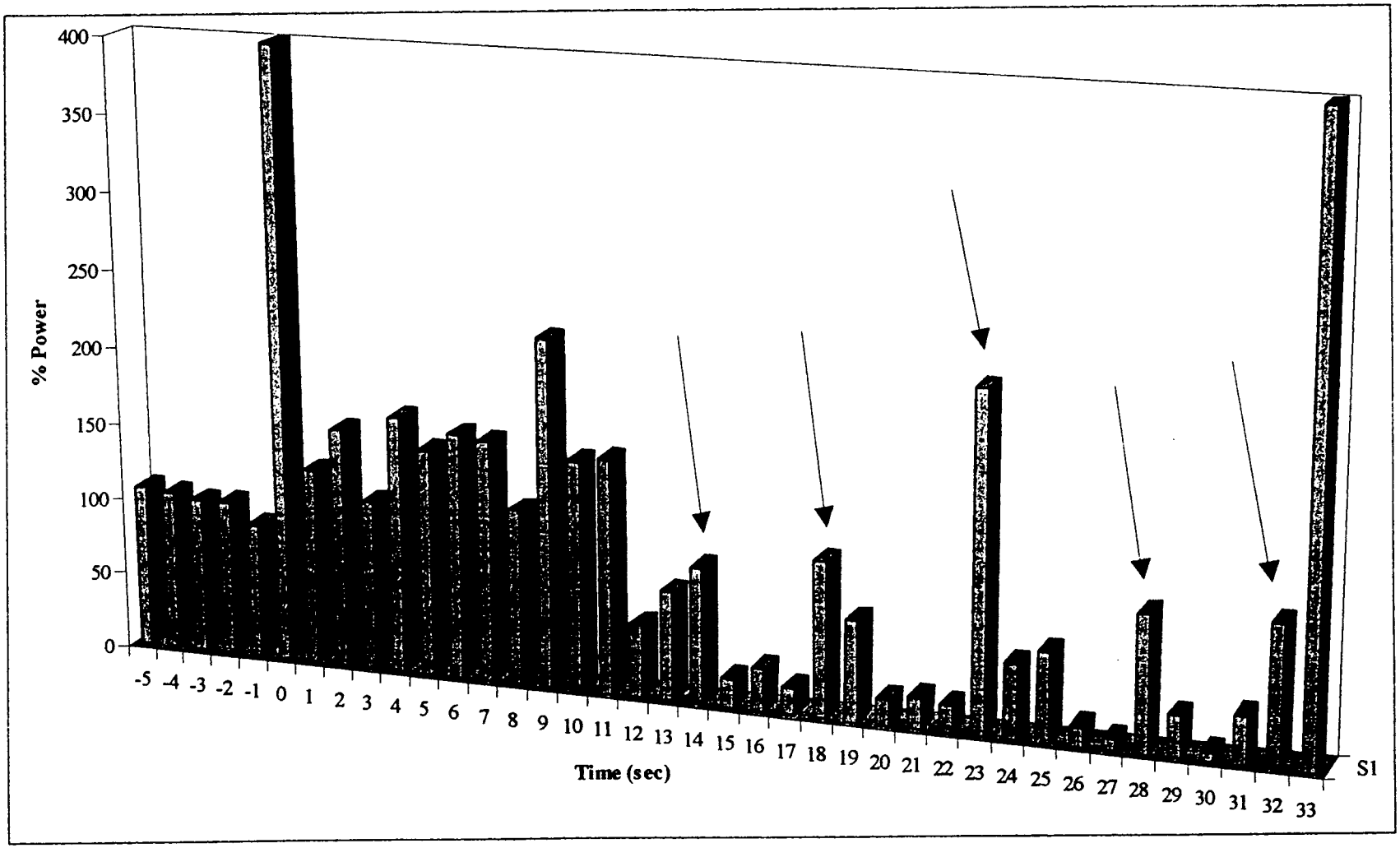

Graph 4

Applications

There are numerous applications for the results of this project. The most obvious is for pilots of high performance aircraft. By having a precise, reliable, and reproducible index of unconsciousness, we are another step closer to being able to prolong G-LOC (Gravitational Induced Loss of Consciousness) induction time, and perhaps even prevent G-LOC. Even if we are unable to completely prevent G-LOC, we can now predict the onset of G-LOC and program an auto-pilot to take control of the aircraft when it detects G-LOC. After the pilot regains his faculties, he can regain control of the aircraft and continue unharmed. Thus we save a life and an airplane.

By having a reliable index of unconsciousness, we have furthered our knowledge of the central nervous system and its mechanisms. Having an index of unconsciousness takes us one step closer to knowing the complete "wiring" of consciousness. This index is a stepping stone to understanding why our brain ceases to function under hypergravic stress.

Limitations

When working with any living system, there is always a major limitation with the behavior of a subject. Each subject is unique such that it behaves differently to stimuli. This fact creates a problem when basing conjecture on behavior. For this reason many subjects are needed for testing to assure the accuracy of the data.

A limitation when working with EEG's is the electrical "noise." The EEG's occasionally produce extremely erratic signals, which we know to be false. If the noise is not identified on the strip chart, then the results can be misleading.

References

Bloom, Floyd E. (1994). Neurotransmission and the Central Nervous System. Neuroscience. 267-288.

Echon, R. M. (1996). Neurophysiological and Pharmcological Characterization of the +Gz Induced Loss of Consciousness. UTHSC of San Antonio and AL/CFTF Brooks AFB.

Giancoli, Douglas C. (1991) Physics. New Jersey: Prentice Hall.

Kool, Kenneth A. (1971). Fundamentals of Electroencephalography. New York: Harper and Row.

Lukatch, Heath. (1996). G-Force Induced Alterations in Rat EEG Activity: A Quantitative Analysis. Electroecephalography and clinical Neurophysiology Journal.

Posner, Michael I. (1994). Review: Attention: The Mechanisms of Consciousness]. Institute of Cognitive and Decision Sciences, 91, 7398-7403.

Newman, James. (1995). [Review: Thalamic Contributions to Attention and Consciousness]. Colorado Neurological Institute, 4, 172-193.

Walker, James S. (1988). Fourier Analysis. New York: Oxford University Press.

Werchan, Paul M. (1991). Physiologic Bases of G-Induced Loss of Consciousness (G-LOC). Aviation, Space, and Environmental Medicine. 612-614.

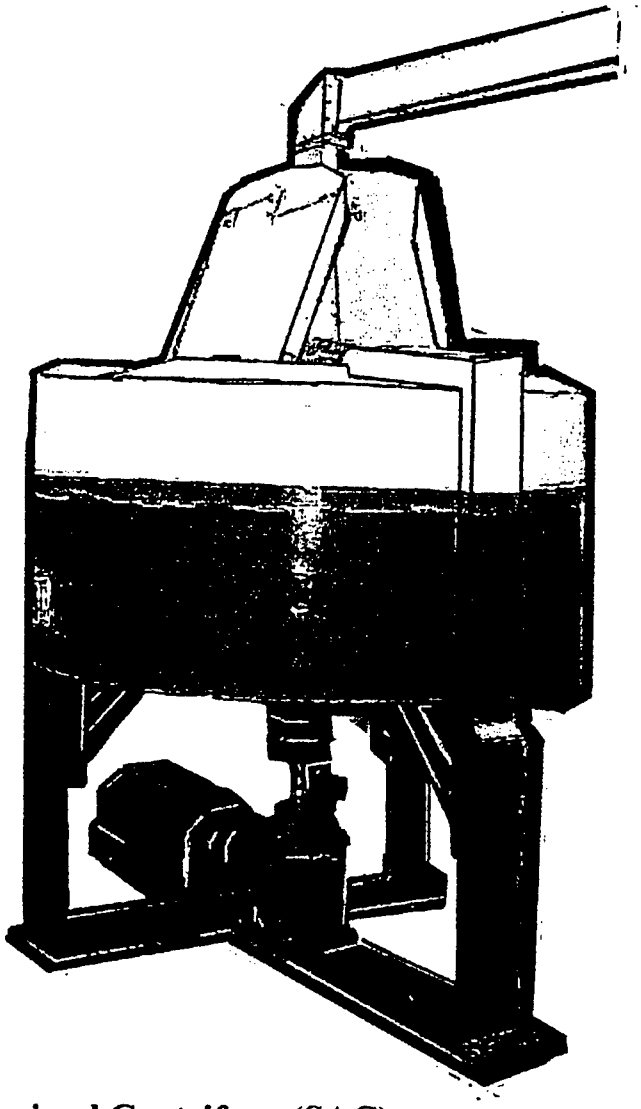

Small Animal Centrifuge (SAC)
-Photograph by Medical Division at Brooks AFB, San Antonio, TX

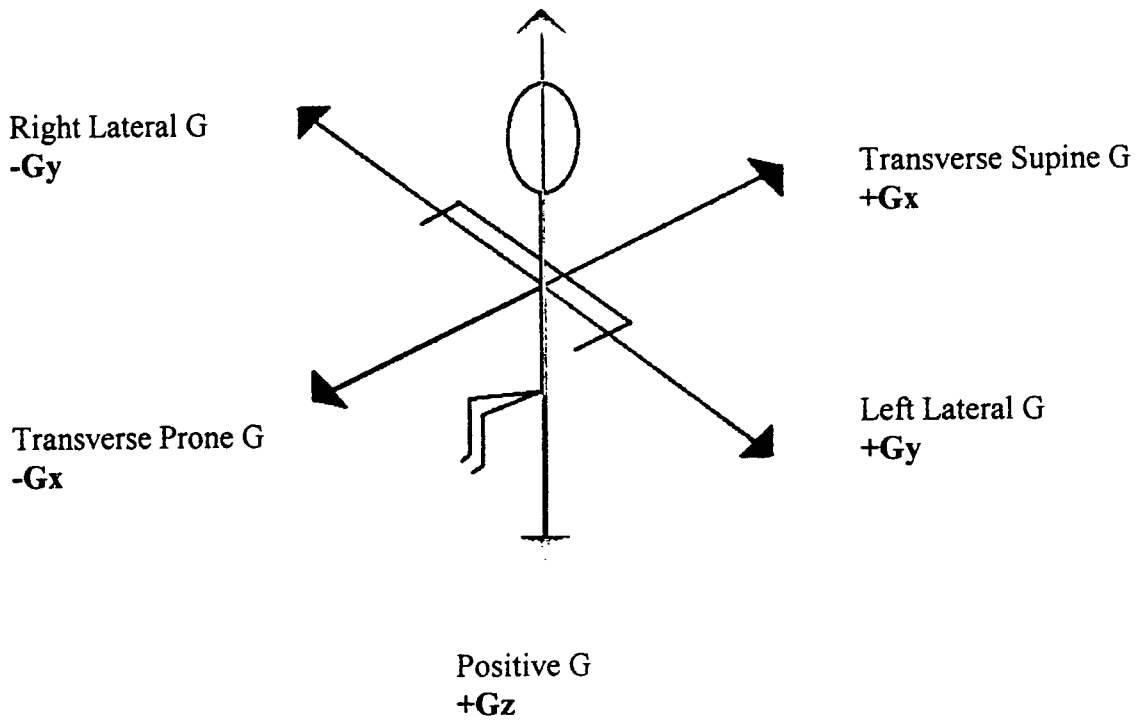

G-force Diagram

A STUDY OF PITCH AND CONTACT ASSOCIATED WITH THE OPENING AND CLOSING OF VOCAL CORDS

Elizabeth M. Cobb

Belmont High School
2323 Mapleview Dr.
Dayton, Ohio 45420

Final Report for:
High School Apprentice Program
Armstrong Laboratory

Sponsored by:
Air Force Office of Scientific Research
Bolling Air Force Base, DC

and

Armstrong Laboratory

August 1997

A STUDY OF PITCH AND CONTACT ASSOCIATED WITH THE OPENING AND CLOSING OF VOCAL CORDS

Elizabeth M. Cobb
Belmont High School

Abstract

The opening and closing of vocal cords was studied. A group of thirteen subjects, 7 women and 6 men were chosen. With the use of the Kay Elemetrics System and CSL (computerized speech lab), each subject performed six lists of fifty MRT words and ten timit sentences. The .egg program was then used to determine the statistics of the data, and Excel was used to process the data onto a spreadsheet. The researcher was then planning to graph and compare the mean contact and pitch for each person.

A STUDY OF PITCH AND CONTACT ASSOCIATED WITH THE OPENING AND CLOSING OF VOCAL CORDS

Elizabeth M. Cobb

Introduction

Data was gathered from a small group of test subjects, six men and seven women. The object was to determine the mean percentage of open and closed vocal cord response . From this data a graph would be produced to show the average differences in pitch and contact for each person. The data could then be compared to each other person as well.

Methodology

This researcher used a variety of computer programs to convert the input into useable information for reporting purposes. The lists of words and sentences to administer to each subject were provided by another researcher. This researcher instructed each subject to palpate his or her throat for vibrations in order to place the laryngograph in the correct place to gather data. The subject then placed a headset on and fixed the microphone mouthpiece to the correct side of their mouth. In the CSL program, the researcher checked the settings for the laryngograph and the microphone for appropriate recording levels. The subject said three test words to determine the appropriate range for recording.

The researcher set the directory files for the correct lists and proceeded to gather the information. The program would save the speech in the .sp directory and the laryngograph information in the .egg directory. At the end of each list, the researcher would listen to the voice information saved in the computer to determine usable information and would visually check the .egg information for the same. Any problems with this information are caught and fixed in another file, then are deleted from the original saved file. This process is repeated for each list, six in total , administered two lists at a time in one week intervals to each subject.

The computer file is transferred from a temporary file into a permanent file per each person's name. The researcher then converted the .egg information to .nsp so the statistical program could read the data. After reading the data and saving each individual word's statistics, another file was created and the data transferred to Excel for spreadsheet information.

From the spreadsheet, averages per person per list were compiled and the researcher was planning to summarize the averages of all the words and lists to determine the complete average per person , the average for the complete subject group and the averages for all males and females. The plan was then to graph the differences between male and female pitch and contact.

Most of the data was compiled in the time allotted for the researcher to complete her project, but time did not allow for all of the statistics necessary to come to any reasonable conclusions.

The Effect of Hyperbaric Oxygenation on the Mitotic Division of Prostate Cancer Cells

Linda Cortina

Theodore Roosevelt High School
5110 Walzem Rd.
San Antonio, TX 78218

Final Report for:
High School Apprenticeship Program
Armstrong Laboratory
Davis Hyperbarics

Sponsored by:
Air Force Office of Scientific Research
Bolling Air Force Base, DC

and

Armstrong Laboratory

August 1997

THE EFFECT OF HYPERBARIC OXYGENATION ON THE MITOTIC DIVISION OF PROSTATE CANCER CELLS

Linda Cortina
Theodore Roosevelt High School

Abstract

Prostate cancer is the most commonly diagnosed malignancy behind skin cancer. It is also the second leading cause of cancer death in U.S. men. Prostate cancer in its advanced stages is currently untreatable, thus there is a critical need for an effective treatment. For the experiment, malignant PC-3 cells were treated with hyperbaric oxygenation. It was hypothesized that the hyperbaric oxygen exposure will slow the growth rate of the cancer cells by stalling mitotic division. Effects of various pressure treatments ranging from 6 ATM to 0.32 ATM were tested. Experimental results indicated that .32 ATM was the most effective.

THE EFFECTS OF HYPERBARIC OXYGENATION ON THE MITOTIC DIVISION OF PROSTATE CANCER CELLS

Linda Cortina

Introduction

Hyperbaric oxygen is the inclusion of 100 percent oxygen at two to three times the atmospheric pressure at sea level. The resulting effect can include arterial oxygen tension in excess of 2000 mm Hg and oxygen tension in tissue of almost 400 mm Hg. The benefits of such oxygen doses include positive biochemical, cellular, and physiologic effects. The pressure expressed for hyperbaric oxygen is in multiples of the atmospheric pressure at sea level, which is 1 atmosphere. At sea level, the blood oxygen concentration is .3 mL per deciliter. Under the administration of 100 percent oxygen at ambient pressure increases the amount of oxygen dissolved in the blood fivefold to 1.5 mL per deciliter.

Methodology

Plating Cells:

Prostate cancer cells were grown in flasks in RPMI-1640 growth media. For experimentation, the PC-3 cells were plated at 10^6 cells per plate in petri dishes. The plating of the cells was accomplished by decanting the media in the flask and adding a 2 mL wash of Trypsin-EDTA. This wash was decanted and then an additional 2 mL of Trypsin-EDTA was added. The flask was then incubated for 5 minutes at 37 C. After incubation the flasks were agitated to dislodge cells from the flask wall and 3 mL of RPMI-1640 media was added. The 5 mL cell solution was then pipetted vigorously to prevent cell clumping. After performing cell counts, cells were diluted to be plated in petri dishes at 10^6 cells per plate in 10 mL of media. The plates were then allowed to incubate overnight to ensure the binding of cells to the culture dish.

Dosing Cells:

After overnight incubation, plates to be dosed were decanted and 2 mL fresh media was added immediately prior to hyperbaric oxygen (HBO) exposure. Plates were then placed in the HBO chamber on a level surface to ensure even distribution of media/oxygen. The chamber was flushed at 10 ft. below sea level for 5 minutes. The pressure was then raised to the desired level at a rate of 1 ft/sec. Once the desired pressure was reached, the dosing continued for 1.5 hours. After the treatment period, the pressure was lowered at a rate of 1ft/sec to bring plates back to surface pressure. Plates then received an additional 8 mL of media and were returned to the incubator.

Fixation of Cells:

Plates remained in incubation for 23.5 hours. They were then spiked with 25 uL of 40 mM BrdU solution. They were then allowed to incubate 30 minutes. The cells were then harvested, saving all solutions in a 15 mL centrifuge tube. The media in the plates was decanted and a 1 mL wash of Trypsin-EDTA was added. This wash was decanted and an additional 1 mL of Trypsin-EDTA was added. The plates were then incubated for 10 minutes at 37 C. After incubation the cell solution was pipetted 30 times to break up and clusters and was then added to the 15 mL centrifuge tube. The plates were then washed with 1 mL of media two times, adding the remaining solution to the centrifuge tubes after each wash. The centrifuge tubes were then spun in the centrifuge at 1 K for 10 minutes. The supernatant was decanted and the pellet was resuspended in 1 mL of 70% EtOH over a period of 5 seconds while vortexing at the lowest possible speed. The fixed cell solutions were immediately placed in 4 C refrigeration and remained there overnight.

Staining of Cells:

The refrigerated cell solutions were spun in the centrifuge at 1 K for 10 minutes. After decanting the supernatant, the pellet was resuspended in 1 mL of PBTB. Each cell solution was then split into 2 microcentrifuge tubes (mct) to be stained. One mct of fixed cells received both Anti-BrdU and PI staining. The solution was centrifuged at 4 K for 8 minutes. The supernatant was decanted and the pellet was

resuspended in 1 mL of 2N HCl and then was incubated at 37 C for 20 minutes. The solution was then spun at 4 K for 8 minutes, decanted, and resuspended in 1 mL of 0.1 M Sodium tetraborate. The solution was allowed to incubate at room temperature for 5 minutes, was then spun at 4 K for 8 minutes, decanted, and resuspended in 1 mL of PBTB. This solution was immediately spun down at the above speed and time. After decanting the supernatant, the pellet was suspended in 20 uL of anti-BrdU FITC conjugated antibody and incubated at 37 C for 30 minutes. After incubation, 1 mL PBTB was added to the mct. The cell solution was then spiked with PI solution (final concentration 50 ug/mL) and RNAase (final concentration 10 ug/mL) and incubated at 37 C for 30 minutes, covered in foil. Following incubation, the stained cells were placed in 4 C refrigeration for no less than 30 minutes. The second mct of cells suspended in 500 uL of PBTB were stained with only the PI and RNAase in the manner described above.

Results:

The results of our experiment are as follows:

Cell Type	**Cell Count**				**Total**
Control PC-3	386	210	178	159	
	200	259	239	176	1807
.32 ATM	83	66	118	96	
	80	172	150	90	855
.75 ATM	133	144	161	120	
	133	126	139	126	1082
1.5 ATM	145	142	200	150	
	152	115	118	105	1127
3 ATM	101	106	115	146	
	118	138	145	241	1110
6 ATM	120	200	108	111	
	93	104	93	103	939

Conclusion:

Based on the data collected, it can be concluded that hyperbaric-oxygenation can be used as an effective treatment for prostate cancer because Treatment would be most successful in stalling mitotic division at pressures of 0.32 ATM and 6 ATM. At .32 ATM, the number of cells decreased by 52.7% while at 6 ATM, the number of cells decreased by 48%.

MERCURY ANALYSIS BY COLD VAPOR BY ATOMIC ABSORTION

Maria Evans

John Jay High School
7611 Marbach Rd.
San Antonio, TX 78227

Final Report for:
High School Apprentice Program
Armstrong Laboratory

Sponsored by:
Air Force Office of Scientific Research
Bolling Air Force Base, DC

and
Armstrong Laboratory
Brooks AFB, TX

August 1997

MERCURY ANALYSIS BY COLD VAPOR BY ATOMIC ABSORTION

Maria Evans
John Jay High School

Abstract

The instrument used to analyze all mercury samples is called Perkin-Elmer Flow Injection Mercury System (FIMS). PE FIMS is specifically designed to determine the concentration of mercury at the low part per billion level. The analytical technique employed is cold vapor, atomic absorption spectroscopy. All samples are digested according a standard operating procedures which were developed by the Environmental Hygiene Agency and the National Institute for Occupational Safety and Health. Sample type include water, waste water, soil sludge, industrial materials and air collected on solid sorbant material. The results of analysis are used to help safeguard the health of Air Force personnel who work with mercury containing equipment and to protect the environment from further contamination during the use of this equipment.

MERCURY ANALYSIS BY COLD VAPOR
BY ATOMIC ABSORTION

Maria Evans

3.1 INTRODUCTION

3.1.1 MERCURY ANALYSIS BY COLD VAPOR

There are several instruments that are used here at Armstrong Laboratory/ Occupational Chemistry Branch. In the Metals Analysis Function: Perkin-Elmer Flow Injection Mercury System (FIMS) Model 400 mercury analyzer, ICP-Mass Spectrometer (MS), Flame Atomic Absorption Spectrometer (AAS), Furnace (AAS) and Argon Plasma- Atomic Emission Spectrometer (ICP).

PE FIMS 400 is specifically designed for determining mercury concentration in the low parts per billion range using cold vapor, atomic absorption spectroscopy. Waste water, air samples, and soil samples are analyzed using these technique.

The method is applicable to water regulated under the National Primary Drinking Water (NPDW) and the National Pollutant Discharge Elimination System (NPDES). These samples are suitable for the determination of total mercury content in the concentration range between 0.2 and 20 ug/L Mercury (Hg).

3.1.2 WHAT KIND OF SAMPLES ARE ANALYZED

Samples containing organic and inorganic mercury are analyzed in aqueous solutions, solid materials, and vapor collected on air sampling absorbent media.

3.2 DISCUSSION OF TECHNIQUE

Organic and inorganic mercury are quantitatively dissolved in aqueous solution by oxidation to the +2 state. In the analytical phase, the mercury cations are reduced to the atomic state by stannous chloride. The absorbance of a specific wavelength of ultra-violet light by the atomic mercury is proportional to the concentration if the mercury present. Sample concentrations can be determined by comparison of the absorbances produced by known mercury concentrations with the absorbance of the unknown.

3.3 METHODOLOGY

3.3.1 SAMPLE PREPARATION

Solids

For solids, 0.200 grams of the sample are added to a 50 mL plastic screwcap. Then, 2 mL of water and 2 mL of aqua regia is added. The samples are heated in a water bath for 2 minutes loosely capped at 95 C. Then the samples were removed and were allowed to cool at room temperature. Then, 15 mL of water and 4 mL of potassium permanganate were added to the samples. Then, all samples were capped and allowed to stand for 15 minutes. If the samples became colorless, an additional 0.5 mL of potassium permanganate was added until a purplish-brown color reappeared. Next, the samples were placed in the water bath which was heated to 95 C. They were allowed to cook for 30 minutes. Then all samples were removed and were allowed cool at room temperature. Next, bubbling air and hydroxylamine solution was added to the sample. All samples had to be

clear of potassium permanganate. Finally, the 25mL was brought up to 50mL and the samples were analyzed by (FIMS).

Waste waters

For waste waters, 25 mL of the sample was pipetted into a 50 mL plastic screwcap tube. Then, 1.0 mL of 0.5 N sulfuric acid and 1 mL of nitric acid was added to the samples. Next, 4 mL of the permanganate solution was added to the samples. All samples were capped and were allowed to stand for 15 minutes. After, the 15 minutes all samples were checked to see if they could retain the potassium permanganate. Following this 2 mL of persulfate solution was added. Then, all samples were capped and cooked for 2 hours in a water bath set to 95'C. Then, all samples were removed and were allowed to cool at room temperature. Next, 1.5 mL of hydroxylamine solution and bubbling air was used to reduce the excess permanganate. If the permanganate persists, an additional 0.5 mL of hydroxylamine is added to the solution. The samples were then ready to be analyzed.

Air

For air samples, the Hopcalite sorbant was removed from the front glass of the wool plug and placed in into a 50 mL plastic screwcap. Then, 2.5 mL of nitric acid and 2.5 ml of hydrochloric acid was added. Then, the samples were allowed to stand for 1 hour or until the black Hopcalite sorbant was dissolved. Next, the samples were diluted to 50 mL with deionized water. Then, the samples were allowed to stand for 30 minutes to an hour or until the samples noticeable solids had been settled. Next, filter any samples that required filtering. The samples were then ready for analysis.

Reagents

Different samples require different reagents here are some that we use: Sulfuric acid, Nitric acid, Hydrochloric acid, Stannous Chloride, Sodium Chloride-Hydroxylamine Hydrochloric solution, potassium permanganate, potassium persulfate, stock mercury solution, blank, Laboratory Reagent Blank (LRB), Laboratory Fortified Blank (LFB).

QC and Standards

There are eight types of quality control samples employed in this procedure. There are blanks, mid-level standard checks, QCs, run duplicates, sample duplicates, run spikes, matrix spikes, and Practical Quantitation Limit (PQL) checks. All of these QCs samples have a percent recovery acceptance criteria. Such as: mid-level standard check 90-110%, QCs 90-100%, and run spike 85-115%. The standards are numbered in this order: blank, 0.2, 0.5, 1, 5, 10, 20, and QCs 10. These standards contain 0 to 2.0 ug of mercury. When the standards have been cooked they are analyzed on FIMS. The QCs and the PQL are done before the samples are analyzed. Once this is done you can proceed with the analysis of the samples. After analyzing the samples, a mid-level should be done. The mid-level check should come out with in 10% of the true value.

3.3.2 INSTRUMENT SET -UP

There are four peristaltic pumps tubes which have to be replaced on FIMS. One tube is located at Pump 1. Pump 1 controls the delivery of the sample. Pump 2 has the other three and they control the delivery of the reductant and the acid carrier stream (fig 1). These tubes should be changed every other day. After changing the tubing you have to check the sample probe, the argon pressure, the system, the area calibrated wavelengths,

check the mercury waste container, and most of all, one has to perform a safety check. Next, change the PTFE-membrane (filter)and check all of the tubes in the manifold (figure [illegible]. After all of these procedures are taken care of you can start the automated or the manual analysis.

3.3.3 ANALYTICAL PROCEDURE

In opening the program for FIMS you would go to AA Winlab Analyst'Icon on the desktop. Then open FIAS. FIAS allows the reagents to go through FIMS and the probe. Here you should also check the tube to insure that all the tubing is connected properly. Next, you should go to workspace and open manual or automatic. Then, you should open the method and begin to analysis the samples. Begin with the standards. Next, do the standards and calibrated 0.20 and the QC should. Then the QC 10 should be done as a sample not as standard. Finally, analyze all samples and do a mid-level check with 10 standard as a sample.

3.3.4 QUALITY CONTROL

The absorbance of each sample standard and quality control is measured 3 separate times. And each time the samples are ran they must be within 5% of the true value. Performance of the QC and mid-level are chartered as the percentage of the true value to determine the long term trends that may indicate out of control analysis parameter.

3.4 RESULTS

3.4.1 INTERPRETATION

Sometimes samples tend to come out high such as a spike. A spike should come out around 8-10 ug/L. If a spike doesn't then it is safe to believe that something maybe interfering with the sample. Any sample reading below .20 is meaning less.

3.4.2 CALCULATIONS

FIMS uses a calibration curve that plots the peak absorbance value of the known standards versus their concentrations. The value unknown is obtained by plotting the determined peak absorbance on the standard curve.

QC calculations are as follows: Take the given calculation (observed mean) from the print out in divide it by 10 (true value). Then multiply it by 100 to get the % recovery. The range should be around 80-120%.

PQL and Mid-Level calculations are as follows: The same as above but the range is 90-110%

Run Duplicate calculations are as follows: The absolute value of the difference divided by the average of the values express as a percentage.

Spike calculations are as follows: The spike value minus sample contribution divided by the true value. The percentage is between 85-115%.

3.4.3 SUBMITTING FINAL ANALYTICAL RUN PACKET

When submitting a final packet the following things must be done. You must fill out a form that is called a RUN NUMBER CONTROL SHEET FOR MERCURY FIMS ANALYSIS. This gives the analytical run a unique number and annotates the analyst. Then a OCCUPATIONAL METALS CHECKLIST must be

completed. This tells the Technical Reviewer who did what, what tasks were performed, the run number, in what machine was used. Next, a form called STANDARD AND QC PREPARATION LOG FOR MERCURY ANALYSIS BY FIMS 400 must be filled out this has the stock reagents, the unique ID number, initial concentration, initial volume, final volume, final concentration for the samples standards and QCs. After, this a Hg Digest Log must be filled out. This states what the run number, the amount of the final volume, sample ID number, date, and stock reagents. Next, a form called QC SUMMARY SHEET FOR FIMS 400 MERCURY. This form is were up put your QCs, PQL, mid-level, run dup., run spike, ms, Ms., and correlation coefficient number results. You also have to do the calculations for the samples in turn it in with this form. Next, a form called PREVENTIVE MAINTENANCE AND FUNCTION form must be filled out. This form is a guideline on checking the machine and making sure that the parts are working correctly. Finally, a form called QC Chart for Hg is used to plot the results onto the graph.

3.5 CONCLUSIONS

Results are used to determine industrial hygiene, and environmental compliance, for Air Force Bases and Support and Maintenance Operations. Since the first World War, warfare has become increasingly industrial and technical in character. Mercury monitoring is just one aspect of insuring the safety and health of people engaged in deployment using modern weapon systems and the integrity of the environment in which they are stored.

3.6 REFERENCES

Perkin-Elmer Environmental Application Note
Perkin-Elmer Method 245.1A DETERMINATION OF MERCURY IN DRINKING WATER AND WASTEWATER BY FLOW INJECTION ATOMIC ABSORPTION SPECTROMERY (COLD VAPOR TECHNIQUE)

DEPARTMENT OF THE AIR FORCE
OE Analytical Services Division (AFMC)
Brooks AFB,TEXAS
OPERATION OF THE PE FIMS 400 MERCURY ANALYZER
METALS ANAYLSIS FUNCTION
STANDARD OPERATION PROCEDURE 48-907
21 FEB 97

Perkin-Elmer FIMS
Flow Injection Mercury System
Part Number 0993-5202
Publication B3118.10
Release 1.1/ Jun 94.

3.2 The FIMS Spectrometer

3.2.1 The FIMS Control System

AA WinLab is the name of the software application which you use to control your analyses.
AA WinLab uses a graphics user interface running under Microsoft Windows.

3.2.2 Components on the Front Panel of FIMS

FIMS-400

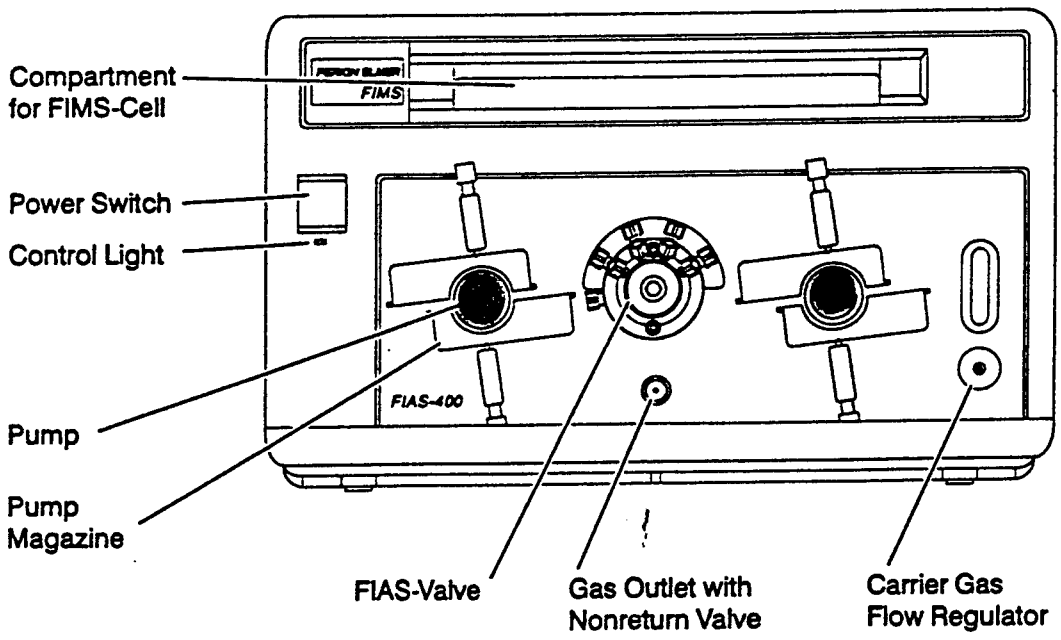

B3118.10 Release 1.0

(FIG. 1)

Key: Pump1 [redacted] Pump2 [redacted]

3-3

1.5.6 Assembling the Manifold

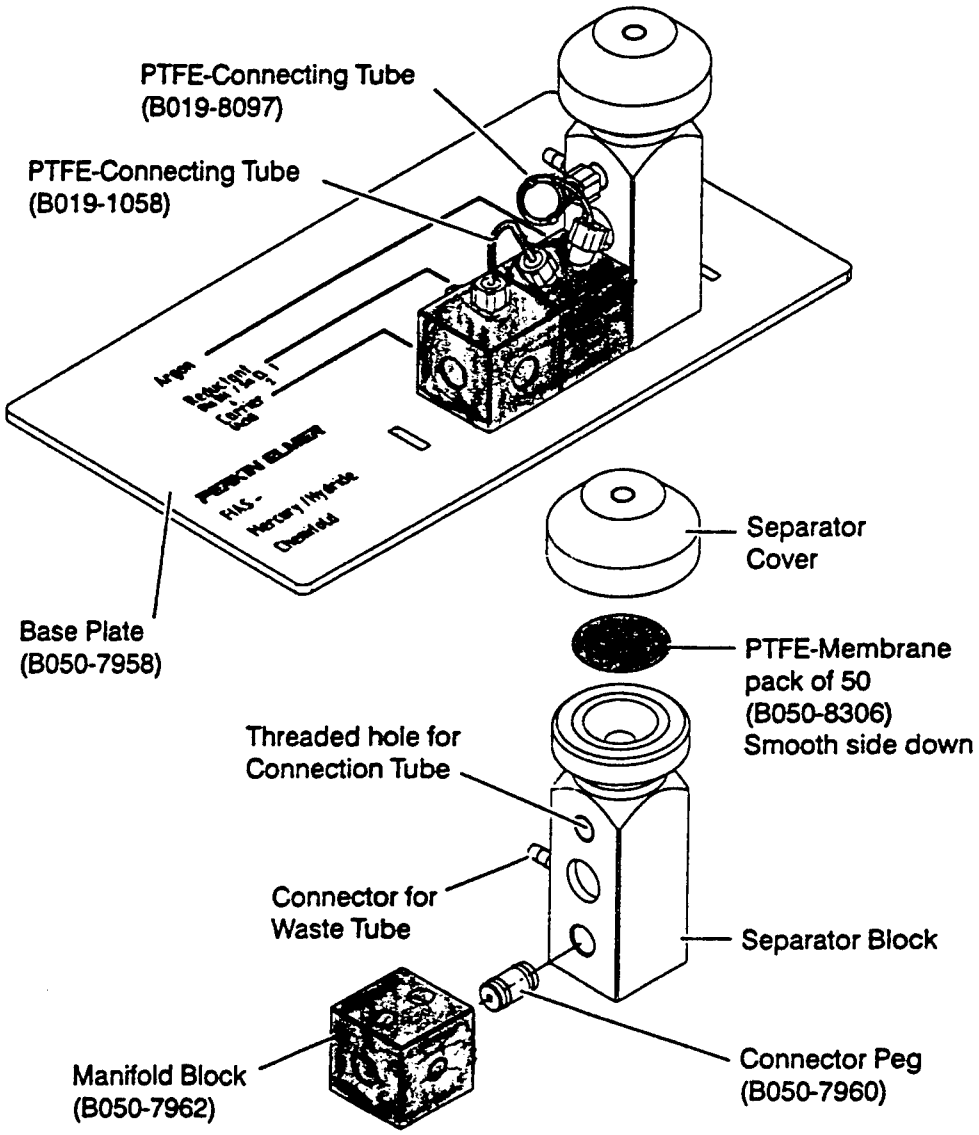

1-22

Key:
Manifold Block
PTFE Tubes

B3118.10 Release 1.0

NEUROPSYCHOLOGICAL EXAMINATIONS FOR PILOTS

Daniel L. Hardmeyer

James Madison High School
5005 Stahl Road
San Antonio, TX 78247

Final Report for:
High School Apprentice Program
Armstrong Laboratory

Sponsored by:
Air Force Office of Scientific Research
Bolling Air Force Base, DC

and

Armstrong Laboratory

August 1997

NEUROPSYCHOLOGICAL EXAMINATIONS FOR PILOTS

Daniel L. Hardmeyer
James Madison High School

Abstract

Neuropsychological testing is administered to UPT pilots, the normal pilot population, and certain special cases. Neuropsychological testing is a factor in the selection of pilots. When pilots are having certain problems (neurological or psychological) they are given these neuropsychological examinations. Testing is also administered under other special circumstances.

NEUROPSYCHOLOGICAL EXAMINATIONS FOR PILOTS

Daniel L. Hardmeyer

Neuropsychological testing is a very important tool in assessing the personality/abilities of pilots and in helping with problems they might be having. UPT pilots are tested to see if they have the personality traits common to pilots, and their results are a factor in whether or not they become a pilot. Pilots with head trauma, depression, alcohol problems, marital problems, and many other such neurological/psychological problems are also tested. There are special cases in which non-pilots and special groups, such as helicopter pilots and gunners are tested, as well.

Many different tests are given. Some personality batteries that are given are: the Minnesota Multiphasic Personality Inventory (MMPI), the NEO Personality Inventory Revised (NEO-PIR), the Millon Clinical Multiaxial Inventory-III (MCMI-III) the Personal Characteristics Inventory (PCI), the Cornell Index, the Beck Depression Inventory (BDI), the Structured Sentence Completion Test, the Recent Life Events questionnaire, the Cockpit Management Attitudes Questionnaire (CMAQ), and the Aircrew Coordination Survey. The MMPI, NEO-PIR, MCMI-III, and PCI are all used to determine personality characteristics. Cornell Index is a true/false questionnaire that asks personal questions. The BDI is used to determine the presence and the level of depression of a patient. The Structured Sentence Completion Test is a page of half written sentences which the patient must finish with the first thing that comes to mind. The Recent Life Events questionnaire asks the patient if specific things have happened within the last year and to rate them in order to determine factors that might be leading to problems a patient is having, or factors caused by problems they are having. The CMAQ and Aircrew Coordination Survey are specifically for pilots, navigators, and aircrew to determine their attitude and approach towards their job.

NEUROPSYCHOLOGICAL EXAMINATIONS FOR PILOTS

Daniel L. Hardmeyer

The other category of tests is the neuropsychological battery. Included are: the Weschler Adult Intelligence Scale Revised (WAIS-R), the Multidimensional Aptitude Battery (MAB), the Selective Reminding test, the Grooved Peg Board, the Weschler Memory Scale Revised (WMS-R), and the Halstead-Reitan Battery. The WAIS-R and the MAB are IQ tests. The Selective Reminding test examines memory loss due to head injury by having a list of words read to the patient that must be repeated. Patients must insert grooved pegs into a pegboard as fast as possible in the Grooved Peg Board in order to test for mental slowing. The WMS-R is a memory test in which current events, digits, letters, words, time, and place must be recalled.

The Halstead-Reitan Battery is a series of tests for head trauma which consists of: the Aphasia Screening Test, the Category Test, the Finger Tapping Test, the Grip Strength, the Seashore Rhythm Test, the Sensory-Perceptual Examination, the Speech Sounds Perception Test, the Tactual Performance Test, and the Trail Making Test. The Aphasia Screening test screens for a partial loss of speech or comprehension resulting from brain damage. The Category Tests use a series of visually presented items to assess brain damage. In the Finger Tapping Test the patient taps their finger as many times as possible for ten seconds, and the results can indicate brain damage. The Grip Strength test is used to detect differences in hand strength to determine if there is lateral brain damage. The Seashore Rhythm Test is a measure of attention and concentration in diagnosing brain damage. In the Sensory-Perceptual Examination parts of the body are touched singly and simultaneously to assess brain damage. In the Speech Sounds Perception Test the patient hears nonsense syllables and must answer which one he is hearing on a multiple choice

answer sheet to determine left brain damage. The Tactual Performance Test tests tactile memory to assess brain damage. The Trail Making Test involves connecting circles to measure visual conceptual and visuomotor tracking.

Specific combination of these neuropsychological tests are given to different cases. The pilot's tests are administered at Brooks AFB in San Antonio, Texas and Wright-Patterson AFB in Ohio.

EFFECTS OF TIMED EXPOSURE TO DIBROMOBENZENE ON ARACHIDONIC ACID LEVELS IN SKIN USING A METHYL ESTERIFICATION QUANTITATION METHOD

Nafisa Islam

Centerville High School
500 E. Franklin Street
Centerville, OH 45459

Final Report for:
High School Apprentice Program
Armstrong Laboratory

Sponsored by:
Air Force Office of Scientific Research
Bolling Air Force Base, DC

and

Armstrong Laboratory

August 1997

EFFECTS OF TIMED EXPOSURE TO DIBROMOBENZENE ON ARACHIDONIC ACID LEVELS IN SKIN USING A METHYL ESTERIFICATION QUANTITATION METHOD

Nafisa Islam
Centerville High School

Abstract

The effect of exposure to dibromobenzene on arachidonic acid levels in rat and guinea pig skin was studied. In order to quantitate arachidonic acid levels by gas chromatography, the acid must be esterified. Thus, a time and temperature study was conducted first in order to optimize time and temperature conditions for methyl esterification of arachidonic acid. Afterward, guinea pigs were exposed to dibromobenzene by dermal contact. While most skin studies are conducted on bald animals, the animals used had hair. Following exposure, the skin was harvested and collected in samples. The epidermis and underlying lipid bilayer were scraped off and an extraction procedure was followed to isolate total lipid fractions, which should include arachidonic acid. The samples then underwent the methyl esterification process, after which they were analyzed by GC. Results were generally inconclusive, perhaps due to inconsistency in scraping off the epidermis.

Introduction

The study of toxicology deals with the effects chemicals may have upon biological systems. The toxicology of occupational chemicals is of particular importance due to possibly harmful effects upon workers who come into contact with that chemical. Dibromobenzene is an occupational chemical used as a solvent for oils, in motor fuels, for top-cylinder compounds and ore flotations, and in organic synthesis. Because dibromobenzene is a liquid, skin would be the most likely contact surface. Therefore, an inquiry into the interaction between dibromobenzene and skin is considered worthwhile.

Discussion of Problem

Arachidonic acid is being considered as a potential biomarker for exposure of skin to dibromobenzene. That is, guinea pig skin is examined for changes in arachidonic acid levels with exposure to dibromobenzene. However, arachidonic acid levels cannot be quantificated directly by GCMS. Samples must first undergo a methyl esterification process, after which the ester may be measured and analyzed. Thus, methyl esterification of arachidonic acid must be optimized as to time and temperature conditions. Then skin samples from different exposure time points are collected, the lipid fraction isolated, put through esterification and analyzed.

Methodology

In order to determine optimal time and temperature conditions for methyl esterification of arachidonic acid, acid solution samples were prepared for esterification at 60, 65, 70, and 75 degrees at 5, 7.5, 10, 15, 20, 25, and 30, minutes. The four temperatures selected were theoretically sufficient to allow the reaction to complete while not initiating decomposition processes in reaction components. With final concentration intended to be approximately 50 ppm, 100 ug arachidonic acid was placed in each sample (50 ul of a 2 mg/ml stock solution). As esterification reactions are acid catalyzed, 10 ul of BF_3, a strong Lewis acid, was added to each sample. To "tie up" the water produced during esterification 60 ul of dimethoxypropane was added to each sample. Also, 200 ul of methanol was added per sample. The excess of the methanol reactant, which provides the methyl group, and the presence of DMP to bind with the water product stress the reaction and cause it to move in a forward direction according to

solution and extract the methyl arachidonate. A second wash is made with another milliliter of hexane. The hexane is made sure to be dry by the addition of some anhydrous sodium sulfate. The hexane extracts can the be analyzed by GCMS. The following table summarizes the results of the esterification optimization. Samples were run in triplicate; area counts in the following table are an average of the three readings.

Time (min.)	Temperature			
	60	65	70	75
5	8663158	11113461	10894216	14346276
7.5	11020623	12100164	13596038	14338799
10	13061657	15891587	13723765	15508908
15	13945664	13868742	13982947	14203114
20	14152536	14346240	16384432	15231259
25	14878297	15748445	13447959	13598395
30	14160382	14651583	14620314	12106950

The next four charts show the relationship between time and area count at each of the four temperatures, and the fifth combines these charts.

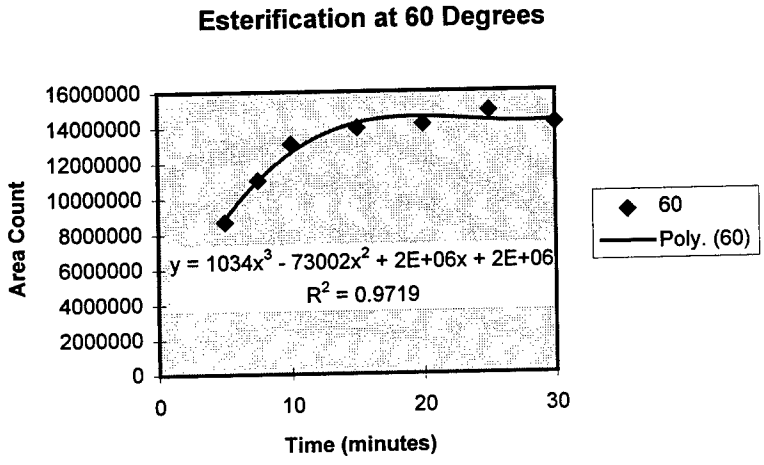

Esterification at 65 Degrees

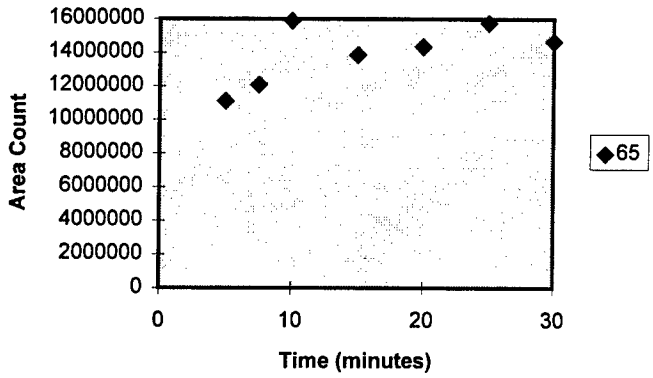

Esterification at 70 Degrees

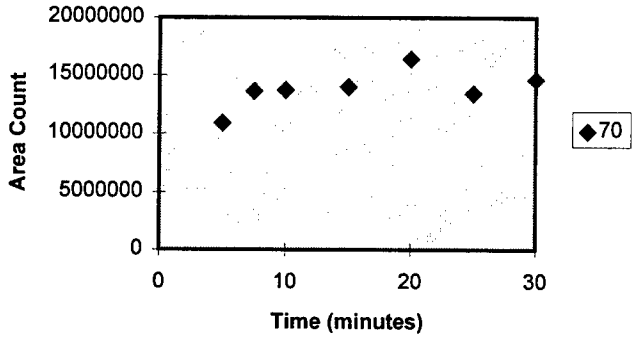

Esterification at 75 Degrees

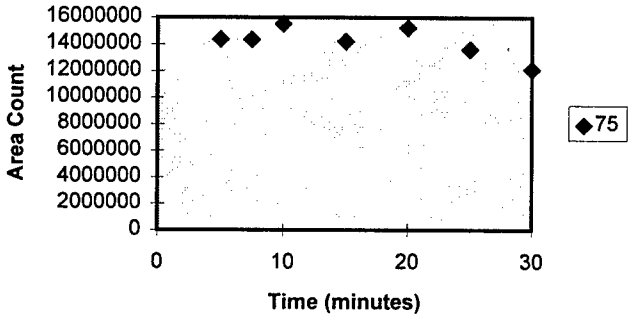

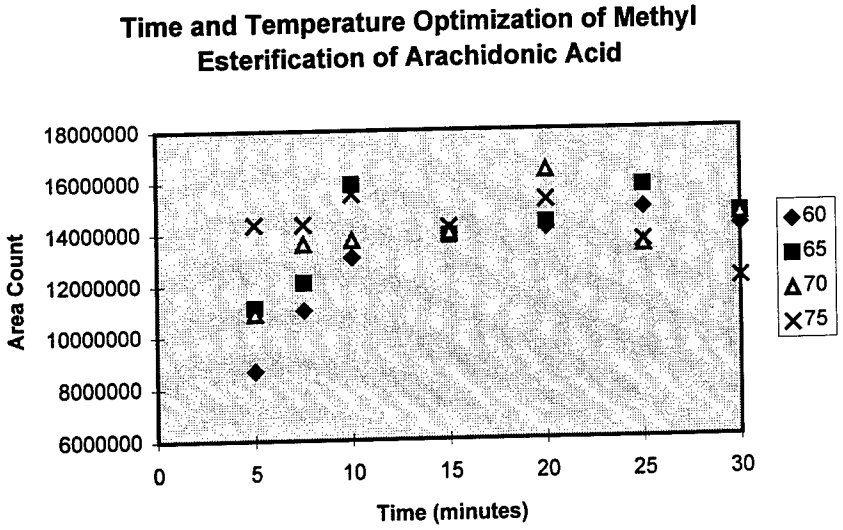

It can be seen from these results that the reaction appears to plateau in the vicinity of 15 million, outliers not exceeding 16 million. However, results are inconclusive as being indicative of optimal esterification conditions. Disregarding error due to instrument variation and human error during the esterification process, it seems that the reaction will go to completion at any of the four temperatures if allowed to incubate beyond ten minutes. Thus, 15 minutes at 70°C was settled upon for the methyl esterification process. At that point, the skin study could begin. Two areas of guinea pig skin were exposed to dibromobenzene with a corresponding area set aside as a control for 15, 30, 45, and 60 minutes. Following exposure the skin was harvested and the controls and exposed areas were cut out and weighed. The skin samples was then placed upon a drop of distilled water and floated on a water bath at 70°C. Immediately following incubation the epidermis and hair were scraped off—the consistency with which this was done is somewhat subject to doubt. Afterward, samples were homogenized by sonication in 400 ul 2:1 methanol-chloroform as done by Ramesha, et. al. (994). All samples were sonicated over an ice bath, then transferred to an extraction filter apparatus equipped with a teflon mesh filter. The sample container and hair were washed three times with 1 ml of a mixture of one part normal saline to 19 parts 2:1 chloroform:methanol. Samples were then dried under a nitrogen stream and reconstituted with 200 ul methanol, 10 ul BF_3, and 60 ul DMP. The samples were then put through the rest of the esterification process and analyzed by GCMS.

Results

The following table summarizes the results of the exposure analysis. Column 1 contains the sample name. For example, C2 15 denotes the control sample of a 15 minute exposure. T2 15 1 and T2 15 2 denote the two dibromobenzene exposures at 15 minutes. Column 2 gives skin weights in grams. Column 3 gives area counts generated by the GC and Column 4 contains area count per unit weight for each sample (the quotient of area count and weight). Column 5 generates sample concentrations based upon area counts and the methyl arachidonate standard curve below the table. Column 6 gives the average of the exposures, and Column 7 calculates percent difference for the exposures.

Column 1	Column 2	Column 3	Column 4	Column 5	Column 6	Column 7
Sample name	**Weight (g)**	**AAM Area Count**	**Ratio**	**Conc. (ppm)**	**Average (exposures)**	**%Diff**
C2 15	0.452	23880	52832	6		
T2 15 1	0.472	30391	64388	8	88354	43%
T2 15 2	0.24	26957	112321	7		
C2 30	0.281	38047	135399	9		
T2 30 1	0.185	28899	156211	7	160540	5%
T2 30 2	0.221	36436	164869	9		
C2 45	0.34	29810	87676	7		
T2 45 1	0.335	31068	92740	8	89262	8%
T2 45 2	0.314	26936	85783	7		
C2 60	0.289	54346	188048	12		
T2 60 1	0.328	16141	49210	5	58162	27%
T2 60 2	0.345	23154	67113	6		

AAM Calibration Curve

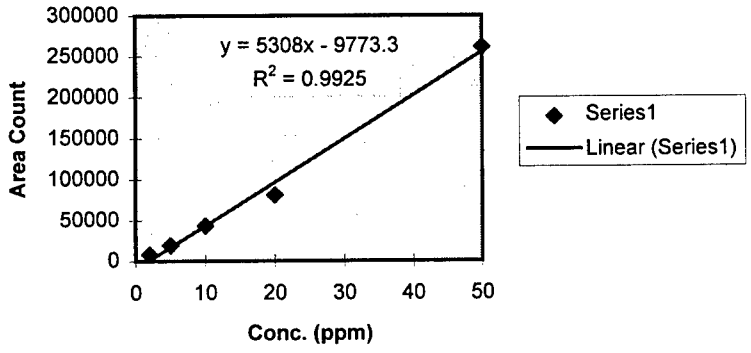

It is important to note the high variability among the controls in area count per weight values, the values used for quantification. Such a result is unexpected and is indicative of high variability in arachidonic acid levels in skin naturally, although a great deal of additional research would be required to determine this conclusively. Exposure values are also variable. Percent difference within the exposure sets at 15 and 60 minutes is considerable. As can be seen from the averaged area count per weight values of the exposure sets, there may be a trend for arachidonic acid levels in skin to rise upon initial exposure and then fall, but this result may be affected by natural variability, amount of epidermis scraped off, GC variability, having only two samples, etc.

Conclusion

At this point the effects of dibromobenzene on arachidonic acid are still inconclusive. Clearly further study is required to determine the natural variability of arachidonic acid content in skin and to what degree such variability would affect quantification following exposure. Perhaps exposures must be conducted for a longer time in order to changes in arachidonic acid levels beyond natural variability. Perhaps samples should be analyzed in replicate sets on the GC in order to reduce variability. Histological analyses should be conducted upon dermal samples after scraping the epidermis to determine how much of the epidermis was actually removed and consequently whether that is a significant source of variability. Certainly the experiment should be repeated several times, possibly with more exposure areas, to determine whether arachidonic acid levels do indeed rise and then fall with prolonged exposure.

References

Ramesha, C.S., Gronke, R.S., Sivarajan, M., and Lands, W.E.M. Metabolic products of arachidonic acid in rats. Prostaglandins. 29, 991-1007 (1985).

EFFECTS OF BRAIN TEMPERATURE ON FATIGUE IN RATS DUE TO MAXIMAL EXERCISE AND RADIO FREQUENCY RADIATION

Kathleen S. Kao

Keystone School
119 East Craig
San Antonio, TX 78212

Final Report for:
High School Apprentice Program
Armstrong Laboratory

Sponsored by:
Air Force Office of Scientific Reasearch
Brooks Air Force Base, TX

and

Armstrong Laboratory

August 1997

EFFECTS OF BRAIN TEMPERATURE ON FATIGUE IN RATS DUE TO MAXIMAL EXERCISE AND 2.07 GHz MICROWAVE RADIATION

Kathleen S. Kao
Keystone High School

Abstract

In previous experiments, it has been observed that fatigue in rats may be linked to hypothalamic temperatures (T_{hyp}) and that exercising rats become exhausted once the T_{hyp} has reached approximately 40.7-41.5°C. We attempted to prove the validity of this observation by subjecting a group of rats to two separate treatments, a microwave (MW) and a sham exposure, each followed by a run to exhaustion. Hypothalamic and rectal temperatures (T_{rec}) were measured continuously during their run. Each rat underwent both the microwave and the sham treatments. For the microwave treatment, the rat was placed in a Styrofoam restrainer and its T_{hyp} was heated with MW radiation up to 41.5°C. During the sham treatment, the rat was also restrained, but not exposed to any microwave radiation. There were significant differences in both pre-run T_{hyp} and T_{rec} between sham and microwave rats. However, there was no significant difference between the two treatments for either the peak T_{rec} or T_{hyp}. Although there existed no significant difference between the mean time to exhaustion of the sham and microwave groups, there was a significant difference between the heating rate and weight loss of the two groups. Because there was no significant difference between the mean peak T_{hyp}, we conclude that there exists a critical brain temperature which limits the ability to perform exercise.

EFFECTS OF BRAIN TEMPERATURE ON FATIGUE IN RATS DUE TO MAXIMAL EXERCISE AND MILLIMETER MICROWAVE RADIATION

Brandon B. Boke

Introduction

Although many different hypotheses have been proposed in an attempt to explain fatigue in mammals under hyperthermic conditions, the physiological mechanism underlying this effect remains unknown. While fatigue in thermoneutral conditions occurs as a result of hypoglycemia and muscle glycogen depletion, in hyperthermic conditions it occurs in the absence of those biological effects (2). It has been observed that exhaustion in exercising rats occurs when the hypothalamic temperature (T_{hyp}) reaches 40.7-41.5°C. (4). This suggests a possible link between T_{hyp} and fatigue in rats. In order to test this link, we performed a series of experiments using both exercise and millimeter microwave radiation (MW) to raise brain temperatures in rats above thermoneutrality. Because the performance ability in rats decreases after T_{hyp} has exceeded 40.7°C, we hypothesize that rats possess a centrally-mediated thermoregulatory response which reduces the large contribution of muscular work to the thermal load of the animal. This mechanism manifests itself in the form of exhaustion, but ultimately serves as a protective function to prevent the brain from reaching damaging levels. The purpose of the experiment is to test this hypothesis. Two different treatments were used in the investigation. One consisted of the rat being restrained and exposed to MW, causing the T_{hyp} to rise to an arbitrary temperature. This was immediately followed by a run to exhaustion on a treadmill with a thermally constant environment. The other treatment served as a control in which the rat was only restrained and then run to exhaustion. If our hypothesis proved to be correct, we would expect the rats to reach exhaustion faster following MW treatment because the T_{hyp} begins at a significantly higher temperature.

Methods

All rats were anesthetized with a combination of Ketamine (70 mg/kg; i.p.) and Xylazine (10 mg/kg; i.p.).

They were then placed on a thermostatically controlled water heating pad set to maintain a rectal temperature (T_{rec}) of 37°C. Stereotaxic surgery was then performed in order to implant Vialon guides (Becton Dickinson) into the hypothalamus of the rat brain. The coordinates for the tip of the hypothalamic guide were 1.8 mm posterior to bregma, 1.5 mm lateral from midline, and 8.3 mm below dura. The top of the hypothalamus guide was equipped with a threaded head cap connected to a Tygon TM tether tube used to contain the thermal probe. The guide was sealed at the bottom and held in place by cranioplastic cement (Plastic One, Roanoke, VA) anchored to nylon screws. These methods have been previously described in detail (3,5)

After two weeks of recovery from the surgery, the rats were familiarized with the Styrofoam restrainer and the motorized treadmill (Model: Dual Economy, Columbus Instruments, Columbus, OH). Each rat received four training sessions spaced no less than two days apart. Every session consisted of a period of familiarization in the restrainer and a ten minute run on the treadmill at a speed of 13.0 m/min. This protocol has been shown not to induce a training effect (1). The periods of familiarization began at 10 minutes and increased in duration up to 25 min.

Every rat in the experiment (n=10) was assigned a number, and each rat was eventually subjected to both treatments. In order to maintain a random design for the experiment two labels were made for all ten rats, one for sham (SH) and one for MW. These labels were then placed into a box and drawn one by one to determine the order in which the rats were used. After a rat had been selected for one treatment, the other label corresponding to that rat was removed until all the rats had been subjected to the first cycle of experiments. The rats were then subjected to the opposite treatment in the same order they were drawn to complete the second cycle of experiments.

All experiments were carried out between 1300-1500 hr. Rats to be used were restricted from feeding the morning before an experiment. Experiments were performed in an anechoic microwave chamber with an environmental temperature (T_{env}) of 21-23°C. Rats were brought into the chamber and weighed before each experiment. Post experiment weights were also measured to account for weight loss. Feces were

also collected from the end of the treadmill and subtracted from the total weight loss to yield fluid weight loss.

For all experiments, the rat was first fitted with a temperature probe inserted 5 cm beyond the rectum to measure rectal temperature (T_{rec}). The nonmetallic temperature probe (+/- 0.1 C, Model 101, Vitek, Boulder, CO) was secured by four pieces of silk surgical tape wrapped around the probe and the tail. With one individual operating the headgate, another experimenter inserted the rat into the rear of the Styrofoam restrainer. With the headgate closed over the rats' neck and a backstop in place behind the rat, the subject was then restricted from movement and ready for MW exposure. In the SH experiments, the rat was simply held in the restrainer for 5 minutes with no MW exposure.

All MW exposures (2.06 Ghz; CW) were conducted at an incident power density of 200 mW/cm^2 at the head with rats in the K, E, H polarization. During both MW and SH experiments, a Vitek probe was inserted into the hypothalamus guide and held in place by the Tygon TM tether and threaded screw. T_{hyp} was monitored at all times. Once the exposure began, T_{hyp} was allowed to rise to 41.5°C and then the MW transmitter was turned off.

Immediately following the MW or SH treatment, the rat was removed from the restrainer keeping both the rectal and hypothalamus probes attached to the rat. The rat was then placed on the treadmill already running at 17.0 m/min. The enclosed treadmill was on an 8% grade and was preheated to the target T_{env} of 35°C by a thermostatically controlled heating source. The T_{env} was maintained throughout the experiment within 1°C of the target T_{env}. In order to encourage the rats to run, the treadmill was also equipped with an electrical shocker on the end of the treadmill belt. The current running through the shocker was held constant throughout all the experiments.

Temperatures were manually recorded every five minutes beginning when the rat was placed upon the running treadmill. Vitek instrument displays and a profile of the running rat were also recorded on videotape for data backup and more detailed analysis at a later time.

Once the rat reached exhaustion, which was defined as the point in time at which the rat, despite electric shock, was no longer able to keep pace with the treadmill, it was removed and allowed to cool off on the

chamber floor. The point of exhaustion was determined by an investigator blind to both the temperature measurements and the exercise time. The rats were given a minimum of two weeks to recover from their first run before undergoing the other treatment.

Statistical analysis was performed using Statistica (Versiion 5.0, StatSoft, Tulsa, Ok) software, t-tests on dependent variables for repeated measures.

Results

During the MW treatments, the mean T_{hyp} following exposure was 40.8 ± 0.06°C. The mean T_{hyp} following the restraining period during the SH treatments was 39.3 ± 0.06°C. This represents a significant difference in pre-run hypothalamic temperatures between the MW and SH treatments (Fig. 1).

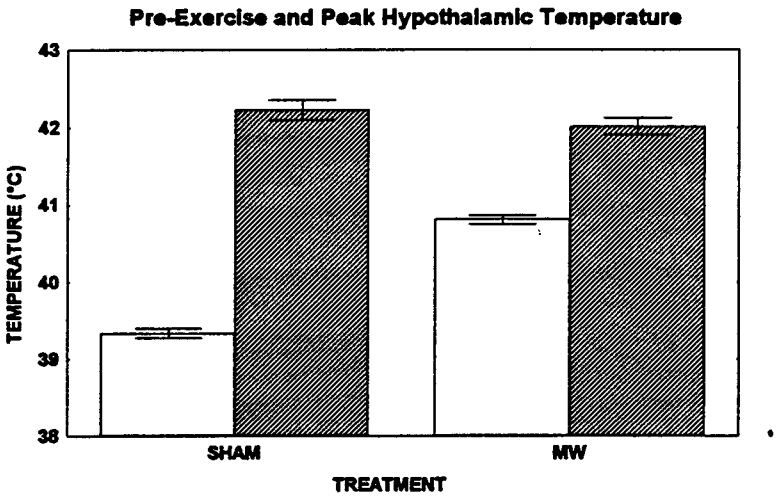

Figure 1.

There was also a significant difference in pre-run rectal temperatures between the two treatments with the MW T_{rec} at 40.4 ± 0.07°C and the SH T_{rec} at 39.4 ± 0.11°C (Fig. 2).

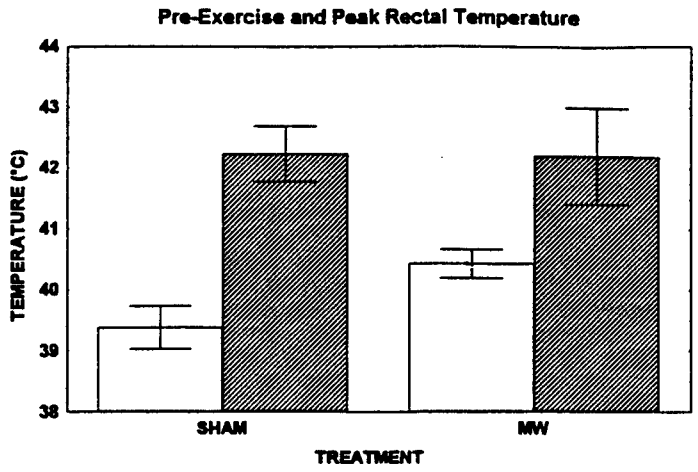

Figure 2.

Peak hypothalamic and rectal temperatures showed no significant difference between the MW and SH treatments. Peak MW T_{hyp} was 42.0 ± 0.11°C, and peak SH T_{hyp} was 42.2 ± 0.13°C (Fig. 1). Peak MW T_{rec} was 42.2 ± .16°C, and peak SH was 42.2 ± 0.27°C (Fig. 2).

The mean time to exhaustion for the MW treatment was 33.5 ± 4.8 min(Fig. 3). For the SH treatment, mean exhaustion time was 44.4 ± 4.8°C(Fig. 3). T-tests on this data showed no significant difference between the two treatments (p=0.067).

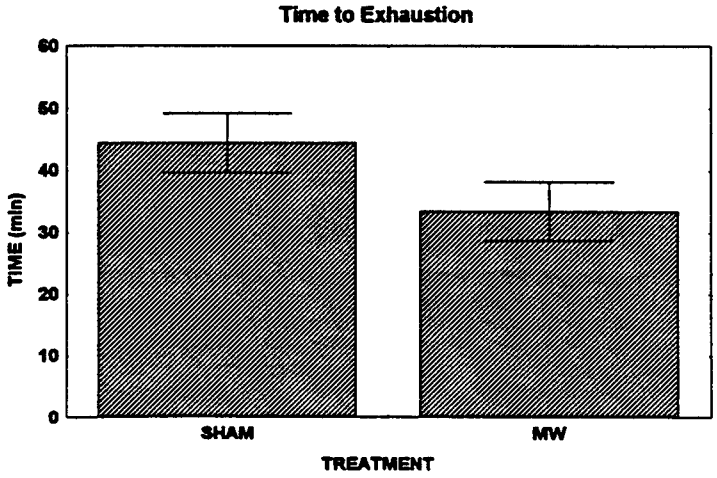

Figure 3.

A significant difference was found when comparing the heating rate of the rats between the two treatments. The mean heating rate was lower for the MW treatment at 0.040 ± 0.006 °C/min., where the rate was 0.073 ± 0.009°C/min. for the SH treatment (Fig. 4).

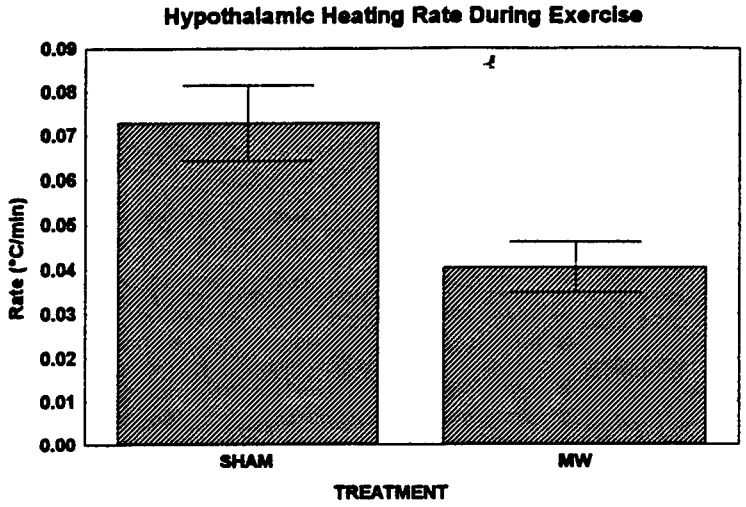

Figure 4.

T-tests looking at the mean weight lost during the runs also revealed a significant difference between the two treatments. During the MW experiments the rats lost an average of 5.0 ± 0.9g of weight. They lost an average of 6.3 ± 0.9g during the SH treatments (Fig. 5).

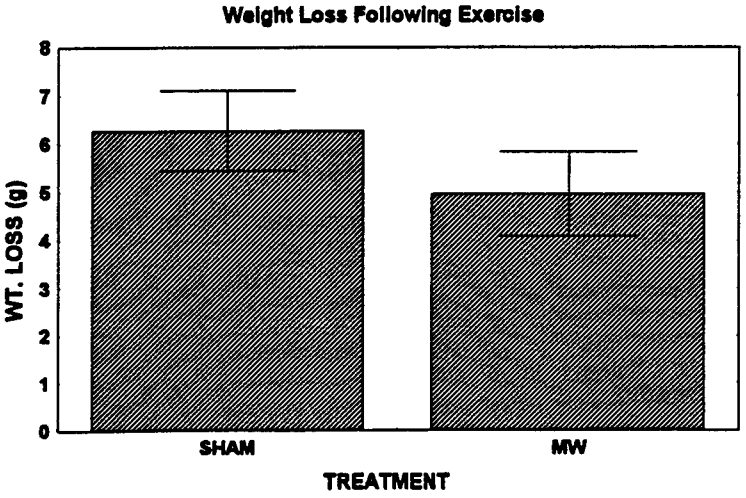

Figure 5.

Conclusion

As we expected, the peak hypothalamic temperatures for both groups showed no significant difference. This indicates that each individual rat has a critical brain temperature beyond which work capability is compromised. This is shown to be true regardless of how fast the animal heated up. The rate of heating could, however, explain why no significant difference was found between the exhaustion times of the two treatments. We expected the animal to reach exhaustion faster during the MW treatment because the rats began their run at a significantly higher temperature. This, most likely, would be the case had the animals' rate of heating been the same in both treatments. Since the rats heated up significantly slower during the MW treatments, it took longer for these rats to reach the critical T_{hyp} which causes exhaustion. There are a number physiological factors that are known to contribute to exhaustion during maximal exercise. Two of these, lactate acidosis and muscle glycogen depletion, are very important, but, unfortunately, measuring their effects is neither practical nor possible in a repeated measures study such as this. An indwelling catheter is required in order to measure lactate levels during exercise. Given the logistic complexity of the study as it is, this procedure would be render the study inoperable. In order to measure glycogen depletion, it is necessary to remove the muscle tissue from the rat so it can be ground and analyzed. Hypoglycemia is another factor to consider, but related pilot studies indicate it does not affect this experiment by significant measures.

One factor that we were able to measure and that could possibly have the most influence of them all is dehydration. By measuring the amount of fluid lost, either by evaporation, urine, or saliva, we found that the rats lost 6-14% of their plasma volume level. This is a significant amount of fluid loss and could greatly affect the time the rats reach exhaustion. Why there was a significantly greater amount of fluid loss during the SH treatments is a question yet unanswered. This and other questions will be addressed further in this ongoing study.

1. Cartee, G., and R. P. Farrar. Exercise training induces glycogen sparing during exercise by old rats. J. Appl. Physiol. 64: 259-265, 1988.

2. Holloszy, J.O., and W.M. Kohrt. Regulation of carbohydrate and fat metabolism during and after exercise. Annu. Rev. Nutr. 16:121-138, 1996.

3. Mason, P.A., T. J. Walters, J.M. Doyle, J.L. Kane, R. Escarciga, and K.E. Purdy. Heat-shock protein and GFAP expression after microwave exposure or warm water immersion. FASEB J. 9: A546, 1995.

4. Walters, T.J., K.L. Ryan, M.R. Tehrany, M.B. Jones, L.A. Paulus, and P.A. Mason. HSP70 expression in the CNS in response to exercise and heat stress in rats. J.Applied Physiol., Submitted.

5. Walters, T.J., K.L. Ryan, J.C. Belcher, J.M. Doyle, M.R. Tehrany, and P.A. Mason. Regional brain heating during microwave exposure (2.06-Ghz), warm-water immersion, environmental heating, and exercise. J. Thermal Biol., Submitted.

Analyses of Metal Concentrations By Flame Atomic Absorption Spectroscopy

Lauren M. Lamm

Keystone School
119 E. Craig Place
San Antonio, Texas 78212

Final Report for:
High School Apprenticeship Program
Armstrong Laboratory

Sponsored by:
Air Force Office of Scientific Research
Bolling Air Force Base, DC

and

Armstrong Laboratory
Brooks Air Force Base, Texas

August 1997

Analyses of Metal Concentrations By Flame Atomic Absorption Spectroscopy

Lauren M. Lamm
Keystone School

Abstract

Atomic absorption spectrometers are instruments used for identification and quantification of metal elements in a variety of different matrices. Before samples of materials in their various forms can be tested to determine the concentration of a given metal they may contain, they must first be digested by concentrated acids in order to produce an aqueous solution in which the target metal is isolated according to methods and standards set by the National Institute Of Safety and Health (NIOSH) and the Environmental Protection Agency (EPA). Because each metal has a unique electron structure capable of absorbing and emitting light energy at specific wavelengths, atomic absorption spectrometers are used to detect the metal atoms within a sample. The light energy absorbed from a hollow cathode lamp is proportional to the concentration of the metal being analyzed. At this point, the results determine whether or not the material is safe for people to work with or dispose of in a normal fashion.

Analyses of Metal Concentrations By Flame Atomic Absorption Spectroscopy

Lauren M. Lamm

Introduction

The purpose of the Analytical Services Division of Armstrong Laboratory at Brooks Air Force Base is to analyze various samples taken from the work place and the environment to insure that the sources of the samples are safe for people to work around and dispose of without causing harm to the environment. Samples are tested for dangerous concentrations of metals such as lead, cadmium, silver, and arsenic.

Spectrometers are instruments used in chemical identification and quantification of metallic elements. Atomic absorption analysis is an efficient means of discovering the concentration of the subject metal within a solution made from a sample.

A wide variety of objects collected from work environments of Air Force Bases throughout the world are tested for unsafe levels of metals. Samples include soils, water, paint, sludges, aqueous bulk mixtures, air, swipes and hazardous waste.

Nearly all samples in their usual form are not immediately ready for testing and so must be properly processed. All samples must be in soluble form without any solids present. Samples are nebulized into a free atomic state so that molecules holding the analyte cannot interfere with the metal's absorption abilities. Chemical digestion and processing become an essential step to overcoming this problem in analysis. Samples are broken down with the use of acids prescribed by EPA; mainly concentrated nitric acid (HNO_3) is used. A solution of 30% hydrogen peroxide (H_2O_2) is added to the digestion procedure to catalyze the chemical breakdown.

Technique

Light and atomic absorption interact in a predictable manner in which the more atoms there are present in the path of a light beam the more of the beam is absorbed. The concentration of an element in a solution can thus be determined mathematically by measuring the difference in light intensity before and after a beam passes through a field of atoms. In the basic setup of a flame atomic absorption spectrometer, a lamp emits a specific wavelength of light which is absorbed by the elemental analyte. Each element has a unique electron structure capable of emitting or absorbing light energy at specific wavelengths. Since a specific wavelength being absorbed by each metal the presence of other metals within a sample causes little interference. This beam transpires a flame into which the sample is aspirated and nebulized. The air/acetylene flame causes the reduction of metal ions into free atoms. Whatever light is not absorbed continues through to a monochromator where all wavelengths of light are diverted except for the specific wavelength which the subject metal is capable of absorbing. This specific remainder finally reaches a photomultiplier detector which measures the remaining amount of light. This process makes a spectrometer an accurate and efficient instrument.

Methodology

Once samples have been properly prepared they are placed into fifteen milliliter tubes which are loaded into enumerated sample tray slots which hold the samples during analyses. A spectrometer will be able to test each of these one at a time in a run. A rinsing solution made up of 3% nitric acid is placed in slots between each sample so that carry over is reduced. Rinsing solutions also serve to monitor the instrument in case of a slip in calibration. The first five slots in a tray are always reserved for a set of solutions whose concentrations are known and are checked against the spectrometer's readings

for accuracy. These solutions range in value from least concentrated to most concentrated and set the minimum and maximum limits of the instrument's accuracy. Should a sample surpass this range it must be diluted and retried and the result readjusted. If a sample falls below this range it is not given a numerical concentration but rather the concentration is reported as too small for detection. Two rinses follow these standard solutions before a final solution known as the quality control sample is tested. A quality control is a solution whose concentration value is known yet was made independently of the other standards to insure that the standards themselves indeed match their presumed values. Between every ten samples a middle standard, which is merely the median standard, is placed to make doubly sure that the calibration of the spectrometer does not slip during the testings. At the very end of the run the middle standard is tested a final time. To make sure that the sample results are accurate a single sample in a run is selected to be tested twice during the run. This sample is called a duplicate. After its testing a duplicate is then spiked with more of the element being tested and given a predicted value which measures accuracy once again when the spike is tested at the end of a run.

The procedure of operating a spectrometer is done through a computer program. Through the program the flame and robotic probe are controlled and the results of testing are recorded. All samples, rinses, standard solutions, duplicates and spike must be listed in the computer according to their slot numbers on the sampling tray so that the right result is matched to the right sample. The computer must be notified of which element it is going to test the concentrations of so that the correct lamp is used. Once the computer program is activated the instrument begins taking concentration readings for the specified element and the computer's printer reports the results in milligrams of metal per liter of solution.

Throughout testing quality control standards as recommended

by EPA are adhered to in order to insure accuracy. Maintenance of the spectrometer is performed on a daily basis and all times of spectrometer use are recorded. Quality control standard solutions must hold a certain percentage of accuracy to the actual values of the solutions in order for any test to be valid. These standards must be renewed on a monthly basis on account of an element's natural tendency to leach out of a solution over time. Because a mathematical linear relationship exists between the element concentration of a solution and the light absorbency of the solution, a correlation coefficient is determined from the standard solutions. The accuracy of the coefficient is another way of safeguarding sound results. The absorption level of the middle standard must also fall into a specified range in order for a test run to be valid.

Results

Once a run is complete, a list is compiled for each sample: the absorbance readings and the average concentration of three measurements is produced. The list must be edited in the event any dilutions were made. The computer program, if notified of a particular sample's dilution, automatically corrects the diluted concentration by multiplying the result by the dilution factor.

A series of calculations for the quality control standards, middle standards, duplicates and spike must be done to show percent accuracy. Observed concentration values of quality control and middle standards are divide by their actual values and then multiplied by one hundred to find percentage accuracy. The final numbers should be as close to 100% as possible. To measure the accuracy of a sample duplicate the difference of the two duplicate measurements is divided by the average of the same two values. When this quotient is multiplied by one hundred the result should be very close to zero percent. A spike's accuracy is calculated by finding the difference between

the observed concentration of the spike and 90% of the duplicate average and then dividing the number by the true concentration of the added spike. The result when multiplied by one hundred should be close to 100%.

After calculations have met specific standards, the percentage accuracy of the quality control and middle standards of a run are placed on charts and compared to percentages of previous runs as a way of monitoring the spectrometer's overall performance. All calculations are recorded and submitted with a list of the run, a computer printout of sample concentration results, and a copy of the quality control and middle standards charts to be reviewed by a technical supervisor before being made into a final report.

Conclusion

After a final report is made for a sample or a set of samples, the information about metal concentrations is sent to the Base from which the sample or samples originated. Should the metallic concentrations exceed EPA regulations, Base personnel use the results germinated by this laboratory to take appropriate measures to ensure the safety of industrial processes and to protect against degradation of the environment.

ABDAR Remote Engineering

Evan Large

Northwestern High School
5650 Troy Road
Springfield, OH 45502

Final Report for:
High School Apprentice Program
Armstrong Laboratory

Sponsored by:
Air Force Office of Scientific Research
Bolling AFB Washington DC
and
Armstrong Laboratory

August 1997

ABDAR Remote Engineering

Evan Large
Northwestern High School

Abstract

The possibility of a medium to be used in long range engineering requests for Aircraft Battle Damage Assessment and Repair was researched. Information was gathered from the World Wide Web, Air Force personnel, and Air Force libraries. Through these research mediums, different computer hardware and software was studied in the hopes of devising a system capable of performing remote engineering requests. The results of this research indicated that such a system is feasible with current technology.

ABDAR Remote Engineering

Evan Large

Introduction

The Concept of Aircraft Battle Damage and Repair dates as far back as the World War I. As the world began to recognize the combat value of airplanes, they were forced to realize the frailties of an airplane in a combat situation. It came to be understood that a method to quickly return damaged aircraft to combat would be a force multiplier, and would have a cumulative effect throughout the conflict.

Most damaged aircraft are not permanently destroyed, but merely injured. As any conflict progresses, the number of combat capable aircraft steadily decreases. An effective ABDR system would make the rate of decrease in the total air power of any country much slower. This would be particularly noticeable in long, drawn-out conflicts, for in these instances, it would not be the sheer power of the aerial force, but the endurance of the aircraft that would decide the final outcome.

The first formal institution of these rapid repair capabilities was during the Vietnam War. During the war, a total of 11,800 U.S. planes received combat damage of some type.. At first, there was little or no support for repairing damaged aircraft. Then, in 1965, the importance of repairing combat damaged aircraft and returning them to combat was fully realized, and additional battle damage support was requested. Rapid area maintenance (RAM) teams, groups of highly skilled members from the Air Material Area depot, were developed and deployed to

Southeast Asia. During the course of the war, these RAM teams repaired or modified more than 1,000 total aircraft. This number may seem insignificant next to the total number of damaged aircraft, but 1,000 aircraft is an extremely significant figure when compared with 0 aircraft.

It was not until the 1980's that the actual separate ABDR program was established. Over the years, the ABDR program has developed training, tools, and procedures to handle the rapid assessment and repair of battle damaged aircraft. The most prominent of these tools is the plane specific Technical Order, or T.O. These are type-written guidelines for the assessment and repair of the aircraft. An ABDR Assessor can compare the damage on an aircraft to the T.O. and then follow its instructions and repair the airplane.

But the ABDR process must be continually up-graded, and this is the purpose of the current Air Force ABDAR program. ABDAR, Aircraft Battle Damage Assessment and Repair, is a program devoted to improving the ABDR process through the use of modern computer and World Wide Web technology. The goal is to put all of the information from the T.O. into a computer format, and to create an ABDAR intranet which will be a repository of all current ABDR operations. With ABDAR, the ABDR practices will be faster, be more accurate, and will require a lot less bulky paper work.

Discussion of Problem:

The ABDR process is generally self-contained. In most cases, the combination of the information in the T.O. and the personal experience and skill of the Assessor and Technicians is enough to handle an aircraft battle damage repair. The Assessor must simple reference the

damage site and type of damage in the T.O., and follow it's directions. But, like any rigid, pre-defined system, the T.O. cannot cover every eventuality; there are limits to it's powers. It has no experience, and no logical processes. It is sufficient for all the types of damage that it has been constructed for in the past, but wars do not happen in the past.

Wars happen now, and there is a reason that the word 'now' is so closely related to the word 'new'. Every time an aircraft is damaged, there is a significant chance that the incurred damage will not be covered in the T.O. When the experience or skill of the Assessor is insufficient, and the T.O. can provide no further answers, then the ABDR Technicians need help. They need the knowledge of an experienced ABDR Engineer. The ABDR Engineer, a specialist in the structural properties of aircraft, uses his knowledge and experience to devise repairs or modifications to battle damaged aircraft that will allow it to be rapidly returned to combat capable status.

The current practice for implementing the ABDR engineer is to send an Engineer trained in the proper aircraft type(s) from the depot to the field that needs his help. Transplanting the Engineer in this matter, however, has certain drawbacks. First, an ABDR Engineer may not be able to bring with him all of the tools that he needs to devise a repair, especially if he does not fully understand the damage. Second, the small number of ABDR Engineers in the Air Force may make sending a true structural specialist to the site impossible, and the Engineer would not be able to contact the specialists at his depot. And lastly, of course, there is the effect that combat conditions could have on the ABDR Engineer's effectiveness. The ABDR Engineer is hustled into a potentially dangerous situation, lacking the mental preparation for his surroundings

and all of the tools he is accustomed to. These are all factors that are likely to affect the performance of an ABDR Engineer.

The electronic medium of the ABDAR system of the future enables the creation of a new, electronic system to handle ABDR Engineering. In fact, current technology makes Remote Engineering Requests possible. Along with the computer-based ABDAR system will be developed a computer-based system that will allow the ABDR Engineer to communicate with the ABDR Assessor and devise repairs and modifications without ever leaving the depot. This would solve all of the problems stated above, while maintaining and perhaps improving the quality and speed of the repairs.

Methodology:

The search for a Remote Engineering Request system was a three-pronged search. First, it had to be determined what tools and abilities the users, Assessor and Engineer, would need to execute their ABDR function. Second, it had to be determined which of these abilities and tools would already be provided in the ABDAR program, and which would have to be added. Lastly, software had to be found that would fulfill all of the functions specified.

Research into the needs of the ABDR functionaries was accomplished through personal interviews with past and present Air Force employees. Through these interviews, the following findings were made. An Assessor would need the ability to take pictures of the damaged aircraft and the damaged site, and send these to an Engineer along with written information on the damage. In most cases, these two types of information would be enough to fully delineate the

location and extent of the damage to the Engineer. However, it was also found that an understanding of some damages can not be gleaned from written descriptions and pictures alone. In this instance, the ABDR Engineer would need the ability to make a more personal inspection of the damage.

Once the Engineer is completely cognizant of the situation, he needs a set of tools and references that will allow him to devise a repair. He would also have to be able to test the repair, making sure that the proposed repair is structurally sound. Then, having solved the Assessor's problem, the Engineer must be able to send instructions back to the Assessor, in the form of written information, diagrams, and pictures. If, for any reason, the Engineer's instructions are unclear, then the Assessor would need to have the ability to consult with the Engineer on trouble areas. These are all of the abilities that needed to be built into a system for ABDR Remote Engineering Requests.

These findings on what abilities are needed in a Remote Engineering Request system were then compared to the abilities that would already be available with the ABDAR program. With ABDAR, each Assessor would have a Personal Maintenance Aid (PMA), which is basically a notebook computer. The software on the PMA would consist primarily of the Netscape Navigator, with a few built in tools such as e-mail and a calculator. The e-mail utility solved the problem of sending information between the Assessor and the Engineer, but the abilities to get pictures of the damage to the Engineer and to consult with the Engineer on misunderstandings were not, as of yet, provided.

It was found that the ABDR Engineer already has all of the tools he needs to complete his

ABDR function at the depot. He has all of the reference materials and tools that he needs to actually devise and test the repair. All that must be provided is the connectivity with the Assessor. His personal computer would already have an e-mail utility. All that has to be provided to the Engineer for a working Remote Engineering Request system is a way to intimately inspect extremely complex damage. So, the unfulfilled requirements of a working system for Remote Engineering Requests are ways to collect and send pictures, and to conduct more intimate communications between the Assessor and Engineer in times of confusion. Also, it was deemed wise to research methods of making the information sent accurate, helpful, and secure as possible.

Once the requirements were established, research into available hardware and software to meet these requirements was begun. This research was conducted mainly through the World Wide Web, but some of the hardware and software was found within the building. The World Wide Web was favorable as a research medium because information on almost any subject, especially computer hardware and software, is easily accessible from a single terminal.

Each potential piece of software or hardware was considered in terms of ease of use, compatibility, and overall usefulness. In cases where no current technology could solve a problem, technologies under development, and future technologies were considered. The problems that cannot be solved now, will be solved in the future.

Results:

The following lists are compilations of all the tools, computer based or otherwise, needed by the

Assessor on his PMA and by the Engineer at the depot. After the name of the software, its primary function in the system is described. Following the two lists is a description of how a Remote Engineering Request would operate. Additional information on the software and hardware elements can be found at the end of this report.

Assessor Requirements:

- Netscape Navigator

The Netscape Navigator is used by the ABDAR intranet. The ABDAR intranet is an on-line compilation of all ABDR information. This program will already be resident on the Assessor's PMA.

- E-mail Utility

E-mail capability would be needed by the Assessor in order to send information about a particular damage to an Engineer. It would also be used to receive repair instructions from the Engineer. Once again, this utility will already be included on the Assessor's PMA under ABDAR

- ViewDirector Pro 2+, by TMSSequoia

This is a plug-in for the Netscape Navigator, which means it installs directly into and works from within Netscape Navigator. This is an attractive feature because the Assessor's PMA will already have the Netscape Navigator. This plug-in allows a user to add annotations to a picture, in the form of text, arrows, squares, and other geometric shapes. These shapes and words can

have a typed note attached to them, or can be hyper-linked to web-pages or even other files. This will be used mainly by the Engineer, but the Assessor must have a plug-in to view the annotations.

- Video Teleconferencing Software

The software that was used for research was CU-SeeMe, and was provided by permission of Cornell University. This software allows for real-time video/audio/white-board teleconferences. This would allow the Assessor and Engineer to meet and discuss the problem in real-time, if the e-mail messages fail to completely clear. In most cases, the e-mail should be sufficient. The video aspect of this program would allow the Assessor to move his video camera wherever the Engineer directs, making the experience as close as possible to actually being there. The white-board program allows the Assessor and Engineer to draw or load pictures on both computers at the same time, and change them, add to them, and discuss them.

- Microphone, Speakers, and Video Camera

These are, of course, the hardware requirements of the teleconferencing software. The microphone and speakers would probably take the form of a headset, to keep the Assessor's hands free. Any type of video camera should be compatible with the software, but the chosen camera should have the clearest picture possible. These three components would not be supplied for each and every PMA. Instead, a small number of each would be resident in a 'equipment library', which they could be borrowed from when needed.

- Digital Camera with software

The digital camera would be used by the Assessor to capture photographs of the airplane and its

damage that would be sent to the Engineer. The software, which comes with the camera, allows the pictures to be converted into a number of common file formats, all of which are supported by the ViewDirector plug-in. Once again, each individual PMA would not have its own camera.

Engineer Requirements

- Netscape Navigator

This web browser would once again be used as an avenue to the ABDAR intranet, and a host for the ViewDirector plug-in

- E-mail Utility

This of course, would be used to transfer information and files between Assessor and Engineer

- Scanner with software

This is another option available to the Engineer at his depot. The Engineer may wish to send additional pictures to the Assessor which are not already in a computer format. These could include schematic diagrams, or even hand-drawn pictures. The software would come with the scanner. Scanners should already be available at the depots.

- Picture Authoring Software

This could be any software which supports common file types. This would allow the Engineer to create more pictures to send to the Assessor if he so desired. This, too, should already be on the Engineer's PC at the depot.

- CAD/FEA Utility

Computer Aided Design and Finite Element Analysis are computer utilities that would allow the

Engineer to test virtual repairs. The Engineer could build models of proposed repairs, and run them through various physical tests. This technology should already be provided at the depot, but if it is not, the Engineer can still perform his function.

- Assorted Reference

This includes everything from volumes on aircraft structure to the expertise of co-workers. These would be available to the Engineer at the depot to help him if he encounters an area where he perceives his knowledge to be incomplete. These, of course, are already resident at the depot.

- ViewDirector Pro 2+, by TMSSequoia
- Video Teleconferencing Software
- Microphone, Speakers, and Video Camera

An ABDR Assessor assesses a damaged aircraft and decides that he cannot conduct repairs without consulting a more knowledgeable party. First, he takes pictures of the aircraft, from close up and afar, that will give the Engineer an understanding of the location and extent of the damage. Then, he writes an e-mail message to the Engineer describing in writing the damage, the circumstances under which the damage was received, and any other information that will aid the understanding of the Engineer. He will find an Engineer's e-mail address in one of two ways. He will either have a roster of all trained ABDR Engineers and their qualifications, or the ABDAR intranet could have pre-programmed mailing lists, from which Engineers could select jobs based on urgency. Once the Assessor has written the message and attached all additional files, he sends it to the Engineer.

Upon receiving the Assessor's message and files, the Engineer studies this information to make sure that he understands the location and extent of the damage. This is the most important part of the operation. If the Assessor's e-mail does not describe the damage to the Engineer's satisfaction, then the Engineer can initiate a teleconference with the Assessor, as described above. Once the Engineer is satisfied that he fully understands what is required of him, he can begin formulating a repair.

To formulate the repair, the Engineer uses all of his assorted reference materials, and possibly a CAD/FEA program. He has everything he needs to devise a repair at the depot. After he devises a viable repair for the damage, he compiles information to send back to the Assessor. He will of course include a written description of the repair instructions, along with any pictures or reference material that he feels will help the Assessor. The pictures could include pictures that the Engineer has annotated using the ViewDirector plug-in, or other pictures that the Engineer has created. Reference materials that the Engineer might send include diagrams or descriptions of techniques for using certain fasteners, adhesives, etc. He then attaches all of this information to an e-mail message, and sends it back to the Assessor.

After the Assessor receives and reads his instructions, he can begin his repairs. If the Assessor doesn't fully understand his instructions, he can initiate another teleconference, but it is highly unlikely that he would ever need to do so. The Assessor can then repair the airplane, ending the ABDR concern with that plane.

Conclusions and Recommendations for the Future:

My conclusions is that a successful system for Remote Engineering Repair Requests is indeed possible. However, the system described above is as of yet incomplete. Before implementation, it would, of course, have to undergo testing and be approved by the actual ABDR functionaries. Due to time constraints, there was little interaction between those developing the system and those for whom it is being developed.

Also, there is one thing missing in this prototype which would be required in an actual, working system; security. It has not been included, but it has been considered. There are two types of technologies that would be needed to ensure the security of this system.

- E-mail encryption

This is a technology that already exists, but was not included in this prototype due to funding restrictions and current debates over its future legality. E-mail encryption would allow the Assessor and Engineer to encode their e-mail transmissions so that the only people who could access them would be those people who knew a certain password. This is essential because of

The Air Force will probably not be affected by the legality issues associated with strong encryption utilities. The reason for the debate is that the government believes that publicly available strong encryption utilities could possibly endanger national security. Since, in this case, encryption would be used specifically for national security, its future legality would not affect its use in ABDR.

- Real-time security

The other security issue with this system concerns the real-time teleconference communications.

During the course of research, no utilities that performed this function were found. Once again, security of these transmissions would be vital due to their sensitive nature. Some type of device or software that would encode outgoing transmissions and decode incoming transmissions in real-time would be ideal. However, this teleconferencing technology is relatively new, and there is no doubt that security utilities for it are on the way.

The two most important things about a system for ABDR Engineering is that it include all of the tools needed by the Assessor and Engineer to conduct quick, accurate repairs, and that it evolve with modern technology. If ever a group of ABDR functionaries decide that they need certain tools available to them, then they should be made available. As the ABDR process evolves, so must the system for ABDR Engineering.

References:

Materials:

Aircraft Battle Damage Repair for the 90s and Beyond, Darrel H. Holcomb, Maj., USAF, March 1994

Integrated Maintenance Information Systems (IMIS): User Field Demonstration and Test, Donald C. Thomas, October 1995

Software Recognition:

TMSSequoia - ViewDirector Pro 2+

Cornell University - CU-SeeMe v .92b2

Netscape Communications Corporation - Netscape Navigator

Special Thanks:

1st Lt. Maurice Azar, AL/HRG

Capt. Mike Clark, AL/HRG

Pat O'connel, NCI

Associate did not participate in the program.

THE ROLE OF MICROSOFT'S DIRECTX 3 SOFTWARE DEVELOPMENT KIT IN THE RAPID DEVELOPMENT OF HIGH FIDELITY SIMULATIONS

Shaun M. Little

Floresville High School
1000 Tenth St.
Floresville TX, 78114

Final Report for:
High School Apprentice Program
Armstrong Laboratory

Sponsored by:
Air Force Office of Scientific Research
Bolling Air Force Base, DC

and

Armstrong Laboratory

July 1997

THE ROLE OF MICROSOFT'S DIRECTX 3 SOFTWARE DEVELOPMENT KIT IN THE RAPID DEVELOPMENT OF HIGH FIDELITY SIMULATIONS

Shaun M. Little
Floresville High School

Abstract

The Role of the DirectX 3 SDK (Software Development Kit) in the development of high fidelity simulations was studied. Borland Delphi Developer 2.0 was used in conjunction with the DirectX 3 SDK header files and the Delphi Games Creator to form the programming environment in which the simulations were created. Careful observation of the development process indicates that the DirectX 3 SDK can significantly increase the fidelity of a simulation while decreasing the time spent in its development and maintaining a high level of experimental control over its testing environment.

THE ROLE OF MICROSOFT'S DIRECTX 3 SOFTWARE DEVELOPMENT KIT IN THE RAPID DEVELOPMENT OF HIGH FIDELITY SIMULATIONS

Shaun M. Little

Simulated training and testing environments play an important role in preparing America's fighting men and women for the many and varied tasks they must undertake. However, until recently there was a growing disparity amongst the various types of simulations (sims) that were being created. As a result of this most sims can be grouped into two very different categories. The first of these categories is comprised of sims that present a very realistic testing environment to the user but offer very little experimental control over that environment i.e., NASA's shuttle simulator. Unfortunately, the complexity of such sims makes them very difficult to build and modify, thereby increasing time spent in development. The second category is comprised of those sims that provide a great deal of control over the testing environment but are very unrealistic. In comparison these sims, though quick and easy to build and maintain, were often berated by users because of their limited believability. However, with Microsoft's introduction of the DirectX 3 SDK the gap between the two categories has been bridged somewhat. By providing real-time access to the hardware acceleration features of today's powerful desktops the DirectX 3 SDK gives the programmer freedom to design life-like three-dimensional simulations that maintain the high performance level associated with their simple two dimensional counterparts.

The main development environment used to design the sims was Borland Delphi Developer 2.0 which uses object Pascal as its underlying language. Since the DirectX 3 SDK header files were originally written in C++ it became necessary to find a set of converted header files. These were provided by the Delphi Games Creator (DGC). The Delphi Games Creator is an independently written addition to Delphi that consists of a set of converted DirectX 3 SDK header files and several units that serve as "wrappers" around the various

DirectX APIs (Application Programming Interfaces). These "wrappers" simplify the use of DirectX by "wrapping up" some of the more complex tasks into simpler function calls. Though the DGC was originally written to design computer games it can be used for much more (Bearne et al., 1996).

During the eight week session there were two main projects that I worked on involving the DirectX 3 SDK. The first project was called the Audio Stroop Task which dealt mostly with the DirectSound API, the audio component of the DirectX 3 SDK. The DirectSound API provides direct access to the sound hardware as well as the ability to introduce three dimensional sounds into any program. Three-dimensional sound takes into account the various physical aspects of sound including muffling, the Doppler effect, and the distance between the listener and the sound source (Microsoft DirectX, 1996). The DGC contains a unit called DGCSound which is basically a wrapper around the DirectSound API (Bearne et al., 1996).

The Audio Stroop Task is a program used to observe how the human brain responds to various auditory and spatial stimuli. There are three facets to each stimulus; the spoken word ("left" or "right"), its location (left or right), and the hand used in response. Previous implementations using two-dimensional sound and monaural audio output had yielded predictable results. If the stimulus word was incompatible with its location, its response hand, or both (i.e. the word was "left" and it seemed to come from the listener's right side) then response times were slower. Unfortunately, the two-dimensional output of the previous programs meant that the user heard the word in either the left or right ear only and no part of the sound was reaching the opposite ear. Upon learning of the three-dimensional capabilities of DirectSound the research scientists requested that the program be modified to make use of them.

In order to convert the program to make use of DirectX I first had to strip out all references to the old audio routines. I then proceeded to

modify the data structures and routines found in DGCSound so that they could work with three-dimensional sounds. Then I went back through the program and put the calls to the new routines in the appropriate places.

Using DGCSound I was able to completely convert the program to three-dimensional stereo sound in a matter of days. I also added five additional sound positions at various distances from the listener. It is believed that with the added realism of three-dimensional sound the results of the test will have more validity. Unfortunately, at the time of this writing there were still some design issues that had to be worked out before the test could be administered.

The second project that I took part in is known as B.R.U.T.E. which stands for Basic Research UAV Task Environment. This is a program designed to simulate the piloting environment of an Uninhabited Aerial Vehicle (UAV). It may also be used to help with UAV pilot selection. This program is still being developed at this time but the current concept for the program is as follows. The main screen is divided into a pilot view and a camera view. The pilot view consists of a small icon representing the UAV which is flying over a two-dimensional map of a given area. The camera view displays a three-dimensional view of the terrain being flown over. The camera view has the ability to zoom in and out and also take pictures of the terrain. There are two operators, one to pilot the UAV and one to control the camera. The two operators are at separate computers linked via a network. The pilot's task is to conform to a certain flight plan while the camera operator takes snapshots of certain targets.

This project makes heavy use of the DirectDraw, Direct3D, and DirectPlay APIs. The DirectDraw API gives the programmer direct access to the display device as well as access to the blitting and buffer-flipping capabilities of the hardware (Microsoft DirectX, 1996). The DGC contains a wrapper around the DirectDraw API known as DGCScreen (Bearne et al., 1996). The Direct3D API

provides an interface that allows programmers to easily incorporate 3D graphics into their applications. The DirectPlay API greatly simplifies the task of connecting computers via a modem or network (Microsoft DirectX, 1996). The DGC contains a wrapper around the DirectPlay API known as DGCPlay (Bearne et al., 1996).

Although I was on the programming team I did not work on the visual parts of the environment very much. However, I did have the opportunity to observe the project from its very conception through its current state. I was simply amazed as I watched the lead programmer take the project from a vague concept to a working two-dimensional prototype in less than a week. This feat is in no small part due the time-saving routines found in the DGCScreen wrapper and the Rapid Application Development (RAD) environment provided by Delphi.

There are many exciting things ahead for this project including the addition of three-dimensional terrain and networking capabilities. For my part, I helped develop pieces of the autopiloting algorithm and I also wrote several test programs that used the DGCPlay wrapper to send messages between networked computers. These test programs were written to help get a better understanding of the DGCPlay wrapper and the DirectPlay API. We are currently using that knowledge to develop an algorithm to synchronize the movements of the UAV between the two networked computers.

The most recent concept for the synchronization routine uses a host-client paradigm wherein the host sends messages about the position of the UAV to the client. Unfortunately the client machine starts to experience a flickering image because the messages from the host are not arriving quickly enough. To compensate for this we have been designing various interpolation routines in order to make a best guess as to the position of the UAV between messages.

Since the program is still being developed it is impossible to tell how well it will be received by those pilots who will use it. We hope that they will find it significantly more realistic than previous simulations. However, even if the simulation runs perfectly it will not be as realistic as those multimillion dollar flight simulators that you see on Discovery Channel.

In conclusion, I believe that although DirectX technology has helped us make many strides towards our goal of bringing real-world simulations to the desktop machine, it cannot rival the capabilities of our more sophisticated simulators. However, what it lacks in realism it more than makes up for in practicality. DirectX provides a relatively inexpensive means to rapidly create good simulations that can be easily modified and maintained.

REFERENCES

Bearne, P., Kurtz, Jeff., & Pullen, J. (1996). The Delphi Games Creator [computer software]. Internet (http://www.ex.ac.uk/~PMBearne/DGC.html).

Microsoft DirectX Software Development Kit. [computer software manual]. (1996). Redmond, WA: Microsoft Corp.

VISUAL ACUITY BETWEEN 6 AND 60 METERS

Katie Lorenz

Chaminade-Julienne High School
505 S. Ludlow Street
Dayton, OH 45402

Final Report for:
High School Apprentice Program
Armstrong Laboratory

Sponsored by:
Air Force Office of Scientific Research
Bolling Air Force Base, Washington, DC

And

Armstrong Laboratory

August 1997

Visual Acuity between 6 and 60 Meters

Katie Lorenz
Chaminade-Julienne High School

Kim Blazer
Oakwood High School

Abstract

Experiments were conducted in order to determine the effect of intermediate distances (between 6 and 60 meters) on visual acuity. The Landolt "C" was chosen as the target for the experiment. Acuity was measured by the minimum angular size of the gap which is just visible in the "C". Factors in the multiple experiments included different target sizes, contrasts, lighting, and orientation, as well as binocular versus monocular vision testing. All of the various factors were controlled for in individual experiments when necessary. Experimental results suggest that there are many variables to be controlled in data collection of this type and that intermediate distances do, in fact, have an unexpected affect on visual acuity. As expected, contrast, lighting, orientation affected the data, but the target size should not have affected the visible angular size of the gap. What should have been equal size to distance ratios were, instead, unequal among all of the subjects tested. As the size of the target increased, the distance did not increase according to the same ratio. Several experiments were conducted attempting to solve this occurrence, but no solution was yet found.

Visual Acuity between 6 and 60 Meters

Katie Lorenz
Kim Blazer

Introduction

The purpose of this research was to vet a technique for the measurement of visual acuity in the Dynamic Visual Assessment Facility (DVAF) or "zoom lane" of the Human Engineering Facility of the Armstrong Laboratory. The zoom lane consists of a sixty meter room equipped with a tracked cart transport system that is able to move an observer in relation to visual stimuli. The facility is used to investigate visual psychophysics, night vision goggle performance, optical assessment of air craft transparencies, and object detection and recognition performance.

Because of the relatively unique capabilities of the zoom lane and its intended uses, standard acuity measurement techniques (based on keeping observers at a fixed viewing distance and adjusting the size of the visual targets) are either precluded or inappropriate. Therefore, the need to develop a more facility-appropriate technique involving observers varying their distance from visual targets of a fixed size. But developing a defensible measurement technique, especially one entailing changing distances, requires that we be sensitive to the subtitles of the concept of visual acuity. This is because of several well-known effects of near distance on vision. The concepts of visual acuity and the factors which affect acuity are reviewed before discussing our research topic.

Visual Acuity

Visual acuity is the ability to resolve small details. This apparently simple definition contains three concepts which are not so simple. In order to understand acuity, what is meant by "details," "small," and "resolve" must be clarified. To conduct useful research and communicate our results, we need a standard detail, a standard procedure for the indexing of smallness or size and determining resolution. Developing these standards and a consensus for their use is not easy and is still an ongoing process. The National Research Council's (NRC) Committee on Vision provided the standard approach to this experiment. They recommended the use of the Landolt "C" because it accounts for the effects of an astigmatism by testing with all four orientations. The NRC also recommended the visual angle recorded in arcminutes versus the decimal notation.

Since arcminute values deal with whole numbers, they are much simpler and easier to deal with than decimal values. The Snellen denominator can then be easily derived from the arcminute value if desired.

Visual Size

A person with good acuity can see a given detail from a further distance than a person with poor acuity. Although several indices of acuity exist, the underlying basis of the various metrics is not the physical size of the detail but rather the visual or angular size. In general, angular size depends in both the physical size and distance of the object. Specifically,

angular size = arctangent (size / distance)

The units of angular size could be degrees or radians, but minutes of arc (arcminutes) are most often used in acuity work. Since the NRC recommends the use of minutes of arc, visual angle is presented in arcminutes.

Visual Detail

There are many visual targets possible including letters, stripped patterns and sinusoidal gratings. We again follow the NRC recommendation and use the Landolt "C" with the gaps oriented four different ways. The reference visual detail in this case is then the width of the gap.

Visual Resolution

The combination of psychophysical technique and the criterion for an observer is what is meant by visual resolution. The psychophysical technique we adopt for a facility featuring observers moving toward a target is a modified Method of Adjustment with the observers approaching the target. Recession trials are not included like they are in the unmodified method since that would make no sense in target acquisition scenarios. The criterion question is more difficult. The NRC report is silent in this question, but experience suggests that subjective criterion effects are not insignificant. As will be discussed later, it is suspected that some of our results might be due to criterion variations across conditions. For now simply note that observers were free to use their own criterion. Also, note that the ability of the observers to see the gap's orientation is not necessarily the same as seeing the gap.

Factors Which Affect Visual Acuity

Visual size (based on the ratio of size and distance) is mot the only factor in visual acuity. That is, the

smallest visible angular extent depends on a number of other factors. These include size, distance, contrast level, luminance, and pupil size. The factors which involve distance, such as accommodation and stereopsis, are generally believed to be inoperative beyond six meters. However, there is some literature that suggests some small effects of distance up to ten meters.

Zoom Lane Experimental Approach

The original purpose of the zoom lane experiments was to evaluate the approach-only Method of Adjustment with a fixed gap-sized Landolt "C". We expected typical effects of variation in parameters such as light level and contrast ratio. For example, greater contrast produces greater acuity. Our goal was to determine the specific range and variance in acuity which we could expect in our unique facility.

Choice of Gap Size

To avoid possible near-distance effects of accommodation and stereopsis, we deliberately wanted a gap size which would require an observer to approach the target no nearer than six meters. Outside of avoiding small gaps to avoid near-distance effects, there is nothing in the visual size equation which would suggest that any particular size gap is to be favored over any other. That is, if a person's acuity is in arcminutes, then for any (large) gap, the observer could be expected to move to a distance which produces a one arcminute size for that gap. A larger gap should merely produce a greater viewing distance such that the size / distance ratio is the same as that for a smaller gap size. Therefore, the actual gap size is arbitrary with the only constraints being the need to avoid viewing distances closer to six meters or greater than sixty meters (the limit of the room).

Preliminary Experiments

In two preliminary experiments, we included two gap sizes (.71 cm and 1.4 cm). We did not expect an effect of these gap sizes but included them solely as good experimental technique. Specifically, except for the "normal" variation, if only one gap size was used, observers would be expected to always position themselves at the same distance from the target. Since the target stand was always fixed in position, this means observers would always move to the same position in the room. This could introduce artifacts if an observer chose to ignore the target and just walk to a visible position referent such as a pillar in the room. The results of these experiments, which included variation in lighting levels, were as expected with respect to contrast and lighting variation. However, we found an unexpected effect of distance. Namely, the bigger gap resulted in a nearer than expected threshold distance. This suggests that angular acuity

worsens with distance. Since the result is contrary to any expectation, it was assumed that an artifact in the procedure was the cause. Therefore, a third experiment was designed to find and eliminate the source of the artifact. This in itself was considered a normal part of the vetting process.

Methodology: Experiment 3

Experimentation included six subjects tested under controlled conditions. These conditions consisted of three target sizes (.71, 1.42, 2.0 cm.), two contrast levels (24% and 71%), four orientations (up, down, right, and left), and a fixed low light level (40V). The set-up consisted of a mounted target (consisting of an 18 cm x 18 cm square with a whitish or gray background depending on contrast condition) with the subject at the end of a 60 meter room as shown in Figure 1. The method of adjustment was used in which the subject adjusts to the stimuli by walking until the gap is just detectable. The observer then indicates the orientation of the "C" by saying "up," "down," "right," or "left." This method has the advantage of giving the subject an active role in the proceedings, hence, the subject is more alert during the testing. This psychophysical method is also the most efficient procedure in gathering thresholds.

After sufficient dark adaptation, the subjects started viewing from a point beyond their visual range of the selected target. Sixty trials of the twelve targets (five repetitions of each) were presented to each subject in random order, and they were asked to walk forward until they could distinguish the orientation of the Landolt "C," shown in Figure 2. Once this was established, the subjects' positions were recorded. These distances were transferred into an Excel spreadsheet where visual angles (in minutes of arc) and Snellen denominators were calculated.

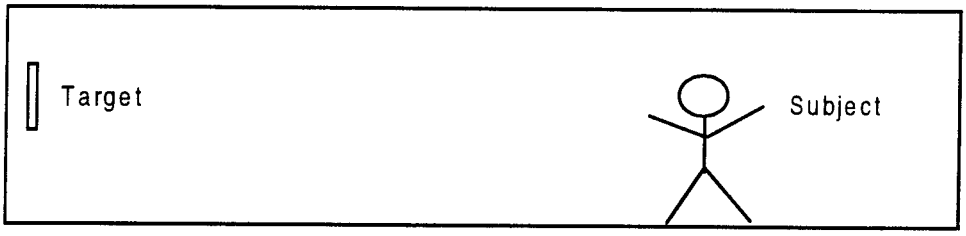

Figure 1. Experiment Set-up

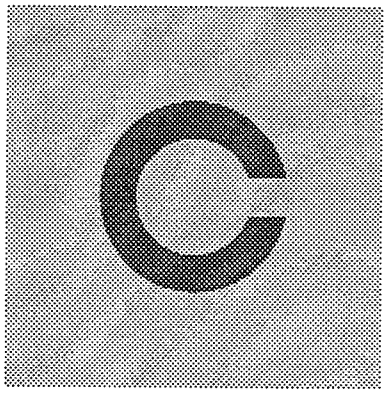

Figure 2. Landolt "C"

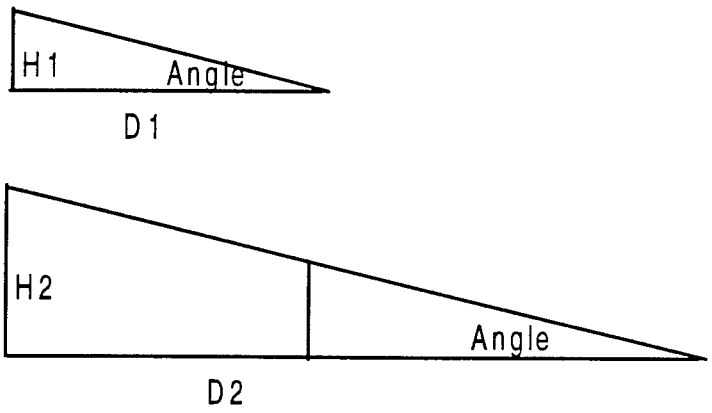

Figure 3. Height to distance ratio: atan angle = H1/D1= H2/D2

Results: Experiment 3

Experimental results showed that the contrast level, orientation, and target size affected the acuity of the subjects. As expected, higher contrast levels produced better acuity. The 24% contrast target produced a grand mean of 2.801 arcminutes, and the 71% contrast target produced a mean of 2.108 arcmin. Due to astigmatic effects, orientation contributed to individual differences in thresholds between horizontal and vertical; the horizontal orientation typically produced lower arcminute values. Orientation, however, did not cause much variation in the data and could be combined as long as both orientations received equal trials.

Target size, on the other hand, produced unexpected results. The primary pattern subjects exhibited was an increase in arcminutes as the target size increased. Instead of a flat function, the size to distance ratio (H/D) showed disproportionate distance values. Table 1 shows the arcminute values for each of the subjects as a function of target gap size. The grand mean for the .7112 cm target is 1.999; the 1.4224

target is 2.457; and the 2.1844 target is 2.909. One subject was eliminated in certain analyses because of his extremely high arcminute values. (Refer to Figure 6) Subjects with such outlying data can be expected in such experimentation but are not necessarily included in data analysis.

Table 1.

Arcminute values for experiment 3.

Subject	Target Gap Sizes (cm)		
	.7112	1.4224	2.1844
1	4.545	5.351	5.761
2	2.061	2.287	2.498
3	0.961	1.975	3.249
4	1.376	1.459	1.161
5	1.051	1.210	1.421
Grand Mean:	1.999	2.457	2.909

Figure 4 presents the range of mean arcminutes at each of the levels of the experimental factors. As anticipated, subjects had the greatest range of variation. Gap size produced the next largest variation. The graph clearly displays this unexpected deviation of arcminutes to their related sizes. Orientation and block numbers affected values slightly. Figure 5 demonstrates the upward tendencies of each subjects' arcminute values. Figure 6 presents all of the subjects' arcminute means. It is apparent that the subject excluded from the calculations was in a range of extremely low visual acuity. To better display the occurring distance phenomena his selective elimination is justified.

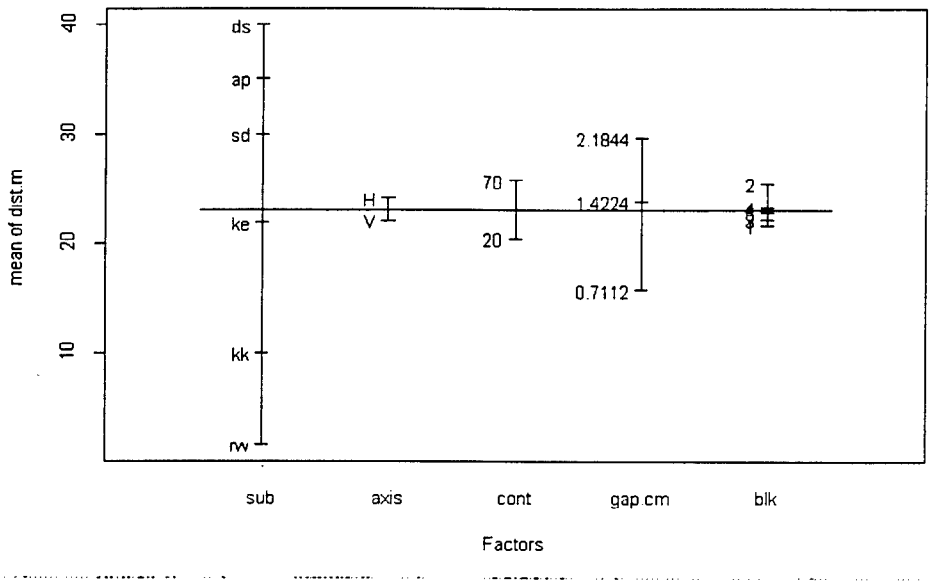

Figure 4. Mean of visual acuity in arcminutes for individual levels of main factors.

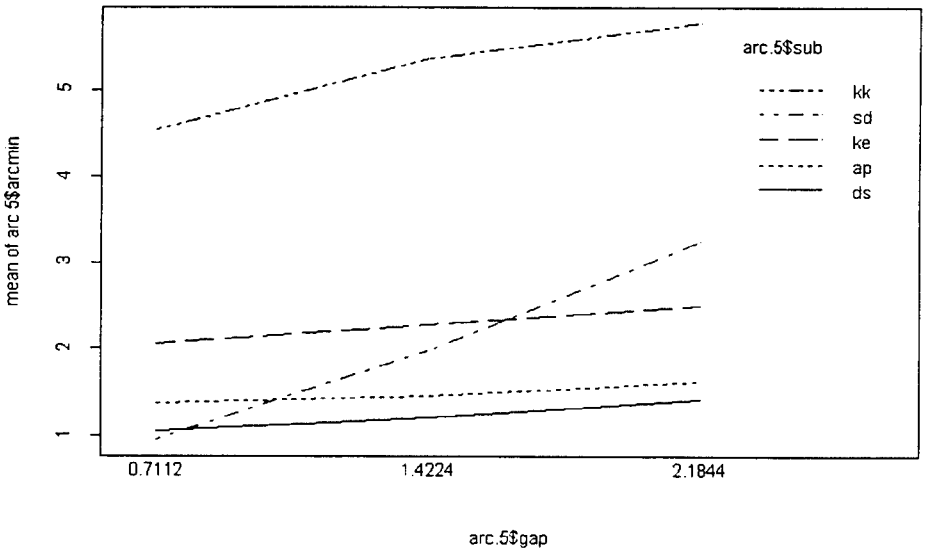

Figure 5. Acuity as a function of gap size for each observer.

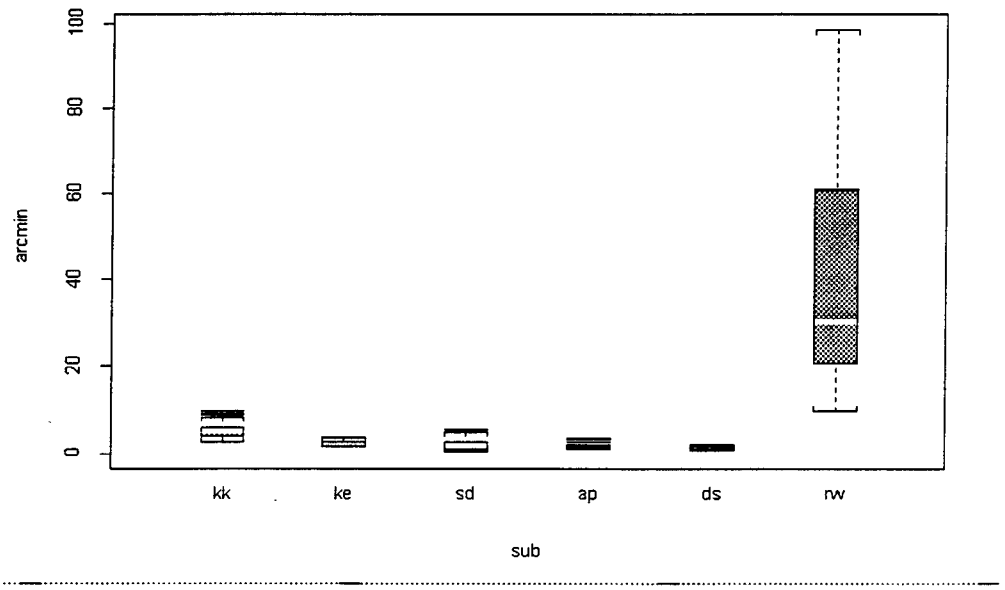

Figure 6. Box plots of acuity for each observer.

Introduction: Experiment 4

Since the distance phenomenon did not disappear in experiment 3, other possible variables were investigated. One possibility for the gap effect was that the use of a 18 cm x 18 cm square background for both sizes introduced an artifact due to differential crowding (the large "C" was more crowded than the smallest "C"), therefore, it was postulated that edge effects could have been causing the unexpected disproportion in distance ratios.

Methodology: Experiment 4

Due to the outcome of experiment 3, edge effects were explored in experiment 4. Although the size of the "C" varied with each display, all of the "C"'s were pasted on 18 x 18 cm foam board cards. Therefore, the immediate, or nearest edge, of each "C" did not scale in size as the target sizes increased. In particular, the large "C"'s were very "crowded" or close to the edge of the frame. To correct this, the targets were made using Landolt "C"'s with an immediate background dimension of twice the circle diameter. This was then attached to a larger square creating a border of more than eight gap widths.

In theory, this set-up would mitigate differential edge and "crowding" effects and potentially solve the size to distance problem.

The approach to experiment four was similar to that of experiment three. To bring out gap effects, the gap range was increased from 3-fold to 4-fold. The variables included two gap sizes (0.5 cm and 2.0 cm), four orientations (up, down , left, and right), one contrast level (17%), and one light level. The procedure was identical to experiment three except that experiment four only consisted of twenty trials (five blocks of four trials), with the mounted target at the end of a 60 meter room and the subject utilizing the method of adjustment. We also reduce the number of contrast levels from 2 to 1 (the more difficult level) in order to reduce the total burden on the observer.

Results: Experiment 4

The results to experiment four were analogous to those of experiment three. It is apparent that the edge effects were not causing the strange distance phenomenon. Figure 7 exhibits the means for acuity (in arcminutes) for the individual factors of the experiment. It's evident that the distance effect is still occurring. Figure 8 reveals the box plot of each observer. As the graph clearly shows, the range of arcminutes the subjects displayed is relatively confined. This graph omits the sixth subject from the analysis because of his extreme data (Refer to Figure 6). Figure 9 constructs an indisputable picture of the upward slope evident when acuity is graphed as a function of gap size. All of the subjects exhibit this upward trend. Figure 10 simply shows acuity as a function of gap size by block. Clearly, the block from which the data is analyzed isn't significant.

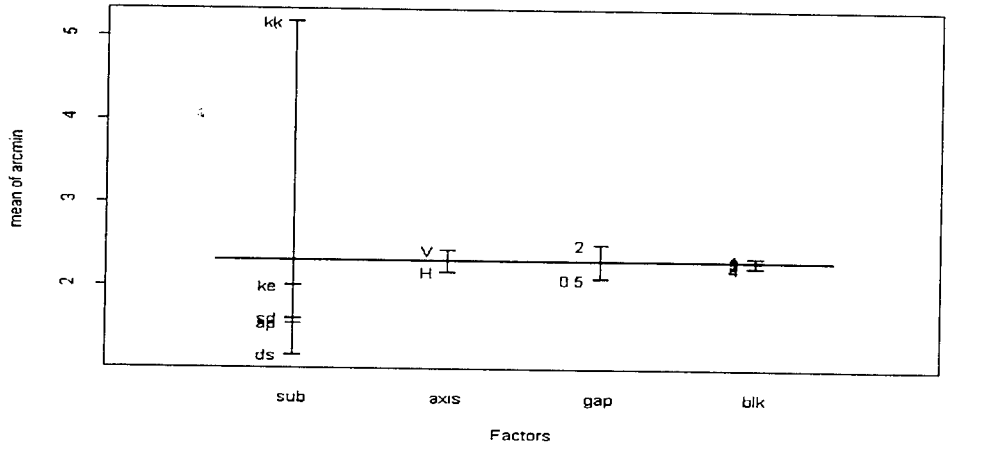

Figure 7. Mean of visual acuity in arcminutes for individual levels of main factors.

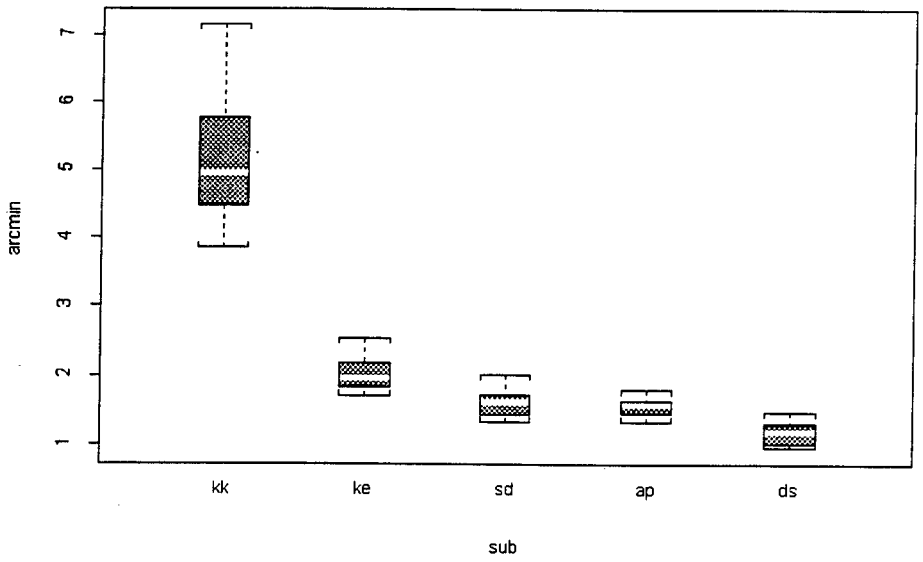

Figure 8. Box plots of acuity for each observer.

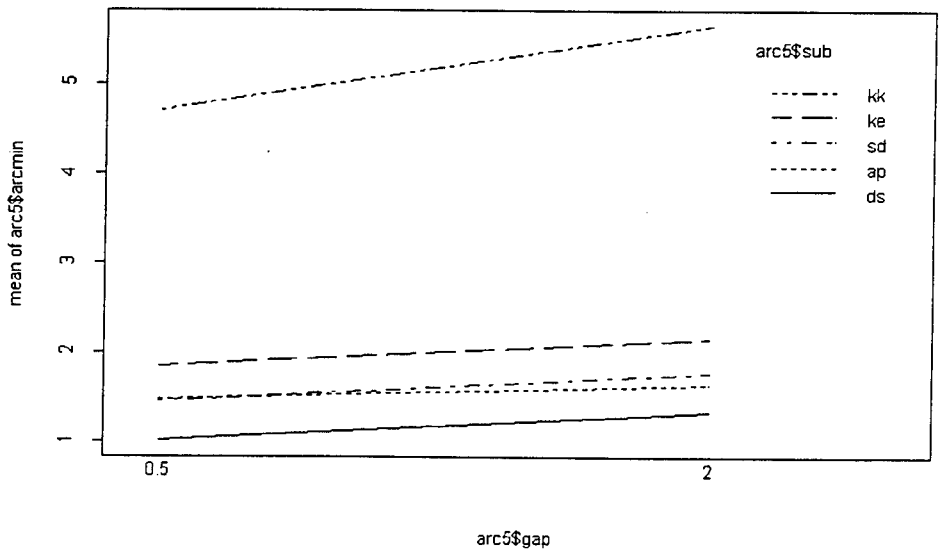

Figure 9. Acuity as a function of gap size for each observer.

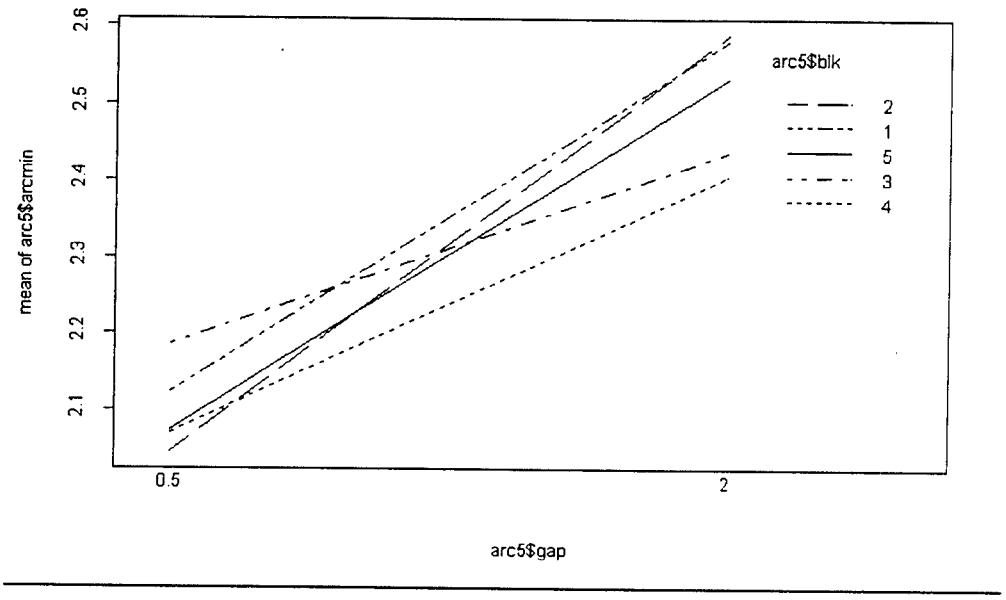

Figure 10. Acuity as a function of gap size for each block.

Introduction: Experiment 5

The results to experiment four were identical to those of experiment three. When examining the acuity as a function of gap size, an upward trend still appeared. Since astigmatism effects and edge effects can be eliminated as possible causes, the effects of binocular vision was explored by running subjects using monocular viewing techniques.

Methodology: Experiment 5

The procedural approach to this experiment was similar to experiment four except that the viewing of the target was monocular instead of binocular. This was done by the subject placing his/her hand over their left eye, only exposing their right eye to the stimuli. The data was also only collected for three subjects instead of six. This was done because the upward trend was so obvious after three subjects that additional runs were unnecessary.

Results: Experiment 5

The solution to the distance phenomenon was not identified with experiment five. The results were comparable to those of previous experiments, displaying the increased visual angle with the increase in target size; the only exception was that monocular viewing led to shorter distances overall. Figure 11

displays the means of acuity for all individual factors involved in the experiment. The unexpected gap effect is apparent, demonstrating that the solution was not monocular viewing. Figure 12 shows the means in arcminutes for the individual subjects. The upward trend in arcminute values as gap size increases is clearly displayed .

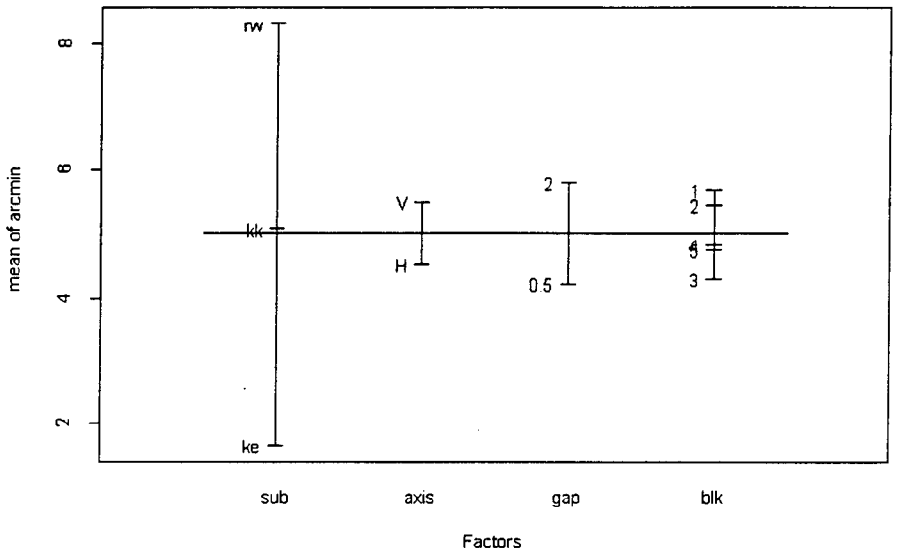

Figure 11. Means of visual acuity in arcminutes for individual levels of main factors.

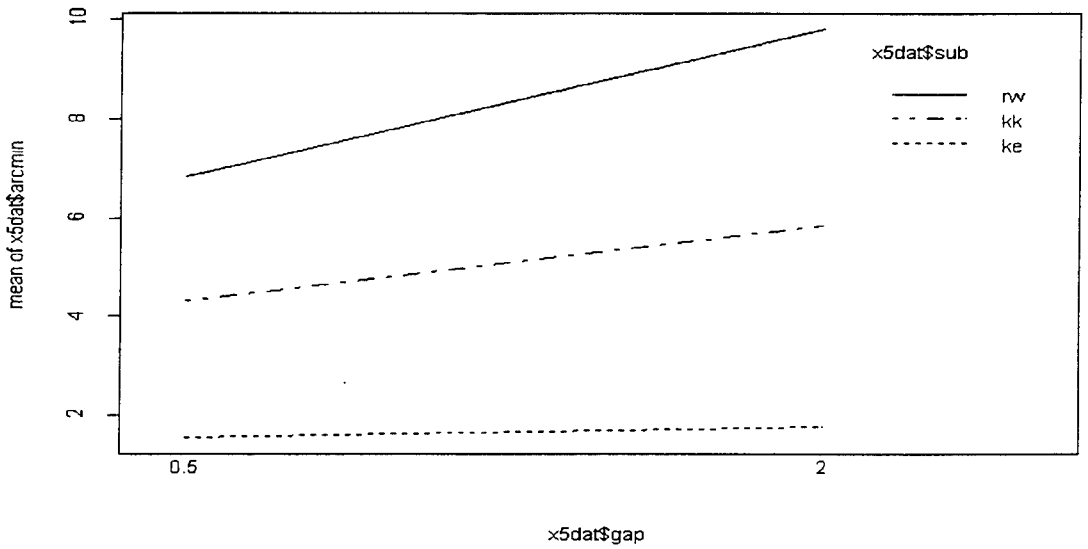

Figure 12. Means of arcminute values for three subjects.

General Discussion:

At this point in the research, the distance effect is still evident. It is known, however, that it is not attributed to crowding, binocular vision, accommodation, or stereopsis. Because the cause is not known additional experimentation must be conducted. Based on the data collected and analyzed to date, this technique cannot be recommended for use in the zoom lane until the cause of the effect is known.

Associate did not participate in the program.

A LOOK INTO THE AIR FORCE'S COMPUTER DEPARTMENT

Priscilla M. Medina

Port St. Joe High School
100 Shark Drive
Port St. Joe, FL 32456

Final Report for:
High School Apprentice Program
Armstrong Laboratory

Sponsored by:
Air Force Office of Scientific Research
Bolling Air Force Base, Washington, DC

And

Armstrong Laboratory

August 1997

A LOOK AT THE AIR FORCE'S COMPUTER DEPARTMENT

Priscilla M. Medina

Technology in our world today is advancing at lightning speed. The world of computers is no exception. At Tyndall Airforce Base, the computer department at AL/EQ is where I spent my 1997 summer research program experience. The experience and tasks I was assigned varied from basic office errands to assisting in the installation of an air force anti-virus screen saver.

The first couple of days was spent getting to know the computer department at AL/EQ. After getting to know the department and personnel, there were several boxes full of old disks which I was given to format and bag with labels for the whole department to use. The department was to begin conducting computer learning sessions in where they had a room for the classess as well as printed material. I helped in setting up the computers in the room and stocking up the shelves with books and videos. I then had to make copies of the booklets needed for the classes. Then most of my time was spent in assisting installing the air force's anti-virus screen saver in every computer in the department. This took several days and took a bit of time considering that people's computers were available.

My 1997 summer research program experience was different than others because I worked at the computer department instead of the lab. I stilled learned with doing basic office tasks. I got to know the department and even the air force better.

A Study of Accuracy and Response Time in Tests of Spatial Ability

Mark T. Meiners

Dobson High School
1501 W. Guadalupe Road
Mesa, Arizona 85202

Final Report for:
High School Apprenticeship Program
Armstrong Laboratory

Sponsored by:
Air Force Office of Scientific Research
Bolling Air Force Base, DC

and

Armstrong Laboratory

July 1997

A Study of Accuracy and Response Time in Tests of Spatial Ability

Mark T. Meiners
Dobson High School

Abstract

Mental rotation is the ability to see three dimensional objects in space and then mentally determine the characteristics of each object. The effect of mental rotation in depth is quite different from the effect found with mental rotation in the picture plane. The angular difference in depth for comparisons of same or mirrored objects was thought to predict the mean response times. An effect called the tandem rotation effect is a counterexample to that hypothesis. Two shapes are separated by an angular difference in depth, then tilted in depth. There is an almost linear variation between the mean response times and the amount of yoked rotation when angular difference is held constant. The tandem effect supports the idea that the mean response time is a function of the area shown to be rotated away from the picture plane; not as a function of the angular difference between the two objects. Tests were done to determine whether or not the area shown on screen has a part in response times. Varying speeds and tilts were incorporated with the angular difference to determine what was playing the key role in response times. After all the tests were done, the data was collected, summed into large databases, and then roughly analyzed with graphs.

A Study of Accuracy and Response Time in Tests of Spatial Ability

Mark T. Meiners

Introduction

For some time now mental, pictured, and tandem rotation have been studied. However, a conclusive hypothesis has not been found to accurately demonstrate these effects. It is still a gray area in which many ideas have been raised. Having the ability to accurately depict the effects can do a great deal of help in the area of computer simulated objects. Increased performance can be reached by weapons systems officers when completing a task more quickly and more efficiently due to the enhancement of the vision systems. The problem remains that an accurate hypothesis has not been universally made which inhibits perfecting the imagery systems on craft.

Methodology

To obtain a better understanding of the mental and pictured effects, a subject would be tested thoroughly within three different experiments. The data was collected and compiled with graphs of the results. The graphs were made to give the results of what happened in the experiment. These gave a rough idea on what to expect from future trials as well. Various graphs of the data were made. They would be three dimensional and sometimes just flat graphs. It depended on the variables being used for that particular experiment. For example, only flat graphs containing the number correct versus cumulative response times.

The three experiments varied in rotation speed, interval of initial rotation, and complete reverse views of the two objects. The subject would then decide if the objects were the same or different from each other. These mental tests were shown on a Silicon Graphics IRIS workstation with IRIX operating system 5.3 using GL graphics library. During all experiments, the subject would use a three button mouse to make the appropriate selection. The left mouse button for the same and the right mouse button would be used if the objects were different. Therefore, the last middle button was used as a pause button for pausing between trials. Experiment one dealt with variable angular difference and variable tilts.

In experiment one the variables were angular difference and tilt. The intervals for the angular difference varied by 10 degrees starting at zero and going up to 180. The other variable, tilt, was any of 5 numbers being 0, 15, 30, 45, and 60 degrees. All the settings for each experiment were setup at the beginning according to the randomized syllabus sheet. The computer would randomize the order of the individual trials. Experiment one contained the four colored dodecahedron as well as the twelve colored one.

These dodecahedron were twelve sided three dimensional objects that would seem to float on the computer screen. The four colors were yellow, green, blue, and a orange/brown color. While in the twelve color object, they had the twelve basic colors, and as a result, all sides had a different color. The four colored object had the colors randomized but never touching a same colored side.

Experiment two introduced speed of rotation in place of tilt. Each object would now be rotating at five different speeds. One being the slowest while five would be the fastest. Both objects would spin at the same rate during the individual sections of the experiment but would vary from section to section. Each section contained three blocks and a total of 342 trials. The interval remained the same as in experiment one, changing from zero to 180 by tens.

Experiment three was quite a different experiment. The objects were completely motionless this time. The one of the objects would be reversed. From this the subject would decide if it was the same or mirrored. In the twelve color portion of the experiment there would be a key at the bottom of the screen which would describe which colors matched with which. This made the task even more difficult during the twelve color sections because the subject would have to memorize the order of the colors to receive better times. In the four color the subject had more visualize what would be on the other side. After the subject made his or her selection the rotated object would turn forward and show its face. From here the subject would be able to see easily wether or not they were correct. This was also different because the subject was now getting feedback on their response.

The subjects would also rotate and take breaks to help relax. This also prepares them for maximum performance from the standpoint of mental fatigue. Some of the various graphs made had to do with mean response times versus the other variables in a three dimensional graph. In the third experiment with the

still objects, simple graphs with the number correct vs. response times were made.

Kirsten Sheffield documented the following on the description of the program:

> The Assessment of Perception-Taking Ability Program is an interactive graphics application developed for Armstrong Laboratory. Psychologists from the Human Factors Division will use this software to study the ability of human observers to determine if the coloring of hidden faces of a dodecahedral are equivalent to the coloring of the faces displayed to the subject. There are two dodecahedral visible on the screen. Each figure is an opaque dodecahedron; each face of each figure is a solid color. In experiment one, four colors are used for the twelve faces of each dodecahedron. In experiment two, each face is a different color resulting in a twelve colored dodecahedron. Both figures are in continuous motion, rotating at the same rate. They appear to tumble in space (i.e. they rotate about the yz and xz planes at constant angles relative to each other).

The program was also capable of being changed and was to fit the needs of the experiment. The objects were motionless sometimes, and then moving at various other speeds. It was not limited to constant motion. However, both objects responded the same to the change in speeds. Both objects moved the same as the other. Kirsten gave a good description what happened in the first experiment.

The program was setup at the start-up screen. From there the subject selected the filename and the variables to be tested from a randomized syllabus sheet. The subject would complete the experiment by pushing the appropriate buttons. Collecting the data, the information was pulled from computer to computer via iFTP. The data files would be in the name form, RESdataXXX, where XXX is a number from 000 to 999 corresponding as the filename entered at setup. The files would then be put into excel files combining a series of ten sections. From here the data was looked at and several new variables were calculated. The natural log of the times were calculated as well as number correct. We were very interested in the number correct. The times are less meaningful if the subject rushed through and missed many of the trials. As time progressed and sufficient data was collected, the data was put into various graphs. These graphs would show response times against tilt and angular difference in a three dimensional graph.

Results and Conclusion

The data of the experiments have not yet been analyzed. Analysis is going to continue later after more data can be collected. Some early results are only showing trends in the mean response times decreasing as well as the number of correct rising. No conclusive results have been made from this data. The research will continue later to further collect data. This study has not made any conclusions as to the effects of mental, pictured, and tandem rotation. More data must be collected in order to sufficiently make a hypothesis for these effects. Time constraints have made it impossible to accurately depict any hypothesis so far relating to these effects. After more is done, then a general and accurate statement can be made.

References

Niall, Keith Dr., 1997. ' Mental rotation ', pictured rotation, and tandem rotation in depth, Acta Psychologica 95 (1997) 31-83.

Sheffield, Kirsten, 1997. "Assessment of Perception-Taking Abilities", unpublished manuscript, Hughes Training, Inc.

AN ANALYSIS OF RADIOFREQUENCY RADIATION-INDUCED TEMPERATURE GRADIENTS IN THE RAT BRAIN

David J. Miller
Mr. William Hurt, OERS
Dr. Patrick Mason, OERB
Dr. David Nelson

Texas Academy of Mathematics and Science
P.O. Box 5307
Denton, TX 76203-0307

Final Report for:
High School Apprentice Program
Armstrong Laboratory

Sponsored by:
Air Force Office of Scientific Research
Bolling Air Force Base, DC

and

Armstrong Laboratory

August 1997

AN ANALYSIS OF RADIOFREQUENCY RADIATION-INDUCED TEMPERATURE GRADIENTS IN THE RAT BRAIN

David J. Miller
Texas Academy of Mathematics and Science

Abstract

Microwaves are a form of electromagnetic radiation that can cause thermal damage to objects exposed to them. High powered microwaves (HPM) have the capability to cause massive thermal damage to an individual exposed to them. Micrwaves are particularly dangerous, because they do not heat uniformly. At the present time, doctors do not realy know what organs are in great danger of being damaged during HPM exposure. The hope is to create a model of a whole human being after creating a model of a rat brain and head. Five mathematical models of increasing complexity have been created that mimic the exposure of a rat head or brain to HPM. The five models are the spherical; cylindrical; homogeneous cylindrical; cylindrical shells; and whole-head, non-homogeneous cylindrical shells models. The results of these models are then discussed and compared to real experimental results.

AN ANALYSIS OF RADIOFREQUENCY RADIATION-INDUCED TEMPERATURE GRADIENTS IN THE RAT BRAIN

David J. Miller

Introduction

Radiofrequency radiation (RF) is electromagnetic radiation that has a longer wavelength than visible light. For purposes of this work, radiofrequency will be considered to extend from 10 MHz to approximately 120 GHz. This includes the microwave frequencies. Microwaves are an example of this type of electromagnetic radiation. On the other end of the electromagnetic spectrum with much shorter wavelengths are the gamma and x-rays. These wavelengths are commonly known as ionizing radiation, because they can ionize an object by breaking the bonds of its atoms. Unlike ionizing radiation, RF produces biological effects almost exclusively via tissue heating. Microwaves, while possessing no ionizing capabilities, deposit most of their energy into the exposed object. Microwaves have the capability to produce massive thermal damage. People may be exposed to HPM near microwave radars and large industrial ovens.

This work is concerned with effects from low frequency microwaves. Microwaves have a range of about 0.5 GHz to 120 GHz. A low frequency microwave can penetrate farther into tissue than a high frequency microwave. Very high frequency microwaves could severely damage peripheral tissue, but leave internal organs undamaged, in contrast low frequency microwaves could damage internal organs, but leave the peripheral tissue looking normal. A microwave oven operates at 2.45 GHz, which is enough to go through about 0.5 to 1.0 ft of material. In the models that are to be discussed here, a frequency of 2.06 GHz was used.

Some terminology should be discussed before proceeding further into the paper. Power density is expressed in energy per time per area (W/cm^2). Power density, which can be measured directly, is the energy passing through a "window in space" per second per the area of that window. In the models to be discussed here, a power density of 1.7 W/cm^2 was used, typical of a high powered microwave (HPM). Specific absorption rate (SAR) is the actual amount of energy absorbed by an organism per time per mass of the organism. It is expressed in energy per second per mass, which is usually in units of Watts per kilogram. Since SAR cannot be measured directly, it must be figured out from the mass, specific heat and total change in temperature of the object, along with the time for that temperature to occur. A higher power density will result in a higher SAR, since there is more energy to absorb. An SAR of 1224 W/kg was assumed at the places with the highest SARs in the models. That is a conversion from 1.7 W/cm^2 found in the paper by Walters et al. (submitted).

Discussion of Problem

High powered microwaves generally do not heat tissue uniformly. Like electricity they have a greater influence at certain areas, such as thin or flat areas, sharp corners or edges, and extreme differences in tissue types. Therefore organs such as the lungs and liver can be seriously damaged by HPM; the liver is susceptible, because it is flat and has sharp edges and corners. The lungs are susceptible, because there is an extreme difference between the air in them and the actual tissue. Also a tissue closer to the surface of the body will be able to dissipate more energy to the outside air than a more central organ could, which will result in the outer organ having a lower temperature.

This work addresses temperature gradients in the rat brain. The rat is a typical lab animal and therefore there is more data regarding exposure of a rat to microwaves. A rat exposed to HPM may have temperature gradients within the brain. Two parts of the brain that have been found to have high temperatures when the rat is exposed to HPM are the hypothalamus and the brain stem. The hypothalamus probably has a high temperature, because it is in a central location in the brain and the mouth and jaw are underneath it. Also there is a large artery running over the brain which would cool the cortex but not the hypothalamus. The brain stem is probably a "hot spot," because it is much narrower than the rest of the brain and HPM have a greater influence at thin areas.

Microwaves are particularly dangerous, because they do not heat tissue uniformly. Someone exposed to HPM could have a whole body SAR that is not above internal safety standards, while certain key organs, such as the lungs, are severely damaged by excess heat. Since doctors do not really know which organs are in danger when a person is exposed to HPM, I have been working on making a mathematical model of the rat brain and head that would show the temperatures at different places in the head after exposure to HPM. The hope is to modify this to a human and make it for the whole body, so that if someone is exposed to HPM, a doctor can look in a handbook and find what organs may be in danger.

Methodology

The first model of the rat brain used was that by Ward et al. (1986). It is a relatively simple model; that is, a small sphere was contained within a larger spherical shell. The smaller sphere has a radius of 2 mm and the spherical shell has a radius of 8 mm. The smaller sphere is meant to be the hypothalamus or another "hot spot" in the rat brain, while the larger sphere is the whole brain. To simplify the model further, the outer layer does not absorb any energy. The density of both spherical layers is assumed to be that of water: 1000 kg/m^3. The specific heat is assumed to be 3600 J/kg/°C and the thermal conductivity is assumed to be 0.500 W/m/°C. The calculations for this model along with all of the other models were done on Mathcad PLUS 6.0 (MathSoft Inc.). The equations entered for this model are shown in Figure 1.

The second model used was a small cylinder within a larger cylinder. By looking at a picture of the rat brain, one can see that it is more cylindrical than spherical. Therefore the next logical step in perfecting the model is to make the model cylindrical. All of the properties except those dependent upon the morphology remain the same as in the spherical model. The radii remain the same length. The length of both cylinders is 1.2 cm. The new equations entered for this model are shown in Figure 2.

In the third model the two cylinders are replaced by one homogeneous cylinder with a radius of 8 mm and a length of 1.2 cm. The density, specific heat of brain tissue, and thermal conductivity are not changed from the previous model. Several things were added to this model to make it more realistic. First blood flow was added to this model. The perfusion rate is assumed to be 9.0 kg/s/m^3 and the specific heat of blood is assumed to be 3800 J/s/°C (Nelson, personal communication). Next, a convection condition was added at the surface. The convection coefficient, h, is assumed to be 5.00 W/m^2/°C. In reality, with the wavelength of microwaves being used, the SAR should not be the same throughout the brain. The inner portion of the brain should have a higher SAR than the outer portions. So a term $e^{-c_1 r}$ was multiplied by the SAR; c_1 is equal to a/R. This term modifies the equations so that the parts of the brain closer to the center have higher SARs than the parts further from the center. The change depends on the value used for a and the value of 0.90937 was chosen. This value will result in the central line of the cylinder having an SAR of 1224 W/kg and the curved surface having an SAR of 493 W/kg. These numbers were found by using the HPM conversion factors for the hypothalamus and cortex, respectively, in the paper by Walters et al. (submitted) on 1.7 W/cm^2. The first equations made for this model are for a steady state. These equations are shown in Figure 3. The steady state shows what temperatures the cylinder will level off at; it produces a function dependent on the radius. All points at the same radius are assumed to have equal temperatures. Steady state temperatures help very little without the time it takes to get close to those temperatures. Since it could possibly take several minutes or even more to even get close to the steady state temperatures. The second set of equations is for time dependent (Figure 4). They show the mean temperature as a function of time. This function reveals about how long it takes for the cylinder to get close to the steady state temperatures.

The fourth main model is the cylindrical shells model. Using a technique called finite-difference approximation, this model allowed us to estimate temperatures as functions of both radial location and time. This model divides the homogeneous cylinder into eleven shells with all but the first and last having equal thicknesses. The first and last have thicknesses of half of the others. Each shell is assumed to be the same temperature throughout. The properties are unchanged from the homogeneous model. The equations for the steady state are shown in Figure 5. Each shell has an equation for the change in its temperature, except for shell eleven, which is assumed to remain at a constant temperature of 37°C, the temperature of the surrounding tisue. The change in the temperature of the shell is dependent upon the temperature of the shell and the shells directly adjacent to it, the blood flow rate and

temperature of blood, and the microwave exposure. The equation for each shell is based upon these factors. To find the steady state all ten of those equations are set to zero (no change is occurring) and the Mathcad software solves them as a system of equations. The time dependent equations (Figure 6) are worked out from the steady state equations. There is no major change in equations, just the way they are implemented. Time is divided into one second sections just as the volume was divided. The equations are now used to figure out the temperature in that shell at the next second. The equations are solved that way for as many seconds as one wants the model to go out for.

The fifth and final main model is the whole-head, non-homogeneous cylindrical shells model. The next logical step is to make a model for the whole head. The radius of the cylinder is increased to 1.3 cm. The inner six shells remain brain matter, but the seventh shell becomes cerebrospinal fluid. The next two shells are the skull and the last two layers are the scalp. The thermal conductivity and perfusion rate are changed for each shell to reflect the new material that it is (Nelson, personal communication). A convection coefficient was added. Shell eleven no longer remains at a constant temperature. The ambient temperature was made 22°C, but the convection coefficient is low enough that shell eleven can remain more than 10°C above the ambient temperature, as real skin would. The temperature of the blood was raised from 37°C to 38°C. The equations for the steady state can be found in Figure 7. The microwave heating was taken out of the steady state equations and replaced by the metabolic heating rates for each type of tissue (Nelson, personal communication). The steady state equations will then return the initial conditions (temperatures) for the time dependent equations to start with. The time dependent equations are shown in Figure 8. They are also changed. The time increment was changed from 1 second to 0.5 seconds. The microwave heating reverts to metabolic heating after 20 seconds to simulate the turning off of the microwaves after 20 seconds as was done in the experiment by Walters et al. (submitted) The metabolic heating rate is so small compared to microwave heating rate that it need not be added to the microwave heating rate.

Results

The spherical model gives a graph of temperature of the inner sphere versus time. The graph is shown in Figure 9. The temperature plateaus at almost 39.5°C after about 20 to 25 seconds of exposure. The temperature levels off because the energy going in equals the energy going out. As the temperature of the sphere gets higher, the amount of energy it loses to the outside environment rises until the energy it is losing is equal to the energy it is absorbing from the microwaves. In actuality, they will never be exactly equal, but they will get very close.

The cylindrical model also gives a graph of temperature of the inner cylinder versus time. This graph is shown in Figure 10. It also levels off for the same reason that the spherical model levels off. The cylinder, though, raises to almost 44°C and reaches this temperature in approximately 90 seconds. The cylinder reaches a higher temperature,

because it has a lower surface area to volume ratio than the sphere. Since it has less surface area per unit volume than the sphere does, the cylinder must dissipate less energy per unit volume than the sphere does. This means that the cylinder will have more energy per unit volume and hence have a higher temperature. If one calculates the volume and surface area of the sphere and cylinder with the values used in the models ($r = 2 * 10^{-3}$ m, $L = 12 * 10^{-3}$ m), one finds that the surface area to volume ratio of the sphere is 15 cm^{-1} and the surface area to volume ratio of the cylinder is 11.67 cm^{-1}. Therefore the cylinder has the lowest surface area to volume ratio.

The steady state homogeneous cylindrical model provides a graph of temperature versus radial location. The graph is shown in Figure 11. The temperatures range from about 59.5°C in the center to 55°C on the surface. At first these temperatures may seem high (on average 20°C above the beginning temperature), but remember these are the steady state temperatures and may take a while to achieve. A look at the time dependent graph (Figure 12) shows that it would take about 3 minutes to get close to the steady state conditions. Rats are usually not experimentally exposed to HPM that long. Even if they were, the rat would die before those extreme temperatures were reached.

The cylindrical shells model provides eleven temperatures for each time step. Actually, it provides only ten since the last temperature remains at a constant 37°C. The steady state graph (Figure 13) shows temperatures from 52°C to 37°C. These temperatures are much lower than the temperatures given by the homogeneous cylindrical model. The time dependent graph (Figure 14) shows that it takes less time to reach those steady state temperatures (1 to 2 minutes) than it took to reach the homogeneous cylinder's steady state temperatures (3 minutes).

The steady state whole-head, non-homogeneous cylindrical shells model provides a graph different from the other two steady state graphs. Instead of providing the steady state temperatures for microwave exposure, the graph gives the steady state conditions for metabolic heating. The graph is shown in Figure 15. The resulting temperatures are low, since they are an approximation for non-exposed conditions. The temperatures range from about 37.7°C to about 36°C. These are entered as the starting temperatures for the time dependent equations. The graph for the time dependent equations is shown in Figure 16. Notice on the graph that the temperatures begin to fall after 20 seconds. This is because the microwave heating rates are changed to the metabolic heating rates (the microwaves have been turned off). The only two temperatures that do not fall immediately after 20 seconds are the two skull temperatures; they actually rise for about 30 seconds after the microwaves have been turned off before they start falling.

Conclusion

So far I have been changing equations, adding variables to them, and changing the values of the variables in order to try to mimic the actual conditions in a rat brain and head. The only way though to test my equations and see how close to reality they are is to compare their theoretical results to actual experimental results. The results I have

chosen to use are taken from a graph in the Walters et al. (submitted) paper. The graph is shown in Figure 17. The graph shows the rectal, cortical, and hypothalamic temperatures as functions of time. The rats were exposed to HPM for a duration of about 20 seconds.

The temperatures of the spherical and cylindrical models are the temperatures for the inner objects. Since the inner objects were meant to be the hypothalamuses, their temperatures can be compared to the temperature of the hypothalamus. The experimental results give the hypothalamus a temperature of 43.5°C after 20 seconds (Figure 17). The spherical model gives a temperature of 39.25 after 20 seconds (Figure 9) and the cylindrical model gives a temperature of 41.25°C after 20 seconds (Figure 10). This supports the idea that a cylinder is a better model than a sphere, since the temperature for the cylinder was closer.

To compare the last three time dependent graphs to the experimental graphs one can use the innermost temperature for the hypothalamus. The homogeneous cylinder model gives a temperature of 42.5 °C after 20 seconds (Figure 12). The cylindrical shells model gives a temperature of 42 °C after 20 seconds (Figure 14) and the whole-head, non-homogeneous cylindrical shells model gives a temperature of 42.5 °C after 20 seconds (Figure 16). All three are fairly close to the experimental result. They are only about 1 to 1.5 °C off. The two time dependent cylindrical shells graphs can also be compared to the cortical temperature by using the outermost brain layer. The cortex is part of the surface of the brain. The experimental result is 39.5 °C after 20 seconds of exposure (Figure 17). The first time dependent cylindrical shells graph gives a result of 38.5 °C after 20 seconds (Figure 14) and the second time dependent cylindrical shells graph gives a result of 39.5 °C after 20 seconds (Figure 16). The second graph is very close. One thing that appears on the experimental graph but not on any of the theoretical graphs is the rising of the cortical temperature after the microwaves are turned off. This behavior is exhibited by the skull temperatures in the last theoretical graph though. Maybe by studying that behavior we can figure out what to add to the cortex to mimic that result.

In conclusion, the last set of equations provide a graph with temperatures very close to the experimental results. With a more fine tuning, I believe it can become a working model of the rat head. Many things can still be added, such as a more accurate brain morphology and differentiation between different properties of the different parts of the rat brain. Also the model could be sliced into even more pieces to make it more accurate. It could be sliced along different axes to differentiate between a top and bottom.

References

Nelson, D. A. personal communication. August 6, 1997.

Walters, T. J., Ryan, K. L., Belcher, J. C., Doyle, J. M., Tehrany, M. R., Mason, P. A. Regional Brain Heating During Microwave Exposure (2.06-GHz), Warm-Water Immersion, Environmental Heating, and Exercise. *Bioelectromagnetics.* Submitted.

Ward, T. R., Svensgaard, D. J., Spiegel, R. J., Puckett, E. T., Long, M. D., Kinn, J. B. (1986) Brain Temperatures in Rats: A Comparison of Microwave and Ambient Temperature Exposures. *Bioelectromagnetics,* 7:243-258.

Appendix

$\rho := 1000$ $\quad c := 3600$ $\quad r_i := 2 \cdot 10^{-3}$ $\quad r_o := 8 \cdot 10^{-3}$ $\quad vol := \frac{4}{3} \cdot \pi \cdot r_i^3$

$R_{th} := \frac{\frac{1}{r_i} - \frac{1}{r_o}}{4 \cdot \pi \cdot k}$ $\quad k := 0.500$ $\quad T_o := 37.0$ $\quad t := 0..50$

$\tau := \rho \cdot c \cdot vol \cdot R_{th}$ $\quad \tau = 7.2$ $\quad q := 1224$

$$T(t) := T_o + \left(q \cdot R_{th} \cdot \rho \cdot vol\right) \cdot \left(1 - e^{-\frac{t}{\tau}}\right)$$

Figure 1: Equations for the spherical model

$\rho := 1000$ $\quad c := 3600$ $\quad r_i := 2 \cdot 10^{-3}$ $\quad r_o := 8 \cdot 10^{-3}$ $\quad L := 12 \cdot 10^{-3}$

$R_{th} := \frac{\ln\left(\frac{r_o}{r_i}\right)}{2 \cdot \pi \cdot k \cdot L}$ $\quad k := 0.500$ $\quad vol := \pi \cdot r_i^2 \cdot L$ $\quad t := 0..150$

$\tau := \rho \cdot c \cdot vol \cdot R_{th}$ $\quad \tau = 19.963$ $\quad T_o := 37.0$ $\quad q := 1224$

$$T(t) := T_o + \left(q \cdot R_{th} \cdot \rho \cdot vol\right) \cdot \left(1 - e^{-\frac{t}{\tau}}\right)$$

Figure 2: Equations for the cylindrical model

$\alpha = \frac{m_i \cdot C_p}{k}$ $\quad \alpha := 6.799 \cdot 10^4$ $\quad \beta = \frac{q}{k}$ $\quad \beta := 2 \cdot 10^3$ $\quad H = \frac{k}{h}$ $\quad H := 0.1$ $\quad R := 8 \cdot 10^{-3}$

$a := 0.90937$ $\quad c_1 := \frac{a}{R}$ $\quad SAR := 1224$ $\quad v_0 := 1$ $\quad load(r1, v) := \begin{pmatrix} v_0 \\ 0 \end{pmatrix}$

$score(r2, \theta) := \theta_0 - \left[-\left(H \cdot \theta_1\right)\right]$

$$D(r, \theta) := \begin{bmatrix} \theta_1 \\ \left[-\left(\frac{1}{r} \cdot \theta_1\right) + \left(\alpha \cdot \theta_0\right)\right] - \left[SAR \cdot \beta \cdot e^{-(r-1)\tau}\right] \end{bmatrix}$$

$S := sbval\left(v, 10^{-306}, R, D, load, score\right)$ $\quad S = 22.40469$ $\quad \theta := \begin{pmatrix} 22.40469 \\ 0 \end{pmatrix}$

$Z := rkfixed\left(\theta, 10^{-306}, R, 300, D\right)$ $\quad i := 0..300$

Figure 3: Equations for the steady state homogeneous cylindrical model

$SAR := 1224$ $\quad \rho := 1000$ $\quad \alpha = m_i \cdot c_b$ $\quad \alpha := 6.799 \cdot 10^4$ $\quad h := 5$ $\quad c_p := 3600$

$R := 8 \cdot 10^{-3}$ $\quad D := 2 \cdot R$ $\quad L := 1.2 \cdot 10^{-2}$ $\quad A_s := (\pi \cdot D \cdot L) + \left(2 \cdot \pi \cdot R^2\right)$ $\quad V := \pi \cdot R^2 \cdot L$

$\theta_0 := 0$

$$D(t, \theta) := \frac{(SAR \cdot \rho) - \left[\left(\alpha + \frac{h \cdot A_s}{V}\right) \cdot \theta_0\right]}{\rho \cdot c_p}$$

$Z := rkfixed(\theta, 0, 1020, 100, D)$ $\quad i := 0..100$

Figure 4: Equations for the time dependent homogeneous cylindrical model

$L := 1.2 \cdot 10^{-2}$ $R := 8 \cdot 10^{-3}$ $\Delta r := \frac{R}{10}$ $k := 0.5$ $q := 1.224 \cdot 10^{6}$ $m_l := 9.0$ $c_b := 3.8 \cdot 10^{3}$

$T_{art} := 37$ $T_{11} := T_{art}$ $l := 1..11$ $r_l := (l-1) \cdot \Delta r$ $a := 0.90937$ $c_l := \frac{a}{R}$

$T_1 := 37$ $T_2 := 37$ $T_3 := 37$ $T_4 := 37$ $T_5 := 37$ $T_6 := 37$ $T_7 := 37$ $T_8 := 37$ $T_9 := 37$ $T_{10} := 37$

Given

$$-\left[-k\cdot\left(\frac{T_2-T_1}{\Delta r}\right)\right]\cdot\left[2\cdot\pi\cdot\left(\frac{\Delta r}{2}\right)\cdot L\right]+\left[q\cdot\pi\cdot\left(\frac{\Delta r}{2}\right)^2\cdot L\right]-\left[m_i\cdot c_b\cdot\left[\pi\cdot\left(\frac{\Delta r}{2}\right)^2\cdot L\right]\cdot(T_1-T_{art})\right]=0$$

$$\left[-k\cdot\left(\frac{T_2-T_1}{\Delta r}\right)\right]\cdot\left[2\cdot\pi\cdot\left(\frac{\Delta r}{2}\right)\cdot L\right]-\left[-k\cdot\left(\frac{T_3-T_2}{\Delta r}\right)\right]\cdot\left[2\cdot\pi\cdot\left(\frac{3\cdot\Delta r}{2}\right)\cdot L\right]+\left[\left[\left[q\cdot e^{-(c_1)\cdot\Delta r}\right]-(m_i\cdot c_b\cdot(T_2-T_{art}))\right]\cdot\pi\cdot\left[\left(\frac{3\cdot\Delta r}{2}\right)^2-\left(\frac{\Delta r}{2}\right)^2\right]\cdot L\right]=0$$

$$\left[-k\cdot\left(\frac{T_3-T_2}{\Delta r}\right)\right]\cdot\left[2\cdot\pi\cdot\left(\frac{3\cdot\Delta r}{2}\right)\cdot L\right]-\left[-k\cdot\left(\frac{T_4-T_3}{\Delta r}\right)\right]\cdot\left[2\cdot\pi\cdot\left(\frac{5\cdot\Delta r}{2}\right)\cdot L\right]+\left[\left[\left[q\cdot e^{-(c_1)\cdot 2\cdot\Delta r}\right]-(m_i\cdot c_b\cdot(T_3-T_{art}))\right]\cdot\pi\cdot\left[\left(\frac{5\cdot\Delta r}{2}\right)^2-\left(\frac{3\cdot\Delta r}{2}\right)^2\right]\cdot L\right]=0$$

$$\left[-k\cdot\left(\frac{T_4-T_3}{\Delta r}\right)\right]\cdot\left[2\cdot\pi\cdot\left(\frac{5\cdot\Delta r}{2}\right)\cdot L\right]-\left[-k\cdot\left(\frac{T_5-T_4}{\Delta r}\right)\right]\cdot\left[2\cdot\pi\cdot\left(\frac{7\cdot\Delta r}{2}\right)\cdot L\right]+\left[\left[\left[q\cdot e^{-(c_1)\cdot 3\cdot\Delta r}\right]-(m_i\cdot c_b\cdot(T_4-T_{art}))\right]\cdot\pi\cdot\left[\left(\frac{7\cdot\Delta r}{2}\right)^2-\left(\frac{5\cdot\Delta r}{2}\right)^2\right]\cdot L\right]=0$$

$$\left[-k\cdot\left(\frac{T_5-T_4}{\Delta r}\right)\right]\cdot\left[2\cdot\pi\cdot\left(\frac{7\cdot\Delta r}{2}\right)\cdot L\right]-\left[-k\cdot\left(\frac{T_6-T_5}{\Delta r}\right)\right]\cdot\left[2\cdot\pi\cdot\left(\frac{9\cdot\Delta r}{2}\right)\cdot L\right]+\left[\left[\left[q\cdot e^{-(c_1)\cdot 4\cdot\Delta r}\right]-(m_i\cdot c_b\cdot(T_5-T_{art}))\right]\cdot\pi\cdot\left[\left(\frac{9\cdot\Delta r}{2}\right)^2-\left(\frac{7\cdot\Delta r}{2}\right)^2\right]\cdot L\right]=0$$

$$\left[-k\cdot\left(\frac{T_6-T_5}{\Delta r}\right)\right]\cdot\left[2\cdot\pi\cdot\left(\frac{9\cdot\Delta r}{2}\right)\cdot L\right]-\left[-k\cdot\left(\frac{T_7-T_6}{\Delta r}\right)\right]\cdot\left[2\cdot\pi\cdot\left(\frac{11\cdot\Delta r}{2}\right)\cdot L\right]+\left[\left[\left[q\cdot e^{-(c_1)\cdot 5\cdot\Delta r}\right]-(m_i\cdot c_b\cdot(T_6-T_{art}))\right]\cdot\pi\cdot\left[\left(\frac{11\cdot\Delta r}{2}\right)^2-\left(\frac{9\cdot\Delta r}{2}\right)^2\right]\cdot L\right]=0$$

$$\left[-k\cdot\left(\frac{T_7-T_6}{\Delta r}\right)\right]\cdot\left[2\cdot\pi\cdot\left(\frac{11\cdot\Delta r}{2}\right)\cdot L\right]-\left[-k\cdot\left(\frac{T_8-T_7}{\Delta r}\right)\right]\cdot\left[2\cdot\pi\cdot\left(\frac{13\cdot\Delta r}{2}\right)\cdot L\right]+\left[\left[\left[q\cdot e^{-(c_1)\cdot 6\cdot\Delta r}\right]-(m_i\cdot c_b\cdot(T_7-T_{art}))\right]\cdot\pi\cdot\left[\left(\frac{13\cdot\Delta r}{2}\right)^2-\left(\frac{11\cdot\Delta r}{2}\right)^2\right]\cdot L\right]=0$$

$$\left[-k\cdot\left(\frac{T_8-T_7}{\Delta r}\right)\right]\cdot\left[2\cdot\pi\cdot\left(\frac{13\cdot\Delta r}{2}\right)\cdot L\right]-\left[-k\cdot\left(\frac{T_9-T_8}{\Delta r}\right)\right]\cdot\left[2\cdot\pi\cdot\left(\frac{15\cdot\Delta r}{2}\right)\cdot L\right]+\left[\left[\left[q\cdot e^{-(c_1)\cdot 7\cdot\Delta r}\right]-(m_i\cdot c_b\cdot(T_8-T_{art}))\right]\cdot\pi\cdot\left[\left(\frac{15\cdot\Delta r}{2}\right)^2-\left(\frac{13\cdot\Delta r}{2}\right)^2\right]\cdot L\right]=0$$

$$\left[-k\cdot\left(\frac{T_9-T_8}{\Delta r}\right)\right]\cdot\left[2\cdot\pi\cdot\left(\frac{15\cdot\Delta r}{2}\right)\cdot L\right]-\left[-k\cdot\left(\frac{T_{10}-T_9}{\Delta r}\right)\right]\cdot\left[2\cdot\pi\cdot\left(\frac{17\cdot\Delta r}{2}\right)\cdot L\right]+\left[\left[\left[q\cdot e^{-(c_1)\cdot 8\cdot\Delta r}\right]-(m_i\cdot c_b\cdot(T_9-T_{art}))\right]\cdot\pi\cdot\left[\left(\frac{17\cdot\Delta r}{2}\right)^2-\left(\frac{15\cdot\Delta r}{2}\right)^2\right]\cdot L\right]=0$$

$$\left[-k\cdot\left(\frac{T_{10}-T_9}{\Delta r}\right)\right]\cdot\left[2\cdot\pi\cdot\left(\frac{17\cdot\Delta r}{2}\right)\cdot L\right]-\left[-k\cdot\left(\frac{T_{11}-T_{10}}{\Delta r}\right)\right]\cdot\left[2\cdot\pi\cdot\left(\frac{19\cdot\Delta r}{2}\right)\cdot L\right]+\left[\left[\left[q\cdot e^{-(c_1)\cdot 9\cdot\Delta r}\right]-(m_i\cdot c_b\cdot(T_{10}-T_{art}))\right]\cdot\pi\cdot\left[\left(\frac{19\cdot\Delta r}{2}\right)^2-\left(\frac{17\cdot\Delta r}{2}\right)^2\right]\cdot L\right]=0$$

$y := \text{Find}(T_1, T_2, T_3, T_4, T_5, T_6, T_7, T_8, T_9, T_{10})$ $y_{10} := T_{11}$

Figure 5:Equations for the steady state cylindrical shells model

$L := 1.2 \cdot 10^{-2}$ $R := 8 \cdot 10^{-3}$ $\Delta r := \frac{R}{10}$ $k := 0.5$ $q := 1.224 \cdot 10^{6}$ $m_l := 9.0$ $c_b := 3.8 \cdot 10^{3}$

$T_{art} := 37$ $T_{11} := T_{art}$ $l := 1..20$ $r_l := (l-1) \cdot \Delta r$ $a := 0.90937$ $c_l := \frac{a}{R}$

$c_p := 3.6 \cdot 10^{3}$ $\rho := 1000$ $\alpha := \frac{k}{\rho \cdot c_p}$ $\alpha = 1.389 \cdot 10^{-7}$ $\Delta t := 1$

$$
\begin{aligned}
F := \;& T1_0 \leftarrow 37 \\
& T2_0 \leftarrow 37 \\
& T3_0 \leftarrow 37 \\
& T4_0 \leftarrow 37 \\
& T5_0 \leftarrow 37 \\
& T6_0 \leftarrow 37 \\
& T7_0 \leftarrow 37 \\
& T8_0 \leftarrow 37 \\
& T9_0 \leftarrow 37 \\
& T10_0 \leftarrow 37 \\
& n \leftarrow 419 \\
& \text{for } m \in 0..10 \\
& \quad G_{0,m} \leftarrow 37 \\
& \text{for } m \in 0..n+1 \\
& \quad G_{m,10} \leftarrow 37 \\
& \text{for } p \in 0..n \\
& \quad T1_{p+1} \leftarrow \alpha \cdot \Delta t \cdot \left[\left[\frac{-\left[-\left(\frac{T2_p - T1_p}{\Delta r} \right) \right] \cdot \left[2 \cdot \pi \cdot \left(\frac{r_2}{2} \right) \cdot L \right]}{\left[\pi \cdot \left(\frac{r_2}{2} \right)^2 \cdot L \right]} \right] + \frac{q}{k} - \frac{m_i \cdot c_b \cdot \left(T1_p - T_{art} \right)}{k} \right] + T1_p \\
& \quad T2_{p+1} \leftarrow \alpha \cdot \Delta t \cdot \left[\frac{\left[-\left(\frac{T2_p - T1_p}{\Delta r} \right) \right] \cdot \left[2 \cdot \pi \cdot \left(\frac{r_2}{2} \right) \cdot L \right] - \left[-\left(\frac{T3_p - T2_p}{\Delta r} \right) \right] \cdot \left[2 \cdot \pi \cdot \left(\frac{r_4}{2} \right) \cdot L \right]}{\pi \cdot \left[\left(\frac{r_4}{2} \right)^2 - \left(\frac{r_2}{2} \right)^2 \right] \cdot L} + \frac{q \cdot e^{-(c1) \cdot r_2}}{k} - \frac{m_i \cdot c_b \cdot \left(T2_p - T_{art} \right)}{k} \right] + T2_p \\
& \quad T3_{p+1} \leftarrow \alpha \cdot \Delta t \cdot \left[\frac{\left[-\left(\frac{T3_p - T2_p}{\Delta r} \right) \right] \cdot \left[2 \cdot \pi \cdot \left(\frac{r_4}{2} \right) \cdot L \right] - \left[-\left(\frac{T4_p - T3_p}{\Delta r} \right) \right] \cdot \left[2 \cdot \pi \cdot \left(\frac{r_6}{2} \right) \cdot L \right]}{\pi \cdot \left[\left(\frac{r_6}{2} \right)^2 - \left(\frac{r_4}{2} \right)^2 \right] \cdot L} + \frac{q \cdot e^{-(c1) \cdot r_3}}{k} - \frac{m_i \cdot c_b \cdot \left(T3_p - T_{art} \right)}{k} \right] + T3_p \\
& \quad T4_{p+1} \leftarrow \alpha \cdot \Delta t \cdot \left[\frac{\left[-\left(\frac{T4_p - T3_p}{\Delta r} \right) \right] \cdot \left[2 \cdot \pi \cdot \left(\frac{r_6}{2} \right) \cdot L \right] - \left[-\left(\frac{T5_p - T4_p}{\Delta r} \right) \right] \cdot \left[2 \cdot \pi \cdot \left(\frac{r_8}{2} \right) \cdot L \right]}{\pi \cdot \left[\left(\frac{r_8}{2} \right)^2 - \left(\frac{r_6}{2} \right)^2 \right] \cdot L} + \frac{q \cdot e^{-(c1) \cdot r_4}}{k} - \frac{m_i \cdot c_b \cdot \left(T4_p - T_{art} \right)}{k} \right] + T4_p \\
& \quad T5_{p+1} \leftarrow \alpha \cdot \Delta t \cdot \left[\frac{\left[-\left(\frac{T5_p - T4_p}{\Delta r} \right) \right] \cdot \left[2 \cdot \pi \cdot \left(\frac{r_8}{2} \right) \cdot L \right] - \left[-\left(\frac{T6_p - T5_p}{\Delta r} \right) \right] \cdot \left[2 \cdot \pi \cdot \left(\frac{r_{10}}{2} \right) \cdot L \right]}{\pi \cdot \left[\left(\frac{r_{10}}{2} \right)^2 - \left(\frac{r_8}{2} \right)^2 \right] \cdot L} + \frac{q \cdot e^{-(c1) \cdot r_5}}{k} - \frac{m_i \cdot c_b \cdot \left(T5_p - T_{art} \right)}{k} \right] + T5_p \\
& \quad T6_{p+1} \leftarrow \alpha \cdot \Delta t \cdot \left[\frac{\left[-\left(\frac{p - p}{\Delta r} \right) \right] \cdot \left[2 \cdot \pi \cdot \left(\frac{10}{2} \right) \cdot L \right] - \left[-\left(\frac{p - p}{\Delta r} \right) \right] \cdot \left[2 \cdot \pi \cdot \left(\frac{12}{2} \right) \cdot L \right]}{\pi \cdot \left[\left(\frac{r_{12}}{2} \right)^2 - \left(\frac{r_{10}}{2} \right)^2 \right] \cdot L} + \frac{q \cdot e^{-(c1) \cdot r_6}}{k} - \frac{m_i \cdot c_b \cdot \left(T6_p - T_{art} \right)}{k} \right] + T6_p \\
& \quad T7_{p+1} \leftarrow \alpha \cdot \Delta t \cdot \left[\frac{\left[-\left(\frac{T7_p - T6_p}{\Delta r} \right) \right] \cdot \left[2 \cdot \pi \cdot \left(\frac{r_{12}}{2} \right) \cdot L \right] - \left[-\left(\frac{T8_p - T7_p}{\Delta r} \right) \right] \cdot \left[2 \cdot \pi \cdot \left(\frac{r_{14}}{2} \right) \cdot L \right]}{\pi \cdot \left[\left(\frac{r_{14}}{2} \right)^2 - \left(\frac{r_{12}}{2} \right)^2 \right] \cdot L} + \frac{q \cdot e^{-(c1) \cdot r_7}}{k} - \frac{m_i \cdot c_b \cdot \left(T7_p - T_{art} \right)}{k} \right] + T7_p
\end{aligned}
$$

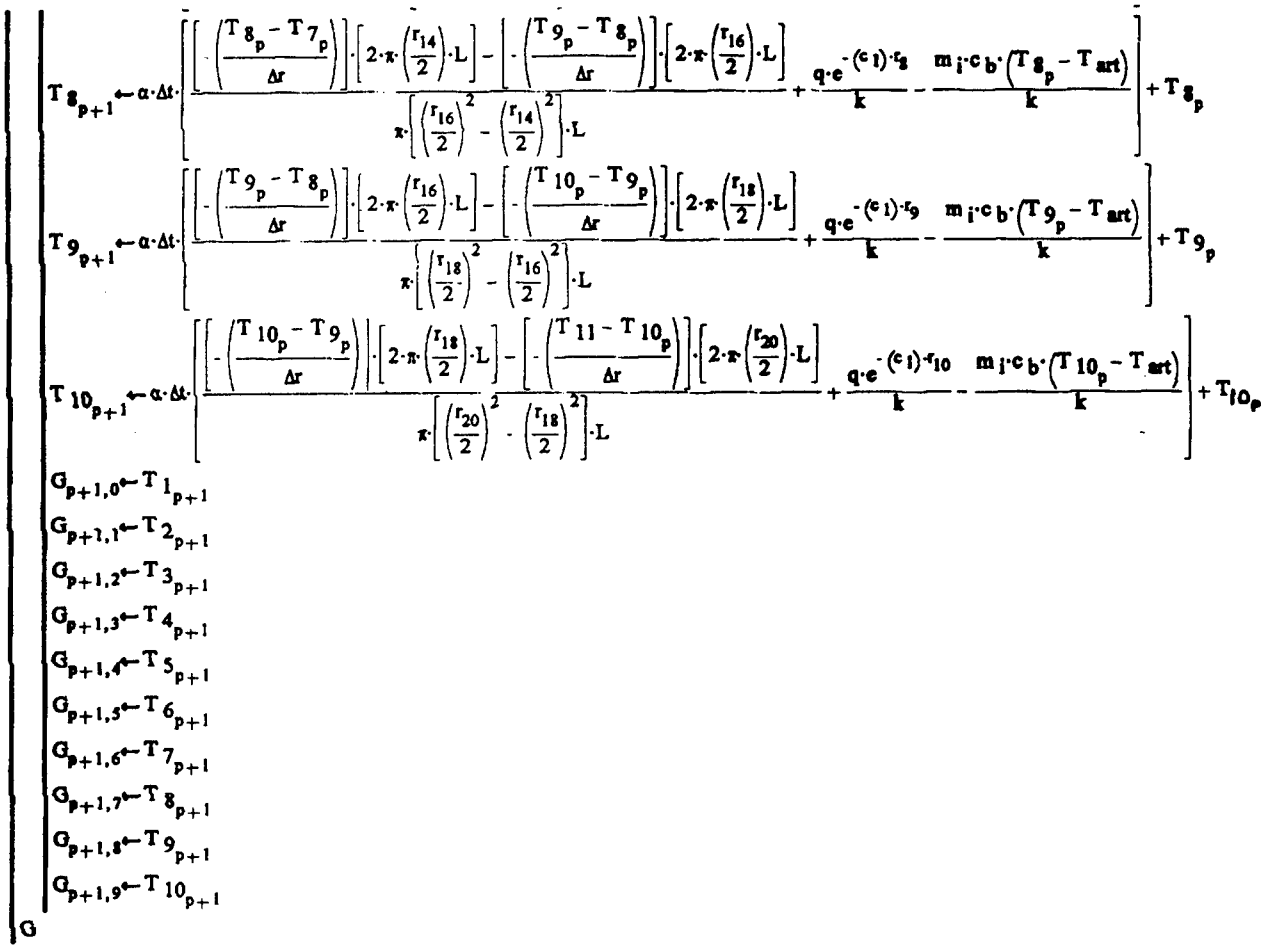

Figure 6: Equations for the time dependent cylindrical shells model

$L := 1.2 \cdot 10^{-2}$ $R := 1.3 \cdot 10^{-2}$ $\Delta r := \frac{R}{10}$ $k := 0.5$ $q := 1.224 \cdot 10^{6}$ $c_b := 3.8 \cdot 10^{3}$

$T_{art} := 38$ $T_{amb} := 22$ $h := 4.00$ $l := 1..11$ $r_l := (l-1) \cdot \Delta r$ $a := 0.90937$ $c_1 := \frac{a}{R}$

$k_{bra} := 0.503$ $k_{csf} := 0.582$ $k_{sku} := 1.16$ $k_{sca} := 0.340$ $w_{bra} := 9.0$ $w_{csf} := 0$

$q_{bra} := 1.10 \cdot 10^{4}$ $q_{csf} := 0$ $q_{sku} := 26.1$ $q_{sca} := 172$ $w_{sku} := 0.3$ $w_{sca} := 0.8$

$T_1 := 37$ $T_2 := 37$ $T_3 := 37$ $T_4 := 37$ $T_5 := 37$ $T_6 := 37$ $T_7 := 37$ $T_8 := 37$ $T_9 := 37$ $T_{10} := 37$ $T_{11} := 37$

Given

$$\left[-k_{bra}\cdot\left(\frac{T_2-T_1}{\Delta r}\right)\right]\cdot\left[2\cdot\pi\cdot\left(\frac{\Delta r}{2}\right)\cdot L\right]+\left[q_{bra}\cdot\pi\cdot\left(\frac{\Delta r}{2}\right)^2\cdot L\right]-\left[w_{bra}\cdot c_b\cdot\left[\pi\cdot\left(\frac{\Delta r}{2}\right)^2\cdot L\right]\cdot(T_1-T_{art})\right]=0$$

$$\left[-k_{bra}\cdot\left(\frac{T_2-T_1}{\Delta r}\right)\right]\cdot\left[2\cdot\pi\cdot\left(\frac{\Delta r}{2}\right)\cdot L\right]-\left[-k_{bra}\cdot\left(\frac{T_3-T_2}{\Delta r}\right)\right]\cdot\left[2\cdot\pi\cdot\left(\frac{3\cdot\Delta r}{2}\right)\cdot L\right]+\left[\left[(q_{bra})-\left[w_{bra}\cdot c_b\cdot(T_2-T_{art})\right]\right]\cdot\pi\cdot\left[\left(\frac{3\cdot\Delta r}{2}\right)^2-\left(\frac{\Delta r}{2}\right)^2\right]\cdot L\right]=0$$

$$\left[-k_{bra}\cdot\left(\frac{T_3-T_2}{\Delta r}\right)\right]\cdot\left[2\cdot\pi\cdot\left(\frac{3\cdot\Delta r}{2}\right)\cdot L\right]-\left[-k_{bra}\cdot\left(\frac{T_4-T_3}{\Delta r}\right)\right]\cdot\left[2\cdot\pi\cdot\left(\frac{5\cdot\Delta r}{2}\right)\cdot L\right]+\left[\left[(q_{bra})-\left[w_{bra}\cdot c_b\cdot(T_3-T_{art})\right]\right]\cdot\pi\cdot\left[\left(\frac{5\cdot\Delta r}{2}\right)^2-\left(\frac{3\cdot\Delta r}{2}\right)^2\right]\cdot L\right]=0$$

$$\left[-k_{bra}\cdot\left(\frac{T_4-T_3}{\Delta r}\right)\right]\cdot\left[2\cdot\pi\cdot\left(\frac{5\cdot\Delta r}{2}\right)\cdot L\right]-\left[-k_{bra}\cdot\left(\frac{T_5-T_4}{\Delta r}\right)\right]\cdot\left[2\cdot\pi\cdot\left(\frac{7\cdot\Delta r}{2}\right)\cdot L\right]+\left[\left[(q_{bra})-\left[w_{bra}\cdot c_b\cdot(T_4-T_{art})\right]\right]\cdot\pi\cdot\left[\left(\frac{7\cdot\Delta r}{2}\right)^2-\left(\frac{5\cdot\Delta r}{2}\right)^2\right]\cdot L\right]=0$$

$$\left[-k_{bra}\cdot\left(\frac{T_5-T_4}{\Delta r}\right)\right]\cdot\left[2\cdot\pi\cdot\left(\frac{7\cdot\Delta r}{2}\right)\cdot L\right]-\left[-k_{bra}\cdot\left(\frac{T_6-T_5}{\Delta r}\right)\right]\cdot\left[2\cdot\pi\cdot\left(\frac{9\cdot\Delta r}{2}\right)\cdot L\right]+\left[\left[(q_{bra})-\left[w_{bra}\cdot c_b\cdot(T_5-T_{art})\right]\right]\cdot\pi\cdot\left[\left(\frac{9\cdot\Delta r}{2}\right)^2-\left(\frac{7\cdot\Delta r}{2}\right)^2\right]\cdot L\right]=0$$

$$\left[-k_{bra}\cdot\left(\frac{T_6-T_5}{\Delta r}\right)\right]\cdot\left[2\cdot\pi\cdot\left(\frac{9\cdot\Delta r}{2}\right)\cdot L\right]-\left[-k_{bra}\cdot\left(\frac{T_7-T_6}{\Delta r}\right)\right]\cdot\left[2\cdot\pi\cdot\left(\frac{11\cdot\Delta r}{2}\right)\cdot L\right]+\left[\left[(q_{bra})-\left[w_{bra}\cdot c_b\cdot(T_6-T_{art})\right]\right]\cdot\pi\cdot\left[\left(\frac{11\cdot\Delta r}{2}\right)^2-\left(\frac{9\cdot\Delta r}{2}\right)^2\right]\cdot L\right]=0$$

$$\left[-k_{csf}\cdot\left(\frac{T_7-T_6}{\Delta r}\right)\right]\cdot\left[2\cdot\pi\cdot\left(\frac{11\cdot\Delta r}{2}\right)\cdot L\right]-\left[-k_{csf}\cdot\left(\frac{T_8-T_7}{\Delta r}\right)\right]\cdot\left[2\cdot\pi\cdot\left(\frac{13\cdot\Delta r}{2}\right)\cdot L\right]+\left[\left[(q_{csf})-\left[w_{csf}\cdot c_b\cdot(T_7-T_{art})\right]\right]\cdot\pi\cdot\left[\left(\frac{13\cdot\Delta r}{2}\right)^2-\left(\frac{11\cdot\Delta r}{2}\right)^2\right]\cdot L\right]=0$$

$$\left[-k_{sku}\cdot\left(\frac{T_8-T_7}{\Delta r}\right)\right]\cdot\left[2\cdot\pi\cdot\left(\frac{13\cdot\Delta r}{2}\right)\cdot L\right]-\left[-k_{sku}\cdot\left(\frac{T_9-T_8}{\Delta r}\right)\right]\cdot\left[2\cdot\pi\cdot\left(\frac{15\cdot\Delta r}{2}\right)\cdot L\right]+\left[\left[(q_{sku})-\left[w_{sku}\cdot c_b\cdot(T_8-T_{art})\right]\right]\cdot\pi\cdot\left[\left(\frac{15\cdot\Delta r}{2}\right)^2-\left(\frac{13\cdot\Delta r}{2}\right)^2\right]\cdot L\right]=0$$

$$\left[-k_{sku}\cdot\left(\frac{T_9-T_8}{\Delta r}\right)\right]\cdot\left[2\cdot\pi\cdot\left(\frac{15\cdot\Delta r}{2}\right)\cdot L\right]-\left[-k_{sku}\cdot\left(\frac{T_{10}-T_9}{\Delta r}\right)\right]\cdot\left[2\cdot\pi\cdot\left(\frac{17\cdot\Delta r}{2}\right)\cdot L\right]+\left[\left[(q_{sku})-\left[w_{sku}\cdot c_b\cdot(T_9-T_{art})\right]\right]\cdot\pi\cdot\left[\left(\frac{17\cdot\Delta r}{2}\right)^2-\left(\frac{15\cdot\Delta r}{2}\right)^2\right]\cdot L\right]=0$$

$$\left[-k_{sca}\cdot\left(\frac{T_{10}-T_9}{\Delta r}\right)\right]\cdot\left[2\cdot\pi\cdot\left(\frac{17\cdot\Delta r}{2}\right)\cdot L\right]-\left[-k_{sca}\cdot\left(\frac{T_{11}-T_{10}}{\Delta r}\right)\right]\cdot\left[2\cdot\pi\cdot\left(\frac{19\cdot\Delta r}{2}\right)\cdot L\right]+\left[\left[(q_{sca})-\left[w_{sca}\cdot c_b\cdot(T_{10}-T_{art})\right]\right]\cdot\pi\cdot\left[\left(\frac{19\cdot\Delta r}{2}\right)^2-\left(\frac{17\cdot\Delta r}{2}\right)^2\right]\cdot L\right]=0$$

$$\left[-k_{sca}\cdot\left(\frac{T_{11}-T_{10}}{\Delta r}\right)\right]\cdot\left[2\cdot\pi\cdot\left(\frac{19\cdot\Delta r}{2}\right)\cdot L\right]-\left[-h\cdot(T_{amb}-T_{11})\right]\cdot\left[2\cdot\pi\cdot(10\cdot\Delta r)\cdot L\right]-\left[\left[(q_{sca})-\left[w_{sca}\cdot c_b\cdot(T_{11}-T_{art})\right]\right]\cdot\pi\cdot\left[(10\cdot\Delta r)^2-\left(\frac{19\cdot\Delta r}{2}\right)^2\right]\cdot L\right]=0$$

$$\gamma := \text{Find}(T_1, T_2, T_3, T_4, T_5, T_6, T_7, T_8, T_9, T_{10}, T_{11})$$

Figure 7: Equations for the steady state whole-head, non-homogeneous cylindrical shells model

Figure 8: Equations for the time dependent whole-head, non-homogeneous cylindrical shells model

Figure 8 had to be eliminated due to spacial limitations. The equations can be found by applying the same changes to the figure 6 equations as the were applied to the figure 5 equations to get the figure 7 equations. Remember to change the microwave heating to the metabolic heating at 20 seconds. (Note: set c1 to zero after 20 seconds also)

Use these values:

$L := 1.2\cdot10^{-2}$ $R := 1.3\cdot10^{-2}$ $\Delta r := \frac{R}{10}$ $k := 0.5$ $q := 1.224\cdot10^{6}$ $c_b := 3.8\cdot10^{3}$

$T_{art} := 38$ $T_{amb} := 22$ $h := 4.00$ $l := 1..11$ $r_l := (l-1)\cdot\Delta r$ $a := 0.90937$ $c_1 := \frac{a}{R}$

$k_{bra} := 0.503$ $k_{csf} := 0.582$ $k_{sku} := 1.16$ $k_{sca} := 0.340$ $w_{bra} := 9.0$ $w_{csf} := 0$

$q_{bra} := 1.10\cdot10^{4}$ $q_{csf} := 0$ $q_{sku} := 26.1$ $q_{sca} := 172$ $w_{sku} := 0.3$ $w_{sca} := 0.8$

$T_1 := 37$ $T_2 := 37$ $T_3 := 37$ $T_4 := 37$ $T_5 := 37$ $T_6 := 37$ $T_7 := 37$ $T_8 := 37$ $T_9 := 37$ $T_{10} := 37$ $T_{11} := 37$

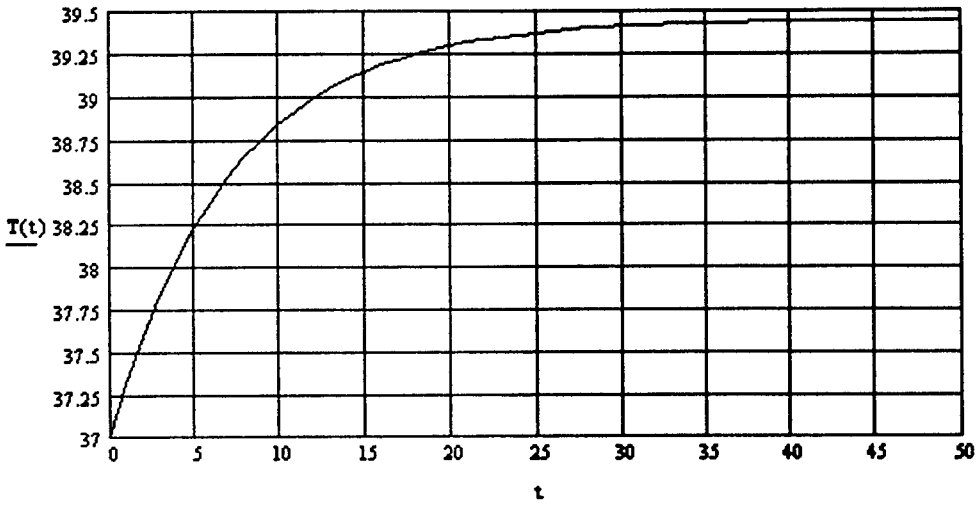

Figure 9:Graph of the spherical model

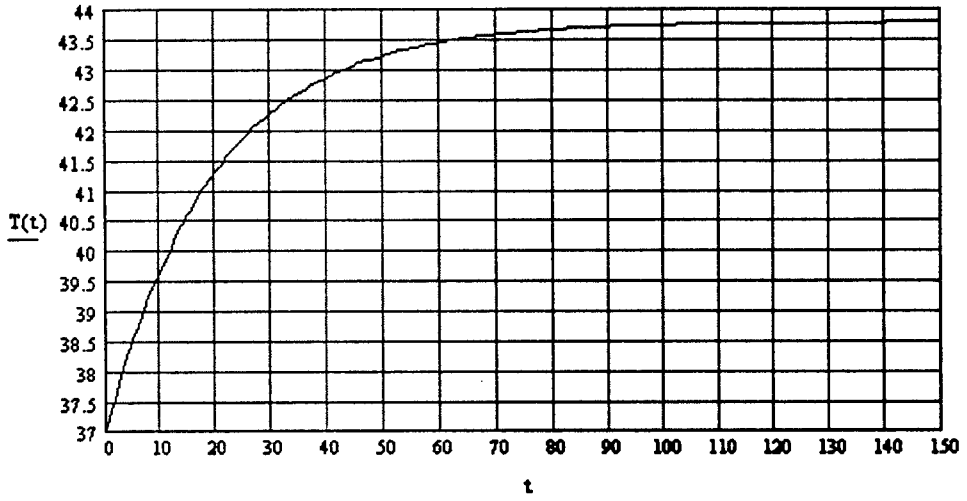

Figure 10: Graph of the cylindrical model

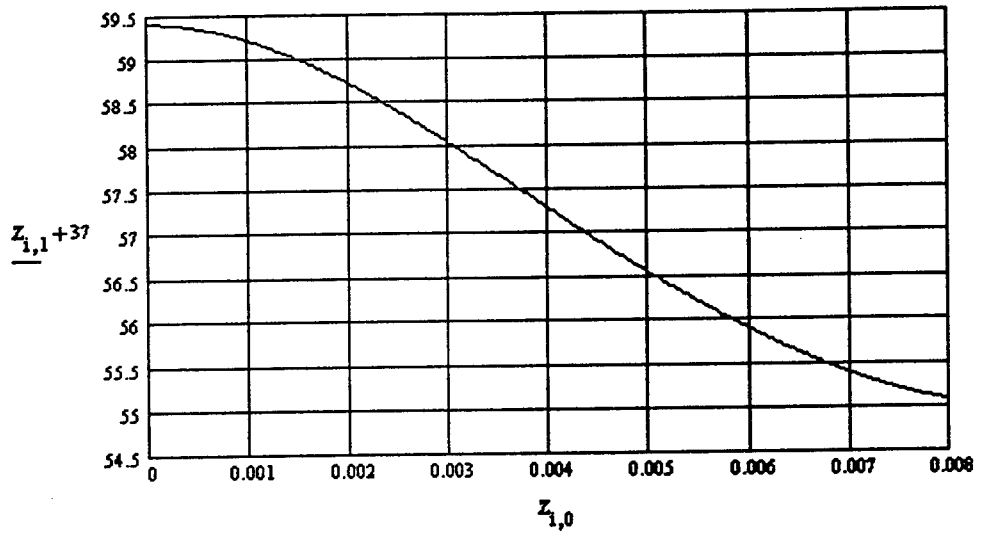

Figure 11: Graph of the steady state homogeneous cylindrical model

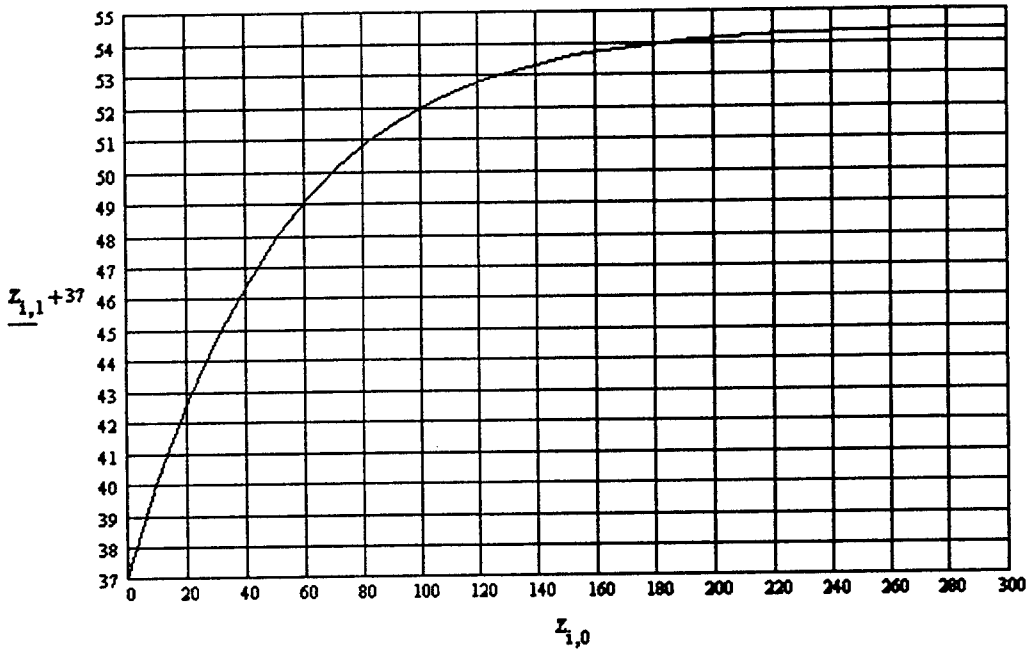

Figure 12: Graph of the time dependent homogeneous cylindrical model

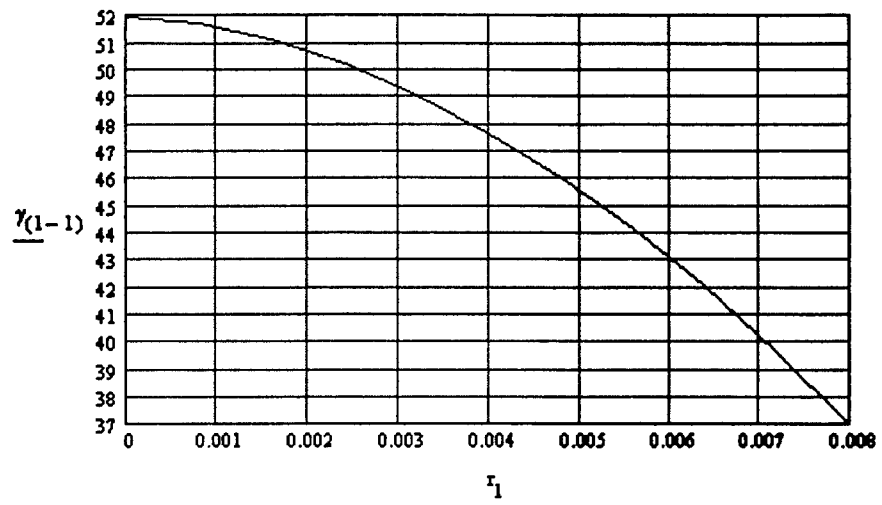

Figure 13: Graph of the steady state cylindrical shells model

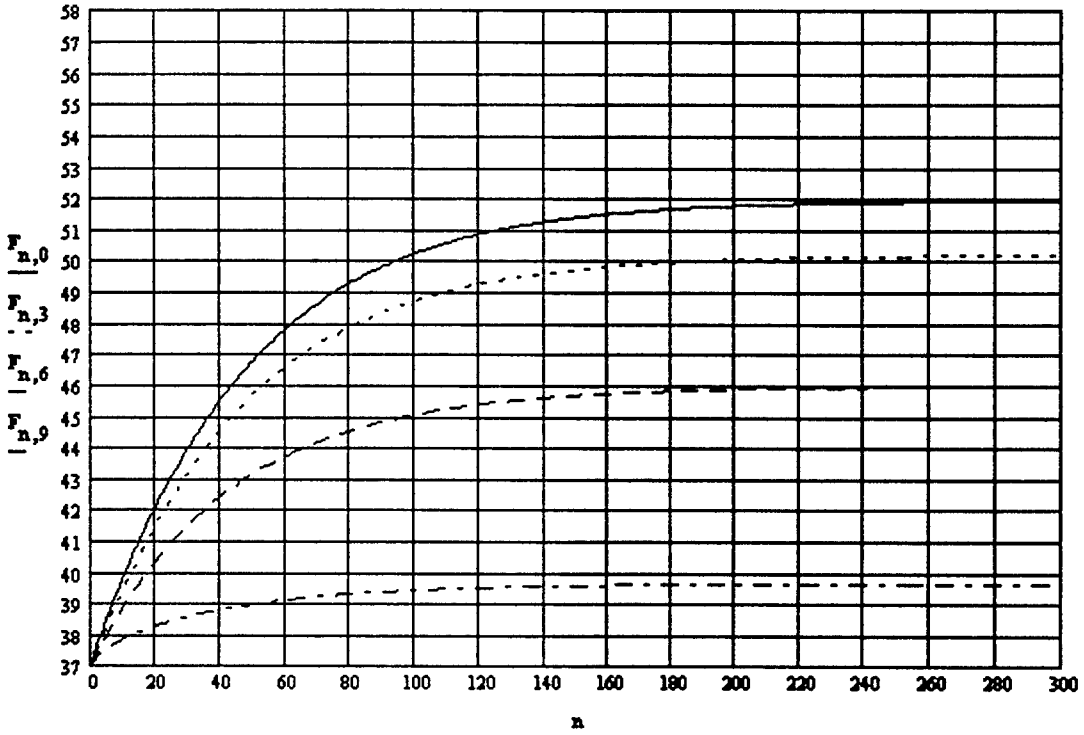

Figure 14: Graph of the time dependent cylindrical shells model

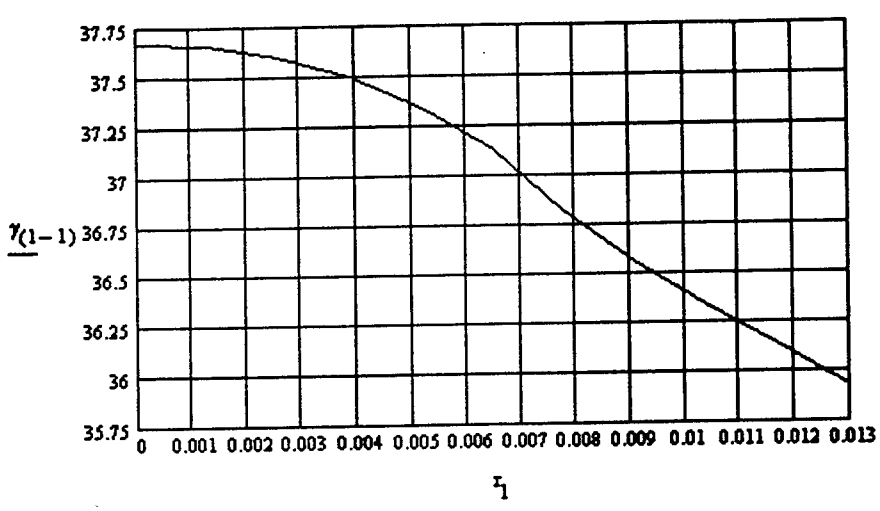

Figure 15: Graph of the steady state whole-head, non-homogeneous cylindrical shells model

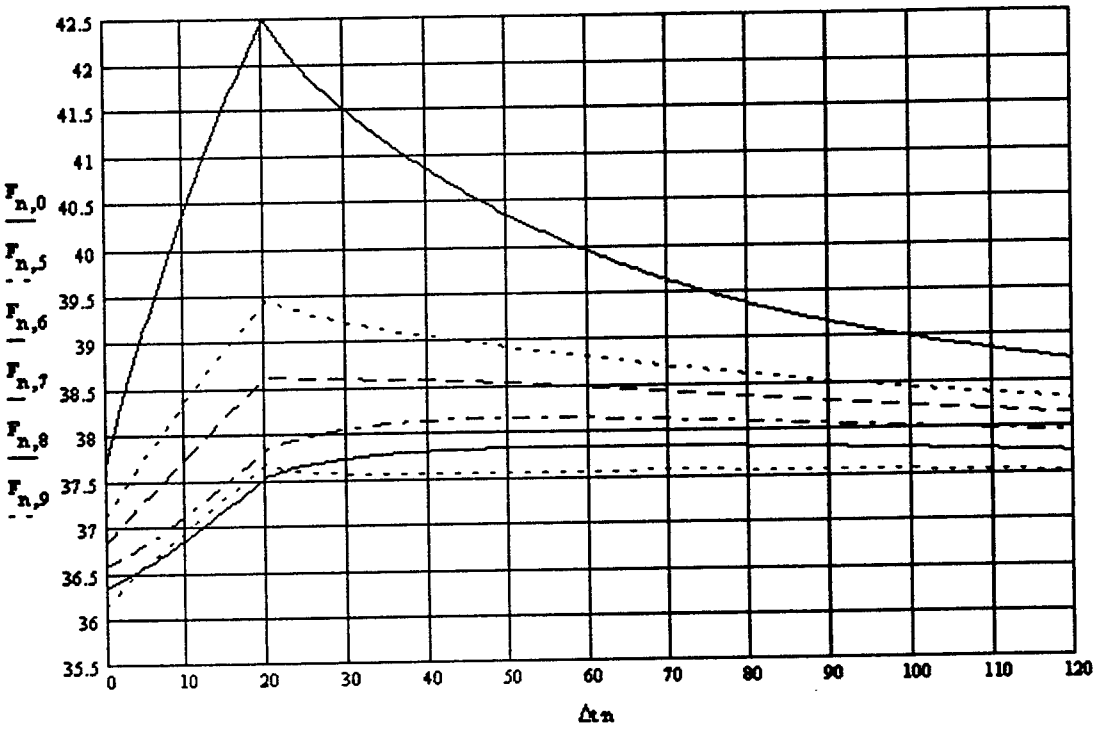

Figure 16: Graph of the time dependent whole-head, non-homogeneous cylindrical shells model

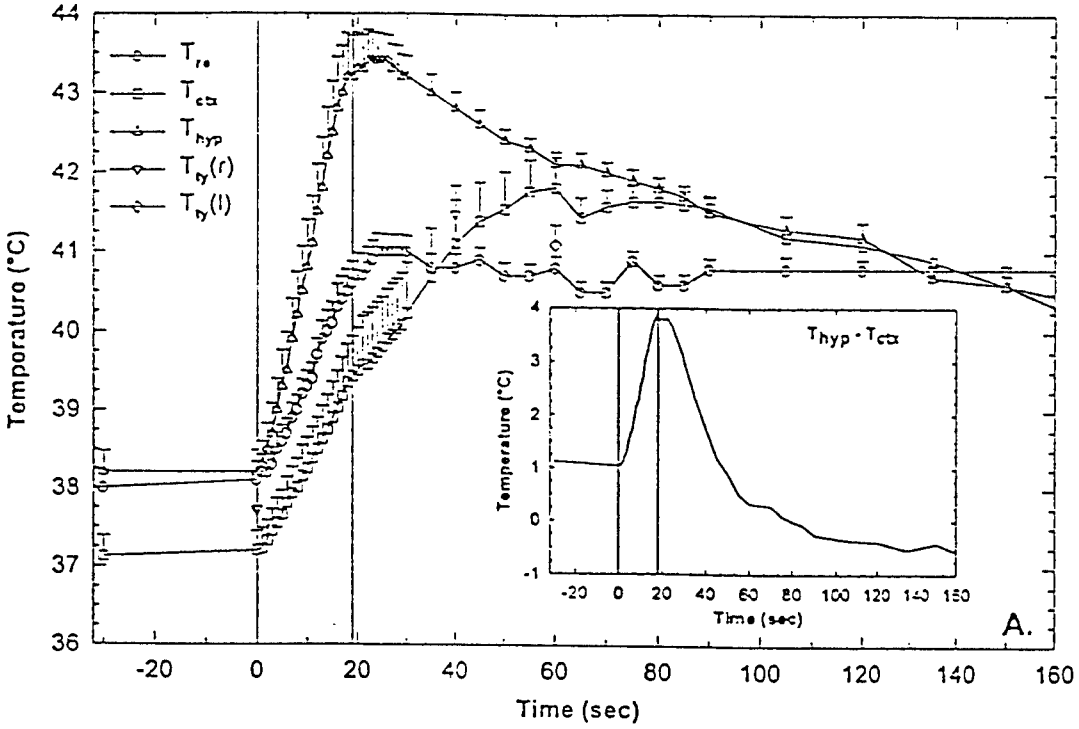

Figure 17: Experimental results of exposure of a rat to HPM

(Note: this graph was taken from the paper by Walters et al.)